

Geoscience Centre

**Department of Geobiology**

*Reinhardt, Manuel*



Univ.Göttingen•GZG•Abt.Geobiologie•Goldschmidtstr.3•37077 Göttingen•Germany

Goldschmidtstr. 3  
37077 Göttingen  
Germany  
Phone: +49(0)551-39 13756  
E-mail: [mreinha@gwdg.de](mailto:mreinha@gwdg.de)  
[http://www.  
geobiologie.uni-goettingen.de](http://www.geobiologie.uni-goettingen.de)

**Associate editor *Biogeosciences***

Dr. Marcel van der Meer



Göttingen, 04/18/2019

**Submission of the revised manuscript bg-2018-513**

Dear Marcel van der Meer,

Also on behalf of my co-authors I would like to thank you, Jan W. de Leeuw, and the two anonymous reviewers for the thoughtful comments.

As requested, we included the previously suggested corrections into the manuscript (see replies to RC1–3, March 9th). In order to help you to track our changes and modifications, we attached the following documents:

- (i) Reply to your comments
- (ii) Replies to all reviewer comments (RC1–3 from March 9th)
- (iii) Tracked changes version of the manuscript
- (iv) Tracked changes version of the supplement

We trust that the revised manuscript will meet the requirements of you and the reviewers.

Yours sincerely,

Manuel Reinhardt

Comment from the editor: “I do think there is one issue you could spend a bit more time on explaining or clarifying. You use the Pleistocene settings as analogs for Archean hydrothermal cherts and I think you need to spend a little bit more time on this to make it more than a way to “sell” your Pleistocene study. The analogy is comparable deposits, hydrothermal cherts, right? I think it is entirely valid to test your approach, methods and types of analysis on a more modern setting to see what works and what doesn’t, what type of information you get etc., before actually working on these really old deposits. I am assuming you are actually going to do that? So that sense it works, in your answer to one of the reviewers you actually mention using methods for these samples you would also use for Archean samples. However, there is a few billion years of evolution between the Archean and Pleistocene, so biologically and on a larger environmental scale these settings are not analogues. Not only in the sense that a lot of organisms were not present in the Archean that were present in the Pleistocene, but even the microorganisms present in the Archean continued to evolve for that enormous amount of time. If the settings are similar, you do expect similar functions in both settings, but how that translates in lipids and isotopic compositions? This, together with all kinds of alterations that take place over time for the Archean organic matter, would make it very useful to study the organic matter from the Pleistocene as complete and detailed as possible and not only using techniques you would use for these really old samples. Things might move in and out of analytical windows with time. So I would like to ask you to put a little bit more time in explaining how you see this analogy in your rebuttal and possibly at some key points in the manuscript as well.”

Author’s response: We consider the Pleistocene hydrothermal chert-generating environment at Lake Magadi more as a (rare) environmental and not so much as an exact biological analog for Archean cherts. So our study is aimed more on the taphonomy (i.e., earliest diagenesis) of organic matter in hydrothermal chert settings. Hydrothermal environments are generally considered unfavorable for the preservation of organic matter, as hot fluid circulation may cause rapid alteration, and destruction of organic compounds. Our data indicate that microbial lipids (in general; not so much specific biomolecules), if produced during the Archean, might well have had a chance to escape syndepositional hydrothermal degradation and be incorporated in the ‘final’ (solid) chert matrix (notwithstanding that any long-term preservation would still be dependent on the post-depositional metamorphic regime). Further, Archean hydrothermal cherts often show organic matter with different maturity fractions that are commonly explained by post-depositional metamorphic overprint and contamination rather than genuine environmental signals (e.g., Ueno et al., 2004; Tice & Lowe, 2006; Olcott Marshall et al., 2012; Sforna et al., 2014; Morag et al., 2016). We show that such different maturity fractions may also be of primary origin, resulting from syndepositional hydrothermal alteration (and circulation). In this way, we believe that our observations from Lake Magadi can certainly aid in the future analysis and interpretation of organic matter characteristics from Archean hydrothermal cherts.

Comment from the editor: “In one of your comments you mention CO<sub>2</sub> limitation as a possible reason for the <sup>13</sup>C enriched lipids in LM-1694. Looking at your table 4, not all compounds are extremely enriched in <sup>13</sup>C relative to the other samples. The short chain alkanols and alkanolic acids are very similar to the other samples, mainly the monoethers and archaeol and to a lesser extend extended archaeol and even phytane perhaps a little are <sup>13</sup>C enriched. The carbon isotopic composition of archaeol seems a bit variable any way. Of course something like CO<sub>2</sub> limitation could play a role, it is a bit strange that you see this mainly in this subset of compounds. In this type of setting it would not be surprising to see other CO<sub>2</sub> fixation pathways with different carbon isotopic fractionation, variable relative contribution from different pathways could potentially explain the observed differences. Any way something to think about.”

Author’s response: We agree and included the possibility of different CO<sub>2</sub> fixation pathways into the discussion.

References cited in the reply:

- Morag, N., Williford, K. H., Kitajima, K., Philippot, P., Van Kranendonk, M. J., Lepot, K., Thomazo, C., and Valley, J. W.: Microstructure-specific carbon isotopic signatures of organic matter from ~3.5 Ga cherts of the Pilbara Craton support a biologic origin, *Precambrian Res.*, 275, 429–449, 10.1016/j.precamres.2016.01.014, 2016.
- Olcott Marshall, A., Emry, J. R., and Marshall, C. P.: Multiple Generations of Carbon in the Apex Chert and Implications for Preservation of Microfossils, *Astrobiology*, 12, 160–166, 10.1089/ast.2011.0729, 2012.
- Sforna, M. C., van Zuilen, M. A., and Philippot, P.: Structural characterization by Raman hyperspectral mapping of organic carbon in the 3.46 billion-year-old Apex chert, Western Australia, *Geochim. Cosmochim. Acta*, 124, 18–33, 10.1016/j.gca.2013.09.031, 2014.
- Tice, M. M., and Lowe, D. R.: The origin of carbonaceous matter in pre-3.0 Ga greenstone terrains: A review and new evidence from the 3.42 Ga Buck Reef Chert, *Earth Sci. Rev.*, 76, 259–300, 10.1016/j.earscirev.2006.03.003, 2006.
- Ueno, Y., Yoshioka, H., Maruyama, S., and Isozaki, Y.: Carbon isotopes and petrography of kerogens in ~3.5-Ga hydrothermal silica dikes in the North Pole area, Western Australia, *Geochim. Cosmochim. Acta*, 68, 573–589, 10.1016/S0016-7037(03)00462-9, 2004.

## ***Interactive comment on* “Organic signatures in Pleistocene cherts from Lake Magadi (Kenya), analogs for early Earth hydrothermal deposits” by Manuel Reinhardt et al.**

**Manuel Reinhardt et al.**

mreinha@gwdg.de

Received and published: 9 March 2019

Comment from referee: “The title suggests more than the contents of the full article, since: 1) Cyanobacteria, Algae, Higher plants, ciliates, fungi and many bacteria and Archaea present in the Pleistocene setting were not present during the “early Earth”, i.e. the (early) Archean. . . ,

Author’s response: We agree in that the organic matter sources of modern and Archean organic matter were certainly not identical. We therefore will use a more cautious wording of the title, avoiding the term ‘analog’ in respect to organic matter.

Printer-friendly version

Discussion paper



Planned changes in manuscript: The title will be reworded.

...2) most, if not all, hydrothermal vents in the early Archean were at the bottom of the oceans, a setting very different from the Pleistocene setting investigated. The analogy is therefore limited to the syngeneity of immature and mature organic matter as a result of the hydrothermal pump hypothesis”.

Author’s response: We do not agree with the referee here. Recent works demonstrated that a variety of early Archean facies in Barberton and Pilbara areas reflect shallow marine hydrothermal (Allwood et al., 2006; Hickman-Lewis et al., 2018) or even terrestrial hot spring environments (Djokic et al., 2017), and several authors have pointed at the similarities of the Magadi cherts and Archean cherts with respect to their formation and lithology (Brenna, 2016; Eugster and Jones, 1968).

Comment from referee: “The authors have analysed the extracts as such by GC/MS. High molecular weight compounds such as Intact GDGTs or their lipid cores, polyesters, etc. (compounds expected to be present in these immature sediments in relative high concentrations), have been missed since the extraction method was not sufficient for extracting such compounds and/or they cannot be analysed by GC/MS. A more polar extraction method in combination with base- and/or acid hydrolysis of extracts and LC/MS analysis would have opened the analytical window very considerably”.

Author’s response: We agree that the use of further analytical techniques may have led to the identification of additional compounds. However, our methodology was not designed as being comprehensive with respect to all (polar) compounds present. As we regard our Pleistocene (10–100 ka old) thermally altered samples essentially as ‘fossil’, we focused more on the GC-amenable alkyl moieties and adhered as much as possible to the techniques typically used on ancient (incl. Archaean) organic matter, i.e., Raman, GC–MS, HyPy, and microscopy. It should nonetheless be noted that we did use acidic hydrolysis on the TOEs to cleave ester-bound compounds (TMCS/MeOH), so

BGD

Interactive  
comment

Printer-friendly version

Discussion paper



that GC-amenable ester-bound moieties have been covered in the bitumen fractions.

Planned changes in manuscript: We will clarify that high molecular weight compounds like GDGTs and polymers were not analyzed in this study (introduction; chapter 3.2.1) and limit our conclusions on archaeal lipid preservation in the Magadi chert kerogens to low/medium molecular weight compounds.

Comment from referee: “The kerogens obtained have not been hydrolysed either, so that non-extracted moderate polar, partly high molecular weight, compounds were not removed and analysed by GC/MS or LC/MS. This implies that the HyPy results of the non-hydrolysed kerogens may be biased by pyrolysis products of relatively polar, high molecular weight immature organic matter which is not the result of hydrothermal maturation”.

Author’s response:

(i) As outlined above we intentionally used the techniques generally applied to study ancient organic matter, hence for kerogen preparation we strictly adhered to the established and commonly used method of Durand (1980), i.e., sequential extraction with different solvents, HCl-treatment, HF-treatment, and repeated extractions of the resulting residue.

(ii) A potential bias by non-extracted low-molecular weight moieties in the kerogen pyrolysis products (‘bitumen II’) can be excluded, because these compounds were removed during the pre-heating step (330 °C) in the HyPy runs. Notably, this step yielded only minor products (thus excluded from discussion).

(iii) DCM/MeOH-based solvent combinations similar to those used in our study were reported to successfully extract lipids of higher molecular weight such as GDGTs (e.g., Pancost et al., 2008). We feel that most lipid-like material including GDGT lipids should have been removed from the kerogen during the sequential extraction and acid dissolution steps. However, the possibility that some biomarkers may partly originate from

[Printer-friendly version](#)

[Discussion paper](#)



residual compounds trapped in the 'kerogen' and missed by the extensive kerogen extraction procedure can hardly be fully excluded (and could hardly be ever excluded in kerogen studies).

Planned changes in manuscript: We will mention the possibility that biphytane may partly derive from incomplete removal of GDGTs during extraction and tone down the implications on archaeal lipid preservation in the kerogens accordingly (see author's response to the previous referee comment).

Comment from referee: "It's also possible that the "kerogen" contains high molecular weight compounds produced through sulfurization of immature functionalized low molecular compounds. I understand very well that the authors have limited themselves analytically. That's OK as long as the consequences of such a narrow analytical window is considered in the results and discussion paragraphs".

Author's response: We agree that the sulfurization of immature compounds may contribute, with or without hydrothermal influence, to the formation of early kerogen-like macromolecules. However, the Magadi cherts have extremely low sulfur contents (Table 1) and these tiny amounts of sulfur are mostly hosted in inorganic oxidized species, mostly gypsum. Therefore we do not consider sulfurization as an important process in this setting. Yet the biomarker inventory revealed evidence for lipid inputs from sulfate reducers, and it may be possible that sulfurization could occur in microscale environments where sulfate reduction was active. Unfortunately this possibility could not be further explored using our analytical setup.

Planned changes in manuscript: The occurrence of sulfates will be specified and the possibility of sulfurization will be discussed.

Comment from referee: "Table 4. Sample LM-1694 seems to have highly deviating isotope values. Why is that? A HyPy m/z 85 trace might be added to Figs 4 and 6".

Author's response: Magadi is an evaporitic environment showing varying salinities,

[Printer-friendly version](#)[Discussion paper](#)

so the  $^{13}\text{C}$  enrichment in compounds from LM-1694 may be explained by a higher salinity/evaporation (stronger  $\text{CO}_2$ -limitation) during deposition of that specific chert.

Planned changes in manuscript: As suggested a  $m/z$  85 HyPy trace of LM-1694 will be added to Fig. 6 and the corresponding bitumen TIC to Fig. 3.

Comment from referee: “The authors note the presence of a clear UMC in sample LM-1697. UMCs are often the consequence of bacterial biodegradation. In this case it’s not clear when this happened, shortly after deposition or recently due to bacterial infection of the outcrop samples. A UMC is also recognized in some of the other samples. I suggest that the authors discuss this topic in more detail”.

Author’s response and planned changes in manuscript: We agree and will discuss biodegradation in the manuscript. However, UCMs may also appear in non-biodegraded low-maturity oils (Peters et al., 2005, p. 106) and the Ph/n-C18 value of LM-1697 is not elevated as compared to other Magadi chert bitumens without pronounced UCMs (see Table 2).

Comment from referee: “For future work related to “kerogen” analysis I suggest that the authors consider to apply Thermally assisted hydrolysis (TMH) in combination with GC/MS (see for example K.G.J. Nierop et al., J. of Anal. and Appl. Pyrolysis, 83, pp 227-231 (2008) instead of HyPy. I’m convinced that by applying this TMH method much more info will be obtained due to the release of functionalized compounds also indicating the mode of chemical binding to the macromolecular matrix, since it can be expected that in this particular case the so called kerogen may partly consist of GDGTs and many other bio(macro)molecules”.

Author’s response: We thank the referee for his suggestion. While we are still convinced that our analytical setup appropriately supports the conclusions drawn in this manuscript, we will certainly consider the TMH method for the design of our future experiments!

[Printer-friendly version](#)[Discussion paper](#)



## References cited in the reply:

Allwood, A. C., Walter, M. R., and Marshall, C. P.: Raman spectroscopy reveals thermal palaeoenvironments of c.3.5 billion-year-old organic matter, *Vib. Spectrosc.*, 41, 190–197, 10.1016/j.vibspec.2006.02.006, 2006.

Brenna, B. L.: The Chemical, Physical, and Microbial Origins of Pleistocene Cherts at Lake Magadi, Kenya Rift Valley, M.Sc. thesis, Department of Geological Sciences, University of Saskatchewan, Saskatoon, 158 pp., 2016.

Durand, B.: Sedimentary organic matter and kerogen. Definition and quantitative importance of kerogen, in: *Kerogen: Insoluble Organic Matter from Sedimentary Rocks*, edited by: Durand, B., Editions Technip., Paris, 13–34, 1980.

Djokic, T., Van Kranendonk, M. J., Campbell, K. A., Walter, M. R., and Ward, C. R.: Earliest signs of life on land preserved in ca. 3.5 Ga hot spring deposits, *Nat. Commun.*, 8, e15263, 10.1038/ncomms15263, 2017.

Eugster, H. P., and Jones, B. F.: Gels Composed of Sodium-Aluminium Silicate, Lake Magadi, Kenya, *Science*, 161, 160–163, 10.1126/science.161.3837.160, 1968.

Hickman-Lewis, K., Cavalazzi, B., Foucher, F., and Westall, F.: Most ancient evidence for life in the Barberton greenstone belt: Microbial mats and biofabrics of the ~3.47 Ga Middle Marker horizon, *Precambrian Res.*, 312, 45–67, 10.1016/j.precamres.2018.04.007, 2018.

Pancost, R. D., Coleman, J. M., Love, G. D., Chatzi, A., Bouloubassi, I., and Snape, C. E.: Kerogen-bound glycerol dialkyl tetraether lipids released by hydrolysis of marine sediments: A bias against incorporation of sedimentary organisms?, *Org. Geochem.*, 39, 1359–1371, 10.1016/j.orggeochem.2008.05.002, 2008.

Peters, K. E., Walters, C. C., and Moldowan, J. M.: *The Biomarker Guide: I. Biomarkers and Isotopes in the Environment and Human History*, 2nd ed., Cambridge University Press., Cambridge, 471 pp., 2005.

BGD

Interactive  
comment

Printer-friendly version

Discussion paper



---

Interactive comment on Biogeosciences Discuss., <https://doi.org/10.5194/bg-2018-513>, 2019.

**BGD**

---

Interactive  
comment

Printer-friendly version

Discussion paper



## ***Interactive comment on “Organic signatures in Pleistocene cherts from Lake Magadi (Kenya), analogs for early Earth hydrothermal deposits” by Manuel Reinhardt et al.***

**Manuel Reinhardt et al.**

mreinha@gwdg.de

Received and published: 9 March 2019

Comment from referee: This study describes the co-occurrence of immature “biolipids” with early to peak oil window maturity “geolipids” in a range of chert samples. Overall, the manuscript provides an interesting case study for such a co-occurrence of organic molecules. The described biolipids appear syngenetic to the samples, as some compounds are constrained to specific environments (e.g. archaeol). However, the thermally mature geolipids can occur in a wide range of settings and are quite abundant. Previous work on hot springs in New Zealand, for example, recorded petroleum seepage as a result geothermal activity. Therefore, the syndepositional hypothesis is valid

[Printer-friendly version](#)

[Discussion paper](#)



from paleoenvironmental settings indicating hydrothermal processes (as in this study). The addition of in-situ Raman evidence for kerogen of a range of different maturities bolsters the validity of the syndepositional hypothesis for the Lake Magadi samples.

Comment from referee: Nevertheless, the authors have not provided any convincing evidence that the occurrence of the geolipids are not an artefact of hydrocarbon contamination - the most parsimonious explanation. While the authors used system blanks to track laboratory contaminants, they did not provide any evidence to account for hydrocarbon contaminants already on the rock samples (prior to laboratory analysis). Such contaminants can be introduced even before sampling/handling and storage. The low organic carbon contents (<0.4 wt%) of the samples makes any introduced contaminants even more visible. In recent years, a range of analytical techniques have been established to quantitatively track hydrocarbons from the outer rock surfaces to the interior. It would have been interesting to see what the results of such a study would have been on the cherts from Lake Magadi.

Author's response and planned changes in manuscript: We are aware of this problem and therefore conducted interior vs. exterior experiments on two Magadi cherts. The results support syngeneity of the geolipids and will be included into the supplement.

---

Interactive comment on Biogeosciences Discuss., <https://doi.org/10.5194/bg-2018-513>, 2019.

BGD

Interactive  
comment

Printer-friendly version

Discussion paper



## ***Interactive comment on* “Organic signatures in Pleistocene cherts from Lake Magadi (Kenya), analogs for early Earth hydrothermal deposits” by Manuel Reinhardt et al.**

**Manuel Reinhardt et al.**

mreinha@gwdg.de

Received and published: 9 March 2019

This is a very nice and detailed study of organic matter in recent, relatively unaltered cherts. Indeed, a good case is made for variable maturity as a result of localized hydrothermal circulation. I have some points of criticism (mostly focusing on the interpretation of the Raman spectral analyses), but these are not critical. There are some issues (as described below) that need to be clarified better, and some references to literature on these issues should be made. Overall, this manuscript can be published after only minor revisions.

Comment from referee: 1) A laser power of 1 mW was used during Raman spec-

Printer-friendly version

Discussion paper



troscopy. These kerogen fractions are very immature, with derived temperatures as low as 40 C. For such unaltered, fragile material, a laser power of 1mW is quite high. Did the authors test if the laser actually affects the kerogen during analysis? For instance causing alteration, or worse, cause combustion?. This should be demonstrated, by a comparison analysis using lower laser power (e.g. 0.1 mW).

Author's response: We agree, and we are fully aware of this problem. In our study, laser energy and exposure time were optimized on representative organic-bearing test spots prior to analyzing the actual spots selected for presentation in the manuscript. With the resulting protocol the degradation of organics (during laser irradiation) was found to be minor.

Changes planned: We will describe the laser power test in the "Materials and Methods" section (2.6 Raman Spectroscopy).

Comment from referee: 2) The very low temperature of alteration (as low as 40C), and the presence of biomarkers for specific groups of prokaryotes, suggests that the Raman spectra of the organic fractions do not only reflect degree of alteration, but also could reflect the type of biologic precursor. For instance, this is suggested by Qu et al. (2015, *Astrobiology*, 15, 825-841) for carbonaceous fractions found in e.g. the Rhynie chert and the Bitter Springs chert. This should at least be expressed as a possibility, that the Raman-based geothermometer (I don't know if Schito et al., 2017, actually address this issue) is influenced by the type of biomass.

Author's response: We agree, this is certainly an important point.

Changes planned: We will refer to the study by Qu et al. (2015) and include the information that the obtained low temperature Raman data possibly reflect both, thermal maturity and the specific type of biological precursor.

Comment from referee: 3) The Raman spectra that are presented in Fig.2 are not of high quality. There is a very low signal to noise ratio. The presented peak-fitting

[Printer-friendly version](#)[Discussion paper](#)

protocol, however, is quite sophisticated and requires a high-quality spectrum. It should be explained in detail then, what the uncertainties actually are of fitting these peaks to the range of Raman spectra that were obtained. Also, in general, the calibration of low-temperature Ramanbased geothermometers is quite difficult. The geothermometer of Schito et al. (2017) is quite new. There are other, well-known geothermometers, that should also be applied to check if similar temperatures are obtained. The most important ones are the Ramanbased determination of H/C-ratio by Ferralis et al. (2016, Carbon, 108, 440-449) and the D1-peak-based geothermometer of Kouketsu et al. (2014, Island Arc, 23, 33-50).

Author's response: Most Raman geothermometers, including those mentioned in this referee comment, focus on temperatures above 150°C, so we feel that they cannot be usefully applied here. Schito et al. (2017) appear to be the only authors attempting Raman thermometry below 100 °C.

Changes planned: CoD-values (R2) for the fittings and a word of caution (see point 2 above) will be added to the manuscript. The signal-to-noise ratio has been addressed under point 1 (see above).

Comment from referee: 4) In the Discussion, on page 14 line 1-5, it is said that hydrothermal processes can cause syndepositional variation in kerogen maturity. This is not new, and has particularly been suggested for carbonaceous fractions in the hydrothermal feeder part of the 3.5 Ga Apex Chert, Pilbara, Western Australia. In the papers Olcott et al. (2012, Astrobiology, 12, 160-166) and Sforza et al. (2014, GCA, 124, 18-33), it is suggested that variation in kerogen maturity is linked to multiple episodes of hydrothermal fluid flow. The authors should better describe this process, and refer to these papers.

Author's response: We agree.

Changes planned: We will rephrase the respective part (p. 14) and include these papers into our discussion.

[Printer-friendly version](#)[Discussion paper](#)

Comment from referee: 5) The last part of the discussion, and end of the conclusions, is quite positive about the prospect of finding biomarkers in kerogen in Archean cherts. The authors argue that this is possible because they find good biomarkers in these hydrothermally influenced cherts at Lake Magadi. However, they should mention that most (if not all) cherts of Archean age have experienced greenschist-facies metamorphism, and that they thus have been buried and heated under pressure for millions of years. That's a very different thermal history than the Pleistocene cherts that are studied here. Time is an important factor. Biomarkers are extremely rare in Archean cherts, and the small fractions that have been described are highly controversial. The authors can work that issue out a bit better, and refer to e.g. French et al. (2015, PNAS, 112, 5915-5920) that described these issues. Nevertheless, the authors have proven an important point, that syndepositional hydrothermal circulation would indeed have created a range of maturities, and possibly have caused preservation of kerogen-bound biomarker molecules. That such biomarkers could be found in the Archean, however, remains to be seen.

Author's response: We agree. The post-depositional thermal history of the Magadi cherts is not comparable with Archean hydrothermal deposits. Nevertheless, our data indicate that not all molecular fingerprints, such as lipid biomarkers, are lost during initial hydrothermal heating and mild diagenesis in hydrothermal environments.

Changes planned: We will tone down our positive view and implement the work by French and colleagues.

References cited in the reply:

French, K. L., Hallmann, C., Hope, J. M., Schoon, P. L., Zumberge, J. A., Hoshino, Y., Peters, C. A., George, S. C., Love, G. D., Brocks, J. J., Buick, R., Summons, R. E.: Reappraisal of hydrocarbon biomarkers in Archean rocks, PNAS, 112, 5915–5920, 10.1073/pnas.1419563112, 2015.

Qu, Y., Engdahl, A., Zhu, S., Vajda, V., McLoughlin, N.: Ultrastructural Heterogeneity

[Printer-friendly version](#)[Discussion paper](#)



of Carbonaceous Material in Ancient Cherts: Investigating Biosignature Origin and Preservation, *Astrobiol.*, 15, 10.1089/ast.2015.1298, 2015.

Schito, A., Romano, C., Corrado, S., Grigo, D., and Poe, B.: Diagenetic thermal evolution of organic matter by Raman spectroscopy, *Org. Geochem.*, 106, 57–67, 0.1016/j.orggeochem.2016.12.006, 2017.

---

Interactive comment on Biogeosciences Discuss., <https://doi.org/10.5194/bg-2018-513>, 2019.

**BGD**

---

Interactive  
comment

Printer-friendly version

Discussion paper



# Organic signatures in Pleistocene cherts from Lake Magadi (Kenya), analogs—implications for early Earth hydrothermal deposits

Manuel Reinhardt<sup>1,2</sup>, Walter Goetz<sup>1</sup>, Jan-Peter Duda<sup>3</sup>, Christine Heim<sup>2</sup>, Joachim Reitner<sup>2,4</sup>, Volker Thiel<sup>2</sup>

<sup>1</sup>Planets and Comets, Max Planck Institute for Solar System Research, 37077 Göttingen, Germany

5 <sup>2</sup>Department of Geobiology, Geoscience Centre, University of Göttingen, 37077 Göttingen, Germany

<sup>3</sup>Department of Earth Sciences, University of California Riverside, CA 92521, USA

<sup>4</sup>'Origin of Life' Group, Göttingen Academy of Sciences and Humanities, 37073 Göttingen, Germany

Correspondence to: Manuel Reinhardt (mreinha@gwdg.de)

**Abstract.** Organic matter in Archean hydrothermal cherts may provide an important archive for molecular traces of earliest life on Earth. The geobiological interpretation of this archive, however, requires a sound understanding of organic matter preservation and alteration in hydrothermal systems. Here we report on organic matter (including molecular biosignatures) enclosed in hydrothermally influenced cherts of the Pleistocene Lake Magadi (Kenya; High Magadi Beds and Green Beds)—~~important analogs for Archean cherts.~~ The Magadi cherts contain low organic carbon (<0.4 wt.%) that occurs in form of finely dispersed clots, layers, or encapsulated within microscopic carbonate rhombs. Both, extractable (bitumen) and non-  
15 extractable organic matter (kerogen) was analyzed. The bitumens contain immature “biolipids” like glycerol mono- and diethers (e.g., archaeol and extended archaeol), fatty acids and –alcohols indicative for, *inter alia*, thermophilic cyanobacteria, sulfate reducers, and haloarchaea. However, co-occurring “geolipids” such as *n*-alkanes, hopanes, and polycyclic aromatic hydrocarbons (PAHs) indicate that a fraction of the bitumen has been thermally altered to early or peak oil window maturity. This more mature fraction likely originated from defunctionalization of dissolved organic matter and/or hydrothermal  
20 petroleum formation at places of higher thermal flux. Like the bitumens, the kerogens also show variations in thermal maturities, which can partly be explained by admixture of thermally pre-altered macromolecules. However, findings of archaea-derived isoprenoid moieties ~~in some of the kerogens~~(C<sub>20</sub> and C<sub>25</sub> chains) in kerogen pyrolysates indicate ~~that a fast~~rapid sequestration of ~~microbial~~some archaeal lipids into kerogen ~~must have occurred~~ while hydrothermal alteration was active. We posit that such early sequestration may enhance the ~~survival~~resistance of molecular biosignatures ~~during~~against *in-situ* hydrothermal (and post-depositional) alteration ~~through deep time~~. Furthermore, the co-occurrence of organic matter with different thermal maturities in the Lake Magadi cherts suggests that similar findings in Archean hydrothermal deposits could partly reflect original environmental conditions, and not exclusively post-depositional overprint or contamination. Our results support the view that kerogen in Archean hydrothermal cherts may contain important information on early life. Our study also highlights the suitability of Lake Magadi as an analog system for hydrothermal chert environments on the Archean Earth.

## 30 1 Introduction

Organic matter trapped in Archean cherts is of utmost relevance for the reconstruction of earliest microbial processes on Earth, but its origin is only poorly constrained. Diagenesis and metamorphic processes have been obliterating the original organic matter over billions of years and complicate its interpretation. Many of the Archean cherts are associated with hydrothermal settings (e.g., [including shallow marine and terrestrial environments](#) (e.g., Brasier et al., 2002; Djokic et al., 2017; Duda et al., 2016, 2018; Hickman-Lewis et al., 2018)). In such environments, organic compounds may rapidly decompose due to elevated temperature and pressure conditions (Hawkes et al., 2015, 2016; Rossel et al., 2017) and may also be redistributed via hydrothermal cycling in the form of bitumen (e.g., Weston and Woolhouse, 1987; Clifton et al., 1990; Leif and Simoneit, 1995) or kerogen (Duda et al., 2018). The interpretation of organic signatures in Archean hydrothermal cherts therefore requires detailed knowledge on the preservation, alteration, and distribution pathways of organic matter in such environments. Some of these aspects can be studied in modern analogs.

Archean cherts generally originate from chemical precipitation or replacement processes of silica rather than biogenic precipitation by silicifying organisms (e.g., Sugitani et al., 2002; van den Boorn et al., 2007). Siliceous sediments associated with chemical precipitation are rare on the modern Earth, but can be found in some hot spring or shallow lacustrine environments. Important sites include the Taupo Volcanic Zone (New Zealand; Campbell et al., 2003), the Geysir hot spring area (Iceland; Jones et al., 2007; Jones and Renaut, 2010), the El Tatio geothermal field (Chile; Jones and Renaut, 1997; Nicolau et al., 2014) and the East African Rift system (Kenya; Renault et al., 2002). Among the latter, the alkaline chert environment of Lake Magadi is of particular interest, as it represents an analog for Archean hydrothermal chert environments (Eugster and Jones, 1968; Pirajno and Van Kranendonk, 2005; Brenna, 2016).

Lake Magadi, the focus of this study, is located in the lowermost depression of the East African Rift Valley (south Kenya; ca. 1°54' S, 36°16' E). The geology of the surrounding hills is dominated by alkali trachyte (1.65 to 0.8 Ma; Baker, 1958, 1986). Cherts occur in three sedimentary units overlaying the trachytes, namely the Oloronga Beds (ca. 0.8 to 0.3 Ma; Fairhead et al., 1972; Behr and Röhrlich, 2000), the Green Beds (*sensu* Behr and Röhrlich 2000; Behr 2002; ca. 40 to 100 ka; Goetz and Hillaire-Marcel, 1992; Williamson et al., 1993) and the High Magadi Beds (9 to 25 ka; Williamson et al., 1993; Tichy and Seegers, 1999). Each of these units represents a different lake stage. Today, trona ( $\text{Na}_3(\text{HCO}_3)(\text{CO}_3)\cdot\text{H}_2\text{O}$ ) is precipitating in large areas of the residual lake (Evaporite Series; Baker, 1958), and Lake Magadi is the type locality for cherts based on the sodium silicate mineral magadiite ( $\text{NaSi}_7\text{O}_{13}(\text{OH})_3\cdot 4(\text{H}_2\text{O})$ ; Eugster, 1967, 1969; Eugster and Jones, 1968; Hay, 1968).

Lake Magadi has strongly been influenced by changes in the local climate ~~and tectonics~~ ([Owen et al., 2019](#)). Today the Magadi basin represents an evaporation pan with a closed hydrological cycle (i.e., no outflow) that is only recharged by ephemeral runoff and hydrothermal springs (ca. 28 to 86 °C at present; Eugster, 1970; Jones et al., 1977). During the Pleistocene, however, the water level has changed several times. The Oloronga Beds (not investigated in this study) were formed in a stratified freshwater lake (Roberts et al., 1993). The Green Beds, in contrast, were deposited in a highly dynamic, alkaline, shallow water environment, probably in periodically flooded hot spring mudflats (Behr and Röhrlich, 2000). Lake levels may then have increased again during deposition of the High Magadi Beds (Behr and Röhrlich, 2000), but the setting remained strongly

evaporitic. However, chemical precipitation of silica gels, the precursor of most cherts at Lake Magadi, was likely induced by hydrothermal processes (Eugster and Jones, 1968), evaporation and microbial activity (Behr and Röhricht, 2000; Behr, 2002). A variety of cherts from Lake Magadi and its surroundings contain microbial structures (Behr and Röhricht, 2000; Behr, 2002; Brenna, 2016). Especially the Green Bed cherts are associated with fingerprints of microbial activity such as stromatolites and silicified cyanobacteria cells (Behr and Röhricht, 2000). Organic matter archived in these cherts potentially encodes important information of geobiological value but has not been characterized so far.

Our study is focused on the origin, alteration and preservation of the organic matter in Pleistocene hydrothermal cherts from Lake Magadi. It is aimed at assessing syndepositional and early diagenetic hydrothermal effects on the organic compounds to support the interpretation of organic matter in early Earth hydrothermal deposits. We essentially consider these ~10–100 ka old cherts as “fossil” and adhere to methods typically applied to ancient (including Archean) organic matter. For our analyses we used several complementary petrographic and organic-geochemical techniques, including (scanning electron) microscopy, Raman spectroscopy, catalytic hydrolysis (HyPy), gas chromatography-mass spectrometry (GC-MS) and gas chromatography-combustion-isotope ratio mass spectrometry (GC-C-IRMS). The combined application of petrographic and geochemical techniques ~~is required to fully~~ opens up an analytical window to understand organic matter characteristics (e.g., appearance on macroscopic and molecular levels, identification of heterogeneities) in context of the depositional environment. Our study is not designed to fully assess the whole organic repertoire of the Magadi cherts, and distinguish between different macromolecular fractions (e.g., biopolymers and kerogen).

## 2 Materials and Methods

### 2.1 Sample material, petrographic and bulk geochemical analyses

Cherts from the Pleistocene High Magadi Beds (LM-1692–1695) and Green Beds (LM-1696–1699) were sampled from different surficial outcrops around the present Lake Magadi (extent area of the Pleistocene Lake Magadi; Röhricht, 1999). A recent siliceous sinter from Great Geysir, Iceland (IC-1700; 64°18'46'' N, 20°18'03'' W) was additionally analyzed as a reference.

Petrographic observation was performed on thin sections using a Zeiss SteREO Discovery.V8 stereomicroscope connected to an AxioCam MRc5 5-megapixel camera (transmitted and reflected light) and with a Leica DMLP microscope coupled to a Kappa Zelos-655C camera (polarized light). Chert fragments (sputtered with Au-Pd, 7.3 nm for 120 s) were furthermore investigated using a LEO 1530 Gemini scanning electron microscope (SEM) coupled with an Oxford INCA X-act energy dispersive X-ray spectrometer (EDX). Contents of organic carbon ( $C_{org}$ ), inorganic carbon ( $C_{inorg}$ ), sulfur and nitrogen were determined with a Hekatech Euro EA elemental analyzer and a Leco RC612 temperature programmable carbon analyzer. Element distributions were analyzed on sample slices using a Bruker M4 Tornado  $\mu$ -XRF scanner equipped with a rhodium target X-ray tube at 50 kV and 200  $\mu$ A. Areas of ca. 50 mm<sup>2</sup> were mapped with scan resolution of 500x300 and using a spot size of 20  $\mu$ m.

## 2.2 Organic-geochemical preparation

All materials used for biomarker preparation were heated to 500 °C (3 hrs) and/or carefully rinsed with acetone. A blank (pre-combusted sea sand) was processed in parallel to track potential laboratory contamination. Outer surfaces (2–5 mm) of the chert samples were removed with a particularly cleaned rock saw, ~~and the~~. The surfaces of the resulting inner blocks were carefully rinsed with dichloromethane (DCM). To keep track of contaminations, interior-versus-exterior experiments were performed (see Table S6 for results). After grinding (Retsch MM 301 pebble mill), inner sample powders (50 g each) were ultrasonically extracted with 100 mL DCM/methanol (MeOH) (2/1, v/v), 100 mL DCM/MeOH (3/1, v/v) and 100 mL DCM (10 min, respectively). The total organic extract (TOE) was then desulfurized with reduced Cu. 10 % of each TOE was transesterified/derivatized with trimethylchlorosilane (TMCS)/MeOH (1/9, v/v; heated at 80 °C for 1 h 30 min ~~at 80 °C~~) and subsequently with *N,O*-bis(trimethylsilyl)trifluoroacetamide (BSTFA)/pyridine (3/2, v/v; heated ~~for 1 h~~ at 40 °C) ~~to convert for 1 h~~, converting carboxyl groups into methyl esters, and hydroxyl groups into trimethylsilyl ethers. Another 50 % of each TOE was separated via column chromatography into a hydrocarbon (F1), alcohol/ketone (F2; including free lipids) and a polar fraction (F3). In brief, 7 g silica gel 60 were filled into a glass column (1.5 cm internal diameter), plugged with pre-extracted cotton wool and sand. The dried TOE was vapor-deposited onto ca. 0.5 g silica gel 60 and added to the column. F1 was eluted with 20 mL *n*-hexane/DCM (8/2, v/v), F2 with 30 mL DCM/ethyl acetate (9/1, v/v) and F3 with 100 mL DCM/MeOH (1/1, v/v) and 100 mL MeOH. F2 and F3 were transesterified/derivatized with TMCS/MeOH (1/9, v/v; heated at 80 °C for 1 h 30 min ~~at 80 °C~~) and with BSTFA/pyridine (3/2, v/v; heated ~~for 1 h~~ at 40 °C for 1 h).

The extraction residues were decalcified with HCl (37 %, 1 d, 20°C) and desilicified with HF (48 %, 7 d, 20°C). The remaining kerogens (i.e., the non-extractable portion of organic matter; Durand, 1980; potentially including insoluble high molecular weight biopolymers) from the Magadi cherts were used for catalytic hydrolysis (HyPy; Sec. 2.3; LM-1692–1693, LM-1695, LM-1697–1698) and Raman spectroscopy (Sec. 2.6; LM-1692–1699). No kerogen could be isolated from the reference sample IC-1700: (Great Geysir, Iceland).

## 2.3 Catalytic hydrolysis (HyPy)

HyPy is an open-system pyrolysis technique for studying the molecular kerogen composition (Love et al., 1995). It involves the gentle release of kerogen-bound compounds through progressive heating under a high-pressure hydrogen atmosphere (150 bar) and in the presence of a sulfided molybdenum catalyst (ammonium dioxodithiomolybdate). HyPy has been demonstrated to be very sensitive and leaving to leave the organic stereochemistry of released compounds largely intact (e.g., Love et al., 1995, 1997; Bishop et al., 1998; Meredith et al., 2014).

Our experiments were conducted with a HyPy device from Strata Technology Ltd. (Nottingham, UK), following existing protocols (e.g., Love et al., 1995; Brocks et al., 2003b; Marshall et al., 2007; Duda et al., 2018). In brief, between 1–10 mg of pre-extracted kerogen (3x ultrasonically extracted in DCM/MeOH (3/1, v/v)) was loaded with 10 wt.% ~~of the~~ sulfide molybdenum catalyst and then pyrolyzed under a constant hydrogen flow of 6 L min<sup>-1</sup>. HyPy was conducted following a two-

step approach. The first step involved heating of the kerogens from ambient temperature to 250 °C (at 300 °C min<sup>-1</sup>) and then to 330 °C (at 8 °C min<sup>-1</sup>, held for 10 min). During this step, residual bitumens and compounds bound via unstable covalent bonds were released. In a second step, the remaining kerogens were heated from ambient temperature to 520 °C (at 8 °C min<sup>-1</sup>), releasing solely covalently bound molecules. Pyrolysates from all steps obtained at each step were separately collected in a silica gel trap cooled with dry ice (Meredith et al., 2004) and subsequently analyzed via GC-MS (Sec. 2.4) and GC-C-IRMS (Sec. 2.5). Blanks were run regularly to ensure constant experimental conditions and track potential contamination.

#### 2.4 Gas chromatography-mass spectrometry (GC-MS)

Molecular fractions were analyzed using a Thermo Trace 1310 gas chromatograph (GC) coupled to a Thermo TSQ Quantum Ultra triple quadrupole mass spectrometer (MS). The GC was equipped with a fused silica capillary column (Phenomenex Zebtron ZB-5MS, 30 m length, 250 µm internal diameter, 0.25 µm film thickness). Samples were injected with a Thermo TriPlus RSH autosampler into a splitless injector and transferred to the GC column at 320 °C. The GC oven was heated under a constant He flow (1.5 mL min<sup>-1</sup>) from 80 °C (held for 1 min) to 325 °C at 5 °C min<sup>-1</sup> (held for 30 min). The MS source operated in electron ionization mode at 70 eV and 240 °C. Organic compounds were analyzed in full scan mode (scan range 50–850 amu) and identified by comparison with published retention times and mass spectra.

#### 2.5 Gas chromatography-combustion-isotope ratio mass spectrometry (GC-C-IRMS)

Compound-specific stable carbon isotope ratios ( $\delta^{13}\text{C}_{\text{V-PDB}}$ ) were measured using a Thermo Scientific Trace GC coupled to a Delta Plus isotope ratio mass spectrometer (IRMS) via a combustion reactor (C). The GC was equipped with two serially linked silica capillary columns (Agilent DB-5 and DB-1, each with 30 m length, 250 µm internal diameter, 0.25 µm film thickness). The combustion reactor contained CuO, Ni and Pt, and was operated at 940 °C. Fractions were injected into a splitless injector and transferred to the GC column at 290 °C. The carrier gas was He with a flow rate of 1.2 mL min<sup>-1</sup>. The temperature program started at 80 °C, followed by heating to 325 °C at 5 °C min<sup>-1</sup> (held for 60 min). Laboratory standards were analyzed to control the reproducibility of measuring conditions and CO<sub>2</sub> gas of known isotopic composition was used for calibration.  $\delta^{13}\text{C}$  of the MeOH used for derivatization (methyl ~~esters~~esters) and androstanol (underivatized, as well as TMS derivative) were measured to track isotopic changes through derivatization. The  $\delta^{13}\text{C}$  values of derivatized compounds were then corrected according to Goñi and Eglinton (1996).

#### 2.6 Raman spectroscopy

Raman spectroscopy was conducted on sample slices (thickness ca. 1 cm) and isolated kerogen flakes (see Sec. 2.2). At least 10 measurements were conducted per sample in order to evaluate internal variation and identify potential outliers. The measurements were performed with a WITEC alpha300 instrument. Spectra (scan range 100–4000 rel. cm<sup>-1</sup>) were generated with a frequency-doubled continuous-wave Nd-YAG laser (532 nm, beam intensity of ca. 1 mW) over 10 s integration time by focusing through a 50x optical power objective. These settings (laser power and integration time) were found to cause only

minor degradation of the organic matter to be characterized, and still allowed for acquisition of spectra with sufficient signal-to-noise ratio for meaningful analysis. The reflected beam was dispersed by a 600 L mm<sup>-1</sup> grating on its way into the detector (CCD, 248 pixels). The diameter of each measurement spot was ca. 0.7 μm. Calibration of the instrument (including stability over time) was routinely controlled by pure mineral phases (quartz, calcite, gypsum, beryl). The WITEC Control and Project FOUR 4.1 software was used to record and process all spectral data (smoothing, baseline correction, fitting). Choosing an appropriate Raman fitting method for organic carbon is not trivial as the established methods refer to specific temperature windows. In this study we applied a 6-Voigt-functions fit (after Schito et al., 2017) for low-temperature organic carbon and a 4-Voigt-functions fit (Beysac et al., 2002; R<sup>2</sup> values for each fitting are listed in Table S5) for high-temperature organic carbon. Band nomenclature for the low-temperature organic carbon follows Rebelo et al. (2016), while the high-temperature organic carbon bands are named after Beysac et al. (2002). Peak temperatures (T<sub>max</sub>; averaged over all valid measurements on each sample) were inferred from (i) the vitrinite reflectance R<sub>0</sub> that in sum was calculated from the Raman band ratio RA2 for low-thermal-maturity spectra (RA2=(S+D1+D)/(Dr+G1+G); Schito et al., 2017; Barker and Pavlewicz, 1994) and (ii) the Raman band ratio R2 for high-thermal-maturity spectra (R2=D1/(G+D1+D2); Beysac et al., 2002).

### 3 Results

#### 15 3.1 Petrography, bulk-geochemistry and Raman spectroscopy

Most of the Lake Magadi cherts studied reveal a dense silica matrix, except LM-1692 and LM-1693 which show microscopic pores of <50 μm (Fig. 1a, d). The cherts exhibit brecciated (Fig. 1f), cloudy (Fig. 1g), and laminated (Fig. 1i–k) textures. Most of the textures resemble microbial mat fabrics and can contain distinct silicified microbial cells and filaments (Fig. 1e).

The samples show C<sub>org</sub> values between 0.01 and 0.34 wt.% and CaCO<sub>3</sub>-contents of 0.05 to 4.47 wt% (Table 1). Total nitrogen (N) and sulfur (S) contents are generally low (<0.02–0.05 wt.%, respectively; Table 1).

The organic matter occurs either layered (up to 0.5 mm; Fig. 1a, h), or finely dispersed in the form of small clots in the chert matrix (<20 μm; Fig. 1b–c). In ~~some samples~~ LM-1694–1696, organic matter is also associated with carbonate aggregates (Fig. 1m–q) and ~~sulfur enrichments~~ (sulfates (probably gypsum; Fig. 1q)). The carbonate aggregates are up to 1 mm in size and partly have a rhombic shape (e.g., in LM-1696: Fig. 1m–q).

25 Raman spectra of isolated kerogen particles show a broad D-band centered at ca. 1354 cm<sup>-1</sup> and a G-band at ca. 1597 cm<sup>-1</sup> (Fig. 2). Vitrinite reflectance R<sub>0</sub> (calculated from RA2; Schito et al., 2017) generally ranges between 0.32 and 0.72 %, corresponding to maximum temperatures in the range of 40–110 °C (Table 2). At such low temperatures the Raman signal does not only encode thermal maturation, but likely also bears the signature of the specific type of biologic precursor (Qu et al., 2015). This implies that the above derived temperature range (40–110°C) must be taken with caution and is mostly useful  
30 in the context of other (supporting) data sets.



Sample LM-1697 exhibited a second kerogen population with D- and G-bands centered at 1357 and 1577  $\text{cm}^{-1}$ , respectively (Fig. 2), corresponding to a maximum temperature of ca. 440 °C (high-temperature, graphitic; Table 2, Fig. 2c; Beyssac et al., 2002).

## 3.2 Bitumen

5 Figure 3 shows GC-MS chromatograms from bitumens of High Magadi Bed cherts (Fig. 3a–e), ~~d~~, and Green Bed cherts (Fig. ~~3d, e~~, and ~~3e, f~~). The bitumen of a ~~recent~~ modern siliceous sinter from Great Geysir ~~in~~ (Iceland) is provided in the supplement (Fig. ~~3fS1i–j~~). The most noticeable compound classes in all samples are *n*-alkanes, *n*-alkanoic acids and *n*-alkan-1-ols (in decreasing abundance), plus glycerol diethers (Fig. 3a–e). GC-amenable aromatic compounds are low in abundance, but some polycyclic aromatic hydrocarbons (PAHs) were identified in all samples. One sample showed a pronounced unresolved  
10 complex mixture (UCM; LM-1697; Fig. 3d).

### 3.2.1 Functionalized lipids

#### *Fatty acids (alkanoic and alkenoic acids)*

*n*-Alkanoic acids typically range from  $\text{C}_{12}$  to  $\text{C}_{32}$  (Fig. 4a) and exhibit a clear even-over-odd-predominance, as expressed by OEP values  $\ll 1$  (odd-to-even-predominance; Scalan and Smith, 1970; Table 3). The most abundant fatty acids are *n*-  
15 hexadecanoic acid ( $\text{C}_{16:0}$ ) and *n*-octadecanoic acid ( $\text{C}_{18:0}$ ). *n*-Alkenoic acids occur at low abundance and include  $\text{C}_{16:1}$ ,  $\text{C}_{18:1}$  (tentatively identified as  $\omega 9\text{c}/9\text{t}$ ) and  $\text{C}_{18:2}$ . Terminally methylated (*iso(i)*- and *anteiso(ai)*-) alkenoic acids are also present, including *i*- $\text{C}_{15:0}$  and *i*- $\text{C}_{17:0}$  (LM-1692–1694) plus *ai*- $\text{C}_{14:0-17:0}$  and *ai*- $\text{C}_{24:0-25:0}$  (LM-1692–1694). IC-1700 additionally shows *i*- $\text{C}_{16:0}$ . Phytanic acid occurs in LM-1692–1695. The  $\delta^{13}\text{C}$  signatures of the short- ( $\text{C}_{12-18}$ ) and long-chain ( $\text{C}_{24-28}$ ) alkenoic acids range from  $-22.4$  to  $-29.6$  ‰ in the Magadi cherts, and from  $-25.2$  to  $-32.5$  ‰ in IC-1700 (Table 4). The values do not differ  
20 much between short- and long-chain homologues ( $\Delta < 2.4$  ‰), except for IC-1700 ( $\Delta = 7.3$  ‰).

#### *Alkanols and alkanones*

*n*-Alkan-1-ols typically range from  $\text{C}_{12}$  to  $\text{C}_{32}$  (Fig. 4b). These compounds show a strong even-over-odd-predominance in all samples (OEP17 between 0.1 and 0.2, OEP29 between  $< 0.1$  and 0.3; Table 3). Hexadecan-1-ol ( $\text{C}_{16}\text{-OH}$ ) and octadecan-1-ol ( $\text{C}_{18}\text{-OH}$ ) show highest abundances. In addition to the *n*-homologues, odd-numbered  $\text{C}_{15-25}$  *ai*-alkan-1-ols are present (see Fig.  
25 4b). Short-chain ( $\text{C}_{12}$  to  $\text{C}_{18}$ ) *n*-alkan-1-ols from the Magadi cherts reveal mean  $\delta^{13}\text{C}$  values between  $-29.4$  and  $-35.9$  ‰ ( $-27.7$  ‰ in IC-1700). With increasing chain length, the homologues get more enriched in  $^{13}\text{C}$  ( $\text{C}_{24-28}$ ,  $\Delta$  up to  $15.7$  ‰ in LM-1694; Table 4).

*n*-Alkan-2-ols occur in diverse ranges (e.g.,  $\text{C}_{15}$  to  $\text{C}_{31}$  in LM-1698; Fig. 5b). The distributions are unimodal (maximum at  $\text{C}_{20}$ ) in LM-1692–1696, or bimodal (maxima at  $\text{C}_{20}$  and  $\text{C}_{31}$ ) in LM-1697–1699. In all samples, medium-chain *n*-alkan-2-ols ( $\text{C}_{18-}$   
30  $_{24}$ ) have no chain-length-predominance (OEP21 between 0.8 and 1.1; Table 3), while long-chain homologues ( $\text{C}_{25-31}$ ) exhibit a clear odd-over-even-predominance (OEP29 between 1.9 and 5.9). IC-1700 shows a bimodal distribution with maxima at  $\text{C}_{14}$  (minor) and  $\text{C}_{20}$ , and no chain-length-predominance.



*n*-Alkan-2-ones typically appear in the range of C<sub>15</sub> to C<sub>31</sub>, but are virtually absent in LM-1699. Some samples show a unimodal distribution with no chain-length-preference (Fig. 5; Table 3), while most reveal a slight odd-over-even-predominance (OEP21 between 1.3 and 2.1). The isoprenoid ketone 6,10,14-trimethyl pentadecan-2-one additionally occurs in every sample and is the most abundant alkan-2-one in LM-1692–1695 and IC-1700. Furthermore, *i*- and *ai*-alkan-2-ones appear in LM-1698 (C<sub>18</sub> to C<sub>23</sub>; Fig. 5c).

#### Other lipids

Glycerol monoethers (1-*O*-alkylglycerols) occur in all samples from Lake Magadi. Their highest diversity is observed in LM-1692–1694, including methyl-branched (*i*-C<sub>16:0</sub>, 10Me-C<sub>16:0</sub>, *i*-C<sub>17:0</sub>, *ai*-C<sub>17:0</sub>, Me-C<sub>17:0</sub>, *i*-C<sub>18:0</sub>), and straight (C<sub>15–18</sub>) alkyl chains (see Fig. 4c). The most prominent monoether is 1-*O*-(10-methyl)-hexadecylglycerol (10Me-C<sub>16:0</sub>). Furthermore, two glycerol diethers, namely di-*O*-phythanylglycerol (archaeol; “A”, Fig. 3a–e*d*) and *O*-phytanyl-*O*-sesterterpanylglycerol (extended archaeol; “ExA”, Fig. 3a–e*d*) appear in LM-1692–1696 and LM-1699. Mono- and diethers show δ<sup>13</sup>C values between –10.9 and –22.2 ‰ (Table 4; Fig. 3a–e*d*), with highest values in LM-1694 (–10.9 and –12.2 ‰, respectively).

Additionally, functionalized sesqui- and diterpenoids are always present and traces of C<sub>31</sub> or C<sub>32</sub> hopanoic acids are found in some samples. LM-1693 and LM-1695–1699 furthermore contain abundant tetrahymanol (δ<sup>13</sup>C between –24.1 and –33.3 ‰). Sterols, particularly cholesterol and sitosterol, appear in small amounts in most samples. Note that high molecular weight lipids such as glycerol dialkyl glycerol tetraethers (GDGTs) or their lipid cores were not assessed using our GC-based analytical setup.

### 3.2.2 Aliphatic hydrocarbons

*n*-Alkanes range from *n*-C<sub>15</sub> to *n*-C<sub>33</sub> and primarily show a unimodal distribution (maximum around *n*-C<sub>21</sub> and *n*-C<sub>22</sub>; Figs. 3, 5a, S1) and no carbon chain-length-preference up to *n*-C<sub>25</sub> (OEP21 between 1.0 and 1.2; Table 3). However, an odd-over-even-preference is always observed for greater chain-lengths (OEP31 between 1.8 and 7.0; Table 3). Furthermore, *i*- and *ai*-alkanes are present (C<sub>18</sub> to C<sub>25</sub>; Fig. 5a), following the distribution trend of the corresponding *n*-alkanes. Pristane (Pr) and phytane (Ph) are visible in all samples except LM-1699 (only Ph; Fig. S1). Pr/Ph ratios are below 0.37, while Ph/*n*-C<sub>18</sub> ratios range between 0.26 and 0.49 (Table 2). LM-1696 furthermore reveals 6-methylheptadecane (6Me-C<sub>17</sub>; Fig. S1e). Medium-chain *n*-alkanes (C<sub>17–24</sub>) show mean δ<sup>13</sup>C values between –29.7 and –33.3 ‰ in the Lake Magadi cherts (–35.7 ‰ in IC-1700), while δ<sup>13</sup>C values of higher homologues (>C<sub>24</sub>) increase up to –26.2 ‰ (Δ between 1.9 and 7.2 ‰; Table 4).

The samples furthermore contain traces of 17α,21β-hopanes (S+R isomers). The S/S+R isomer ratios of the C<sub>31</sub> pseudohomologues range between 0.49 and 0.61 (Table 2). Steranes are below detection limit.

### 3.2.3 Polycyclic aromatic hydrocarbons (PAHs)

All samples contain low amounts of (monomethyl-) phenanthrenes, while anthracene is only observed in IC-1700. The methylphenanthrene indices (MPI-1, after Radke and Welte, 1983) vary between 0.48 and 1.02, resulting in calculated vitrinite reflectances (R<sub>c</sub>, after Boreham et al., 1988) between 0.56 and 0.94 % (Table 2). Traces of dimethylphenanthrenes are detected

in LM-1692–1698. Other PAHs observed are fluoranthene (Flu) and pyrene (Py) with Flu/(Flu+Py) ratios between 0.48 and 0.96 (Table 2).

### 3.3 Kerogen (high temperature HyPy step, up to 520 °C)

5 Results from the low-temperature pyrolysates (up to 330 °C) were excluded from interpretation, as this fraction may be biased by residual low molecular weight compounds that are adsorbed, but not covalently bound to kerogen (see 2.3). The high temperature HyPy pyrolysates (up to 520 °C; see Sec. 2.3) can be divided in two groups according to their compositions. LM-1692 and LM-1693 show a strong aromatic character (aliphatics/aromatics of 0.4 and 0.2, respectively), which is not observed in LM-~~1694~~–1695 and LM-1697–1698 (aliphatic/aromatic of 1.1, 2.7, 1.0 and 1.5, respectively). All pyrolyzed kerogens reveal varying distributions of *n*-alkanes (Fig. 6; see below).

#### 10 3.3.1 Aliphatic hydrocarbons

Kerogen-bound *n*-alkanes exhibit maxima around *n*-C<sub>18</sub> (LM-1693, LM-1695, LM-1698), *n*-C<sub>21</sub> (LM-1692–~~1693~~1694, 1697) and *n*-C<sub>32</sub> (LM-1695, LM-1697–1698), and range from *n*-C<sub>18</sub> to *n*-C<sub>36</sub> (LM-1692–1693), *n*-C<sub>18</sub> to *n*-C<sub>43</sub> (LM-1694), *n*-C<sub>14</sub> to *n*-C<sub>44</sub> (LM-1695) or *n*-C<sub>16</sub> to *n*-C<sub>46</sub> (LM-1697–1698). No carbon chain-length-preference is visible up to *n*-C<sub>26</sub> (OEP21 always 1.0, except for LM-~~1694~~–1695; Table 3; Fig. ~~6e~~6), but a slight even-over-odd-preference is observed for longer chains (OEP31 15 between 0.7 and 0.9; Table 3). Moreover, all pyrolysates contain few *i*- and *ai*-alkanes (Fig. 6). Mean δ<sup>13</sup>C values of medium-chain *n*-alkane moieties (C<sub>17–24</sub>) range from –23.5 to –34.2 ‰, whereas long-chain *n*-alkanes (C<sub>25–40</sub>) reveal values between –21.9 and –30.2 ‰ (Δ between 1.3 and 7.1 ‰; Table 4).

The regular acyclic isoprenoids phytane (Ph) and 2,6,10,14,18-pentamethylcosane (PMI<sub>reg</sub>; identified via mass spectrum; Fig. S2; Risatti et al., 1984; Greenwood and Summons, 2003) appear in LM-1692–~~1693~~1694 and LM-1695 (Ph/*n*-C<sub>18</sub> between 0.49 20 and 1.89). The regular acyclic isoprenoids Farnesane (Far), norpristane (Nor) and pristane (Pr) are only present in LM-1695 (Pr/Ph = 0.24; Table 2), and biphytane occurs in LM-1693 and LM-1695 (Fig. 6b–~~e~~, d). The detection of phytane and PMI<sub>reg</sub> in the kerogens of LM-1692–~~1693~~1694 and LM-1695 coincides with the appearance of archaeol and extended archaeol in the corresponding bitumens (Fig. 3a–~~ed~~). δ<sup>13</sup>C values of PMI<sub>reg</sub> vary between ~~–22.0~~–14.5 and –24.6 ‰, while phytane exhibits δ<sup>13</sup>C values between –25.1 and –28.5 ‰ (Table 4; Fig. 6a–~~ed~~).

#### 25 3.3.2 PAHs

All kerogen pyrolysates except LM-1694 contain (mono- and dimethylated) phenanthrenes, anthracene, plus various 4- and 5-ring PAHs. MPI-1 ranges from 0.89 to 1.69, corresponding to R<sub>c</sub> values between 0.85 and 1.41 % (Table 2). Fluoranthene (Flu) and pyrene (Py) with Flu/(Flu+Py) ratios between 0.23 and 0.44 are also present. Methyl naphthalenes only occur in LM-1693 and LM-1695, while di- and trimethyl naphthalenes appear in LM-1693, LM-1695 and LM-1698.

## 4 Discussion

### 4.1 Thermal maturity and syngeneity of the organic matter

The studied Lake Magadi cherts are of Pleistocene age and have not been buried. This is in good accordance with several molecular characteristics of the bitumens that suggest an immature nature of the organic matter. These features include the OEP29 of *n*-alkanoic acids (0.3–0.5) and *n*-alkan-1-ols (<0.1–0.3), the OEP31 of *n*-alkanes (2.3–7.0), and the presence of intact functionalized lipids (e.g., archaeol, extended archaeol and monoethers). On the other hand, the OEP21 of medium-chain *n*-alkanes (1.0–1.2), Ph/*n*-C<sub>18</sub> ratios ( $\leq 0.49$ ), MPI-1 ratios (0.48–1.02, mean 0.75), R<sub>c</sub> values (0.56–0.94 %, mean 0.74 %) and C<sub>31</sub> S/(S+R) ratios (0.49–0.61, mean 0.56) are in line with early to peak oil window maturity (see ten Haven et al., 1987; Killops and Killops, 2005; Peters et al., 2005, 2005b; Table 2). Hence, the bitumen preserved in the Magadi cherts consists of ~~at least two fractions~~, a “fresh” immature portion co-occurring with a thermally mature component.

A similar maturity offset is also reflected in bulk- and molecular kerogen characteristics. A low thermal maturity is for instance indicated by low Raman-derived T<sub>max</sub>-signatures in some samples (LM-1697 and LM-1698; ca. 40 and 50 °C; Fig. 2c; Table 2), and a slight even-over-odd preference of long-chain *n*-alkanes in all kerogen pyrolysates (OEP31 between 0.7 and 0.9; Table 3). At the same time, MPI-1 ratios ( $\leq 1.69$ ), R<sub>c</sub> values ( $\leq 1.41$  %), the OEP21 of medium-chain *n*-alkanes (1.0 = no preference) indicate an elevated thermal maturity, which is in good accordance with Raman temperatures from the High Magadi Bed cherts and LM-1696 (T<sub>max</sub> of up to 110 °C; Table 2). Some of the Raman spectra from the LM-1697 kerogen even evidence the presence of a high-temperature graphitic component (i.e., T<sub>max</sub> ~440 °C; Fig. 2d, Table 2).

Such offsets between different thermal maturity parameters are typically related to an emplacement of organic material from another source (e.g., modern endoliths; e.g., Golubic et al., 1981; Hallmann et al., 2015). Most of the Lake Magadi cherts studied reveal a dense silica matrix, but a few samples (LM-1692, LM-1693) indeed show small pores that would allow for such emplacements. However, a recent emplacement is unlikely for the following reasons:

- (i) The analyzed samples did not show any viable microbial colonization (e.g., biofilms, or endolith borings).
- (ii) No carbonaceous microbial remains were discovered via SEM coupled to EDX and all detected microfossils are silicified (see Fig. 1e).
- (iii) ~~Kerogens contain fingerprints of~~ High-temperature HyPy products of kerogens matched up with functionalized moieties in their corresponding bitumens (e.g., C<sub>20</sub> and C<sub>25</sub> isoprenoids appear only in kerogens that show archaeol and extended archaeol in their corresponding bitumens; Figs. 3 and 6).
- (iv) The  $\delta^{13}\text{C}$  values of long-chain *n*-alkanes from the Green Bed chert kerogens ~~matches~~ were consistent with the  $\delta^{13}\text{C}$  values of long-chain *n*-alkanoic acids from bitumens ( $\Delta \leq 3$  ‰), ~~supporting their taphonomic relation.~~ ‰).
- (v) Interior-versus-exterior experiments on LM-1692 and LM-1695 revealed similar concentrations for medium-chain *n*-alkanes and glycerol diethers in outer and inner sample parts (*n*-C<sub>21</sub> and *n*-C<sub>22</sub> are even slightly more abundant in the interior; Table S6).

Consequently, both, the rather immature and the thermally altered organic matter can be considered syngenetic to the Pleistocene cherts.

## 4.2 Geobiology of the Lake Magadi during chert deposition

### 4.2.1 Prokaryotes

5 Archaeol and extended archaeol appear in all High Magadi Bed and two Green Bed chert bitumens (LM-1696 and LM-1699), and their molecular fossils are important contributors to the corresponding kerogens. While archaeol is a common constituent of Euryarchaeal lipids (e.g., Koga, 1993; Pancost et al., 2011; Dawson et al., 2012; Villanueva et al., 2014), extended archaeol is restricted to alkaliphilic and non-alkaliphilic haloarchaea (e.g., De Rosa, 1982; Teixidor et al., 1993; Dawson et al., 2012) and, in traces, to some methanogens (e.g., Grant et al., 1985; Becker et al., 2016). Archaeol and extended archaeol were also  
10 found in various halophilic archaea from recent Lake Magadi (e.g., *Natronobacterium pharaonis*, *Natronobacterium magadii*, *Natronobacterium gregoryi*, *Natronococcus occultus*; Tindall et al., 1985) and haloarchaea are abundant in recent Lake Magadi hot spring communities (Kambura et al., 2016). It is therefore likely that these halophiles have contributed the archaeols to the Lake Magadi cherts. The variable  $\delta^{13}\text{C}$  values of archaeol and extended archaeol in the analyzed samples (Table 4), however, may indicate contributions from organisms with different  $\text{CO}_2$ -fixation pathways.

15 Cyanobacterial contribution to primary production is directly evidenced by 6Me- $\text{C}_{17}$  in LM-1696 (Fig. S1e), which is typically produced by the nitrogen-fixing thermophile *Fischerella* (Coates et al., 2014). Bacterial activity in the chert environment is also indicated by the  $\text{C}_{32}$ -hopanoic acid in LM-1693 and LM-1694, an early degradation product of bacteriohopanepolyols (Farrimond et al., 2002). Further molecular traits of bacteria are  $\text{C}_{15}$  and  $\text{C}_{17}$  *i-/ai*-fatty acids (cf., Parkes and Taylor, 1983) and monounsaturated and saturated  $\text{C}_{16}$  and  $\text{C}_{18}$  fatty acids, although the latter can also derive from algae (e.g., Taipale et al., 2013,  
20 2016) or higher plant polymers (Kolattukudy, 1980).

The monoethers found in the High Magadi Bed chert bitumens occur in various bacteria, and are particularly prevalent in sulfate reducers (e.g., Yang et al., 2015; Vinçon-Laugier et al., 2016 and references therein). Given the hydrothermally influenced setting, the broad variety of these compounds in the Magadi cherts ( $\text{C}_{15}$  to  $\text{C}_{19}$  moieties) may be attributed to thermophiles. Indeed, *i*- $\text{C}_{16:0}$ ,  $\text{C}_{16:0}$  and *ai*- $\text{C}_{17:0}$  monoethers are dominant in Thermodesulfobacteria (Langworthy et al., 1983;  
25 Hamilton-Brehm et al., 2013), while  $\text{C}_{18:1}$  and  $\text{C}_{18:0}$  monoethers were reported from Aquificales (Huber et al., 1992; Jahnke et al., 2001). The most abundant monoether in the Magadi cherts, 10Me- $\text{C}_{16:0}$ , was recently detected in mesophilic heterotrophic Desulfobacterales, i.e. sulfate-reducing bacteria (Vinçon-Laugier et al., 2016).

All archaeal lipids in bitumens show an enrichment in  $^{13}\text{C}$  compared to the fatty acids ( $\Delta$  up to +14.6 ‰ between archaeol and short-chain fatty acids in LM-1694). Such heavy values are known from  $\text{CO}_2$ -limited hypersaline environments (e.g.,  
30 Schidlowski et al., 1984; Schouten et al., 2001) and may be amplified by high bioproductivity (e.g., deDes Marais et al., 1989; Schidlowski et al., 1994). Halobacteria, however, are heterotrophs and use an organic rather than an inorganic carbon source (e.g., Tindall, 1984; Dawson et al., 2012). If so, these organisms must have fed on an isotopically heavy, thus autochthonous

pool of primary produced organic matter (cf., Birgel et al. 2014). This is also in good agreement with the fact that all monoethers are enriched in  $^{13}\text{C}$  compared to other lipids (Table 4) and underpins that the cherts formed in an evaporitic environment.

#### 4.2.2 Eukaryotes

5 Tetrahymanol is typically produced by ciliates (Mallory et al., 1963; Harvey and McManus et al., 1991), but may also originate from few bacteria (e.g., Kleemann et al., 1990; Banta et al., 2015), ferns (Zander et al., 1969) and fungi (Kemp et al., 1984). It is furthermore associated with alkaline environments (e.g., ten Haven et al., 1989; Thiel et al., 1997), which is well in line with the evaporative setting of Lake Magadi.

The presence of only small amounts of typical algal sterols (cholesterol and sitosterol; cf., Taipale et al., 2016) in the Lake  
10 Magadi cherts indicates minor contributions from these primary producers. Long-chain alkanolic acids and alkan-1-ols with an OEP29 of  $\ll 1$  in bitumens as well as the corresponding *n*-alkanes with an OEP31 of 0.7–0.9 in kerogens (Table 3) indicate inputs from higher land plants (Eglinton and Hamilton, 1967). Further biomarker evidence for plant input is provided by functionalized sesqui- and diterpenoids (e.g., Otto and Simoneit, 2002; Hautevelle et al., 2006; Fig. 3a). However, the overall predominance of prokaryotic biomarkers (Sec. 4.4.2) and the petrographic observations of silicified microbial mat remains and  
15 microbial cells (Sec. 3.1; Fig. 1e–h) suggest a minor importance of eukaryotes in the lake ecosystem.

The  $\delta^{13}\text{C}$  signals of long-chain *n*-alkanoic acids from Lake Magadi (between  $-22.4$  and  $-29.6$  ‰; Table 4) are in the range of the short-chain homologues ( $\Delta$  between  $+2.4$  and  $-2.6$  ‰), while the Icelandic reference sample ( $-32.5$  ‰) shows a pronounced  $\delta^{13}\text{C}$  depletion ( $\Delta +7.3$  ‰). All  $\delta^{13}\text{C}$  values are in the range of  $\text{C}_3$  plants (Schidlowski, 2001). The slightly heavier  $\delta^{13}\text{C}$  values of compounds in the Magadi cherts may indicate additional contributions by  $\text{C}_4$  plants (cf., Chikaraishi et al., 2004;  
20 Schidlowski, 2001) which are common in latitudes of the Magadi area (Still et al., 2003). Unlike the *n*-alkanoic acids, long-chain *n*-alkanes in LM-1695–1697 bitumens reveal more depleted  $\delta^{13}\text{C}$  values around  $-31$  ‰, pointing at a different origin (unknown).

#### 4.2.3 Hydrothermal impact on organic matter

In all Lake Magadi cherts a narrow, bell-shaped pattern of *n*-alkanes with a maximum around *n*- $\text{C}_{21}$  is dominant in the bitumens  
25 (Figs. 3a–e, 5a, S1a–h). This *n*-alkane distribution is also present in the bitumen from the Great Geysir reference sample (IC-1700; Figs. 3f, Fig. S1i–j) and has been frequently reported from other hydrothermal sites (e.g., Simoneit, 1984; Weston and Woolhouse, 1987; Clifton et al., 1990; Simoneit et al., 2009). As the hydrothermal system of the Magadi basin consists of a dilute ground water reservoir, deep brines, and recycled lake brines (Eugster, 1970; Jones et al., 1977), it appears plausible that immature organic compounds from the lake environment have been thermally altered by hydrothermal cycling, resulting,  
30 *inter alia*, in a loss of functional groups (cf., McCollom and Seewald, 2003; Hawkes et al., 2016; Rossel et al., 2017). Consequently, the *n*-alkanes from bitumens might represent stable thermal alteration products of originally functionalized compounds, such as linear fatty acids and *n*-alkanols.

Such hydrothermal processes may also yield compounds through the *in-situ* cracking of macromolecular organic matter from the cherts (e.g., alkanes and hopanes, see Sec. 3.2.2). However, temperatures of hydrothermal waters from present springs at Lake Magadi are not higher than 86 °C (Eugster, 1970; Jones et al., 1977). Furthermore, two kerogens from the Green Bed cherts still show relatively low Raman-derived  $T_{\max}$  values (ca. 40–50 °C; Table 2). *In-situ* maturation near hot springs within the lake may therefore not sufficiently explain the presence of thermally mature organic components in all ~~cherts~~-analyzed cherts.

Alternatively, organic matter from older lake sediments (Oloronga Beds) may have been penetrated by hot fluids, resulting in the formation of hydrothermal petroleum, a process known from other hydrothermal environments (e.g., Clifton et al., 1990; Weston and Woolhouse, 1987; Czochanska et al., 1986; Leif and Simoneit, 1995). This is in good accordance with the early to peak oil window maturity of some bitumen compounds as e.g. indicated by the MPI-1 ratios ( $\leq 1.02$ ) and  $C_{31} S/(S+R)$  ratios ( $\leq 0.61$ ; Peters et al., ~~2005~~2005b; Table 2). Cooling and pressure decline of ascending hydrothermal fluids would have led to decreasing solubility of the compounds entrained, resulting in precipitation and thus, fractionation (cf., Simoneit, 1984; Clifton et al., 1990). Such hydrothermal “geochromatography” (Krooss et al., 1991) may explain the narrow distribution of medium-chain *n*-alkanes present in the chert bitumens. In addition, short-chain alkanes might have been lost to microbial consumption (e.g., Tissot and Welte, 1984; Peters et al., 2005a and references therein). Such biodegradation may also have led to the pronounced UCM in LM-1697 (Fig. 3e). Slight to moderate biodegradation, however, is often accompanied by elevated Ph/ $n$ - $C_{18}$  as compared to non-biodegraded bitumens (Peters et al., 2005b), which is not the case here (0.37 in LM-1697 vs. 0.29–0.49 in other Magadi cherts; Table 2). The lack of short-chain *n*-alkanes in the Magadi chert bitumens (also in LM-1697) therefore likely results from evaporation or hydrothermal “geochromatography”.

Hydrothermal petroleum generation may furthermore be supported by the unimodal distribution patterns of medium-chain *n*-alkan-2-ones and *n*-alkan-2-ols in bitumens, although the exact origin of these compounds is difficult to elucidate. *n*-Alkan-2-ones with similar distributions have previously been reported from hydrothermal oils and may originate from pyrolysis of aliphatic moieties (with *n*-alkan-2-ols as intermediates; Leif and Simoneit, 1995) or pyrolysis of fatty acids with subsequent  $\beta$ -oxidation and decarboxylation (George and Jardin, 1994). Further, both, *n*-alkan-2-ones and *n*-alkan-2-ols were experimentally produced by Fischer-Tropsch-type reactions under hydrothermal conditions (Rushdi and Simoneit, 1999; Mißbach et al., 2018). In addition to these thermally driven reactions, *n*-alkan-2-ones may also derive from microbial oxidation of *n*-alkanes (e.g., Cranwell, 1987; van Bergen et al., 1998), potentially also with *n*-alkan-2-ol intermediates (Allen et al., 1971; Cranwell et al., 1987).

The relatively low abundance of PAHs in the bitumens may indicate low formation temperatures of hydrothermal petroleum (cf., Simoneit, 1984; Simoneit et al., 1987; Clifton et al., 1990). This could be due to a shallow sedimentary source which is well in line with the geological situation at Lake Magadi. The Oloronga Beds (maximal thickness of 45 m; Behr, 2002) are the oldest sediments in the young rift basin (ca. 7 Ma; Baker 1958, 1986; geothermal gradient of ca. 200 °C km<sup>-1</sup>; Wheildon et al., 1994) and were not deeply buried at the time of the Green Bed chert deposition. PAHs are common in dissolved organic matter from hydrothermal fluids (e.g., Konn et al., 2009, 2012, McCollom et al., 2015; Rossel et al., 2017), but may also derive from



wildfires. Incomplete combustion of biomass ~~may~~might be a relevant source particularly in LM-1694 and LM-1699, as Flu/(Flu+Py) ratios of about 0.61 (~~see~~-Table 2) are considered indicative for a wildfire origin (Yunker et al., 2002).

Hydrothermal activity may not only have impacted the bitumens. Kerogen from LM-1697 shows highly mature graphitic particles (Raman-based  $T_{\max}$  of ca. 440°C; Fig. 2; Table 2). These particles may either originate from hydrothermal processes (Luque et al., 2009; van Zuilen et al., 2012), or alternatively from wildfires (Cope and Chaloner, 1980; Schmidt and Noack, 2000, and references therein). As the Flu/(Flu+Py) ratio in the LM-1697 kerogen is substantially lower as expected for a wildfire source (0.23 vs. 0.61; Yunker et al., 2002) and also the bitumen fraction shows no indication of biomass combustion (Flu/(Flu+Py) = 0.79; Table 2), the high temperature particles in LM-1697 most likely do not originate from combustion.

We propose that the graphite was produced at depth through the hydrothermally mediated alteration (cf., Luque et al., 2009) of the surrounding trachyte and/or by mineral-templated growth (cf., van Zuilen et al., 2012) during hydrothermal circulation of bitumen-rich fluids. The hydrothermal fluids may then have transported graphite particles into the lake. Like graphite, thermally altered macromolecular particles from older lake sediments may have also been introduced by hydrothermal fluids which would explain the elevated mean Raman temperatures of LM-1692–1693 and LM-1696 kerogens (Raman-based  $T_{\max}$  of 100–110°C; Table 2), the high MPI-1 (up to 1.69) and  $R_c$  (up to 1.41 %; Table 2) in all kerogens and the strong aromatic character of LM-1692 and 1693 kerogens (see Sec. 3.3).

The occurrence of thermally mature organic components in the studied materials is therefore most likely due to syndepositional hydrothermal processes and reflects an environmental signature.

#### 4.3 Organic signatures from the Magadi cherts: implications for the Archean

~~A fraction of the organic matter preserved in the Magadi cherts may have been introduced by hydrothermal fluids. Such hydrothermally driven redistribution of organic matter has recently been proposed as an important process for kerogen in Archean hydrothermal vein cherts (“hydrothermal pump hypothesis”; Duda et al., 2018). Another similar feature to findings from Archean cherts is the variability of organic matter characteristics on a small spatial scale observed in the Lake Magadi samples (i.e., heterogeneous thermal maturities of organic matter within a given sample; The visual appearance of organic matter in the Pleistocene Lake Magadi cherts (i.e., in clots, layers or carbonate rhombs;–) and its thermal heterogeneity even within given samples is, to some extent, similar to findings from Archean cherts (see Ueno et al., 2004; Allwood et al., 2006; Tice & Lowe, 2006; Glikson et al., 2008; Morag et al., 2016). In case of ancient cherts, such heterogeneities the Archean record, varying organic matter characteristics are generally interpreted as a result of post depositional commonly related to metamorphic processes that significantly post-dated chert formation (e.g., Ueno et al., 2004; Tice & Lowe, 2006; Olcott Marshall et al., 2012; Sforza et al., 2014; Morag et al., 2016) rather than syndepositional hydrothermal activity (e.g., Allwood et al., 2006; Glikson et al., 2008). Our results highlight the possibility). Variations in kerogen maturity in the ca. 3.5 Ga old Apex chert (Pilbara Craton, Western Australia) could, for instance, reflect younger hydrothermal alteration events that were entirely unrelated to the original formation of the host rock (Olcott Marshall et al., 2012; Sforza et al., 2014). Our results demonstrate that organic matter of very different nature and maturity may already be enclosed into hydrothermal chert~~

precipitates *a priori*. ~~Such~~ (i.e., during the initial formation of the deposit, prior to potential metamorphic processes), and that this is largely driven by hydrothermal circulation. A similar syndepositional hydrothermally driven *in-situ* mixing of different organic components ~~should also be considered in the interpretation~~ has been proposed for a variety of Archean chert environments (see Allwood et al., 2006; Glikson et al., 2008; Morag et al., 2016; Duda et al., 2018). ~~Of course, the heterogeneous maturity signals still have to be in accordance with~~ Our results highlight that thermal heterogeneities of Archean organic matter may indeed reflect syndepositional hydrothermal activity rather than post-depositional metamorphism in some cases (if the maturity is not significantly lower than the overall estimated peak metamorphic history temperature of the host rock).

In addition, our kerogen data ~~show~~ indicate that archaeal lipid biomarkers (C<sub>20</sub> and C<sub>25</sub> isoprenoids) are preserved in the macromolecular network (Fig. 6; the occurrence of biphytane in kerogens from LM-1693 and LM-1695, however, may be biased by incomplete removal of GDGTs during extraction). Their presence in the kerogens that show a high thermal overprint (LM-1692–1693; Table 2) implies a rapid incorporation of their parent molecules archaeol and extended archaeol into macromolecular organic matter, while hydrothermal alteration is active. The kerogen matrix can form an effective shield against oxidation, biodegradation and thermal maturation, thus promoting the preservation of bound compounds over geological time. It has been shown that archaeal lipids can be bound rapidly into macromolecular networks in non-hydrothermal marine sediments (Pancost et al., 2008). ~~We cannot completely exclude, however, that some isoprenoids were released from high molecular weight polymers that are not part of the kerogen. Kerogen-like macromolecules can form early during diagenesis, e.g., through sulfurization (Sinninghe Damsté and de Leeuw, 1990; Wakeham et al., 1995). Sulfur is generally limited in the analyzed Magadi cherts and mostly hosted in gypsum. Sulfurization, however, requires reduced sulfur species that may have been available in microscale environments where sulfate reduction was active.~~

The fact that ~~archaeal lipid biomarkers~~ the C<sub>20</sub> and C<sub>25</sub> isoprenoids were yielded during the high temperature HyPy step (up to 520 °C) of the Magadi kerogens evidences that these compounds may survive mild diagenetic influences. In this view, a conservation of kerogen-bound molecular biosignatures into kerogen, before significant metamorphism took place, appears plausible also ~~in~~ for early Archean hydrothermal cherts (see Marshall et al., 2007; Duda et al., 2018) ~~appears plausible~~. All studied organic matter-bearing Archean rocks were generally subjected to significant thermal overprint that may have completely obliterated indigenous molecular biosignatures (cf., French et al., 2015). Whether genuine biomarkers such as isoprenoids can be detected in Archean macromolecules, remains to be seen. Our results, ~~together~~ in context with current findings from Archean hydrothermal systems (Duda et al., 2016, 2018; Djokic et al., 2018), ~~therefore~~ nevertheless underline the enormous potential of hydrothermal cherts as valuable archives for biosignatures of early life on Earth.

## 30 5 Conclusions

The depositional record of Lake Magadi (Kenya) contains Pleistocene cherts with different maturity fractions of organic matter, remarkably feature similar to Archean cherts from the Pilbara Craton (Western Australia) and the Barberton



Greenstone Belt (South Africa). We found that a significant portion of the bitumens (extractable) and kerogens (non-extractable) in these cherts from Lake Magadi is thermally immature and contains biomarkers of various prokaryotic microorganisms (e.g., thermophilic cyanobacteria, sulfate reducers, and haloarchaea). ~~The presence of thermophilic organisms is well~~, in line with an evaporitic hydrothermal environment. At the same time, both the bitumens and kerogens also exhibit a thermally mature fraction. We explain this apparent offset between different maturity parameters ~~in the Lake Magadi cherts~~ (immature vs. mature) as a result of ~~a~~ syndepositional hydrothermal alteration (e.g., defunctionalization, pre-maturation) and redistribution of organic matter in the environment. These processes include hydrothermal petroleum expulsion in underlying sedimentary units (Oloronga Beds) and ~~a subsequent~~ the fluid-based introduction of the ~~thermally mature resulting~~ cracking products and mature macromolecules into the lake. Our findings aid in the interpretation of heterogeneous organic signatures in Archean rocks, which may, in cases, reflect original environmental conditions ~~in some cases~~ rather than post-depositional metamorphism or contamination. In addition, the preservation of archaeal lipid biomarkers (C<sub>20</sub> and C<sub>25</sub> isoprenoids) in Magadi chert kerogens ~~demonstrates~~ suggests that some biomolecules ~~can~~ may survive initial destructive hydrothermal processes through rapid polymerization and condensation. ~~In this view, a~~ Such rapid sequestration would support the preservation of kerogen-bound molecular biosignatures even in ~~early Archean~~ very ancient hydrothermal cherts ~~appears plausible~~, depending on the post-depositional thermal regime.

## Supplement

### Author contributions

MR, VT, WG, JR and JPD designed the study. MR and JR conducted petrographic analyses. MR conducted organic-geochemical analyses and catalytic hydrolysis (HyPy). WG and MR performed Raman spectroscopy. CH and MR conducted  $\mu$ -XRF measurements. MR wrote the manuscript with contributions from all co-authors.

### Competing interests

The authors declare that they have no conflict of interest.

### Acknowledgements

We ~~thank~~ are grateful to M. van der Meer, J. W. de Leeuw, and two anonymous reviewers for their thoughtful comments. G. Arp, W. Dröse, J. Dyckmans, A. Hackmann, D. Hause-Reitner, H. Mißbach, A. Reimer, and B. Röring are thanked for scientific and technical support. We furthermore thank A. Schito for providing Raman fitting parameters. This work was financially supported by the International Max Planck Research School (IMPRS) for Solar System Science at the University

of Göttingen, the Deutsche Forschungsgemeinschaft (grants DU 1450/3-1 and DU 1450/4-1), and the Göttingen Academy of Sciences and Humanities. WG specifically acknowledges support by the Deutsche Zentrum für Luft- und Raumfahrt (DLR, grant 50QX1401).

## References

- 5 Allen, J. E., Forney, F. W., and Markovetz, A. J.: Microbial subterminal oxidation of alkanes and alk-1-enes, *Lipids*, 6, 448–452, 10.1007/BF02531227, 1971.
- Allwood, A. C., Walter, M. R., and Marshall, C. P.: Raman spectroscopy reveals thermal palaeoenvironments of c.3.5 billion-year-old organic matter, *Vib. Spectrosc.*, 41, 190–197, 10.1016/j.vibspec.2006.02.006, 2006.
- Baker, B. H.: *Geology of the Magadi area*, Geological Survey of Kenya, 1958.
- 10 Baker, B. H.: Tectonics and volcanism of the southern Kenya Rift Valley and its influence on rift sedimentation, in: *Sedimentation in the African Rifts*, edited by: Frostick, L. E. et al., Geol. Soc. Spec. Publ., London, 45–57, 1986.
- Banta, A. B., Wei, J. H., and Welander, P. V.: A distinct pathway for tetrahymanol synthesis in bacteria, *PNAS*, 112, 13478–13483, 10.1073/pnas.1511482112, 2015.
- Barker, C. E., and Pawlewicz, M. J.: Calculation of Vitrinite Reflectance from Thermal Histories and Peak Temperatures, in: *Vitrinite Reflectance as a Maturity Parameter*, edited by: Mukhopadhyay, P. K., and Dow, W. G., Am. Chem. Soc., Washington, DC, 216–229, 1994.
- 15 Becker, K. W., Elling, F. J., Yoshinaga, M. Y., Söllinger, A., Urich, T., and Hinrichs, K.-U.: Unusual butane- and pentanetriol-based tetraether lipids in *Methanomassiliicoccus luminyensis*, a representative of the seventh order of methanogens, *Appl. Environ. Microbiol.*, 82, 4505–4516, 10.1128/AEM.00772-16, 2016.
- 20 Behr, H.-J.: Magadiite and Magadi chert: a critical analysis of the silica sediments in the Lake Magadi Basin, Kenya, in: *Sedimentation in Continental Rifts*, edited by: Renaut, R. W., and Ashley, G. M., SEPM Spec. P., Tulsa, Oklahoma, 257–273, 2002.
- Behr, H.-J., and Röhrich, C.: Record of seismotectonic events in siliceous cyanobacterial sediments (Magadi cherts), Lake Magadi, Kenya, *Int. J. Earth Sci.*, 89, 268–283, 10.1007/s005319900070, 2000.
- 25 van Bergen, P. F., Nott, C. J., Bull, I. D., Poulton, P. R., and Evershed, R. P.: Organic geochemical studies of soils from the Rothamsted Classical Experiments—IV. Preliminary results from a study of the effect of soil pH on organic matter decay, *Org. Geochem.*, 29, 1779–1795, 10.1016/S0146-6380(98)00188-0, 1998.
- Beysac, O., Goffé, B., Chopin, C., and Rouzaud, J. N.: Raman spectra of carbonaceous material in metasediments: a new geothermometer, *J. Metamorph. Geol.*, 20, 859–871, 10.1046/j.1525-1314.2002.00408.x, 2002.
- 30 Birgel, D., Guido, A., Liu, X., Hinrichs, K.-U., Gier, S., and Peckmann, J.: Hypersaline conditions during deposition of the Calcare di Base revealed from archaeal di- and tetraether inventories, *Org. Geochem.*, 77, 11–21, 10.1016/j.orggeochem.2014.09.002, 2014.

- Bishop, A. N., Love, G. D., McAulay, A. D., Snape, C. E., and Farrimond, P.: Release of kerogen-bound hopanoids by hydrolysis, *Org. Geochem.*, 29, 989–1001, 10.1016/S0146-6380(98)00140-5, 1998.
- van den Boorn, S. H. J. M., van Bergen, M. J., Nijman, W., and Vroon, P. Z.: Dual role of seawater and hydrothermal fluids in Early Archean chert formation: Evidence from silicon isotopes, *Geology*, 35, 939–942, 10.1130/G24096A.1, 2007.
- 5 Boreham, C. J., Crick, I. H., and Powell, T. G.: Alternative calibration of the Methylphenanthrene Index against vitrinite reflectance: Application to maturity measurements on oils and sediments, *Org. Geochem.*, 12, 289–294, 10.1016/0146-6380(88)90266-5, 1988.
- Brasier, M. D., Green, O. R., Jephcoat, A. P., Kleppe, A. K., Van Kranendonk, M. J., Lindsay, J. F., Steele, A., and Grassineau, N. V.: Questioning the evidence for Earth's oldest fossils, *Nature*, 416, 76–81, 10.1038/416076a, 2002.
- 10 Brenna, B. L.: The Chemical, Physical, and Microbial Origins of Pleistocene Cherts at Lake Magadi, Kenya Rift Valley, M.Sc. thesis, Department of Geological Sciences, University of Saskatchewan, Saskatoon, 158 pp., 2016.
- Brocks, J. J., Buick, R., Logan, G. A., and Summons, R. E.: Composition and syngeneity of molecular fossils from the 2.78 to 2.45 billion-year-old Mount Bruce Supergroup, Pilbara Craton, Western Australia, *Geochim. Cosmochim. Acta*, 67, 4289–4319, 10.1016/S0016-7037(03)00208-4, 2003a.
- 15 Brocks, J. J., Love, G. D., Snape, C. E., Logan, G. A., Summons, R. E., and Buick, R.: Release of bound aromatic hydrocarbons from late Archean and Mesoproterozoic kerogens via hydrolysis, *Geochim. Cosmochim. Acta*, 67, 1521–1530, 10.1016/S0016-7037(02)01302-9, 2003b.
- Campbell, K. A., Buddle, T. F., and Browne, P. R. L.: Late Pleistocene siliceous sinter associated with fluvial, lacustrine, volcaniclastic and landslide deposits at Tahunaatara, Taupo Volcanic Zone, New Zealand, *Trans. R. Soc. Edinburgh: Earth Sci.*, 94, 485–501, 10.1017/S0263593300000833, 2003.
- 20 Chikaraishi, Y., Naraoka, H., and Poulson, S. R.: Hydrogen and carbon isotopic fractionations of lipid biosynthesis among terrestrial (C3, C4 and CAM) and aquatic plants, *Phytochemistry*, 65, 1369–1381, 10.1016/j.phytochem.2004.03.036, 2004.
- Clifton, C. G., Walters, C. C., and Simoneit, B. R. T.: Hydrothermal petroleums from Yellowstone National Park, Wyoming, U.S.A., *Appl. Geochem.*, 5, 169–191, 10.1016/0883-2927(90)90047-9, 1990.
- 25 Coates, R. C., Podell, S., Korobeynikov, A., Lapidus, A., Pevzner, P., Sherman, D. H., Allen, E. E., Gerwick, L., and Gerwick, W. H.: Characterization of Cyanobacterial Hydrocarbon Composition and Distribution of Biosynthetic Pathways, *PLoS ONE*, 9, e85140, doi.org/10.1371/journal.pone.0085140, 2014.
- Cope, M. J., and Chaloner, W. G.: Fossil charcoal as evidence of past atmospheric composition, *Nature*, 283, 647–649, 10.1038/283647a0, 1980.
- 30 Cranwell, P. A., Eglinton, G., and Robinson, N.: Lipids of aquatic organisms as potential contributors to lacustrine sediments—II, *Org. Geochem.*, 11, 513–527, 10.1016/0146-6380(87)90007-6, 1987.

- Czochanska, Z., Sheppard, C. M., Weston, R. J., Woolhouse, A. D., and Cook, R. A.: Organic geochemistry of sediments in New Zealand. Part I. A biomarker study of the petroleum seepage at the geothermal region of Waiotapu, *Geochim. Cosmochim. Acta*, 50, 507–515, 10.1016/0016-7037(86)90100-6, 1986.
- Dawson, K. S., Freeman, K. H., and Macalady, J. L.: Molecular characterization of core lipids from halophilic archaea grown under different salinity conditions, *Org. Geochem.*, 48, 1–8, 10.1016/j.orggeochem.2012.04.003, 2012.
- De Rosa, M., Gambacorta, A., Nicolaus, B., Ross, H. N. M., Grant, W. D., and Bu'Lock, J. D.: An Asymmetric Archaeobacterial Diether Lipid from Alkaliphilic Halophiles, *J. Gen. Microbiol.*, 128, 343–348, 10.1099/00221287-128-2-343, 1982.
- Des Marais, D. J., Cohen, Y., Nguyen, H., Cheatham, M., Cheatham, T., and Munoz, E.: Carbon isotopic trends in the hypersaline ponds and microbial mats at Guerrero Negro, Baja California Sur, Mexico: Implications for Precambrian stromatolites, in: *Microbial Mats: Physiological Ecology of Benthic Microbial Communities*, edited by: Cohen, Y., and Rosenberg, E., American Society for Microbiology, Washington, DC, 191–203, 1989.
- Djokic, T., Van Kranendonk, M. J., Campbell, K. A., Walter, M. R., and Ward, C. R.: Earliest signs of life on land preserved in ca. 3.5 Ga hot spring deposits, *Nat. Commun.*, 8, e15263, 10.1038/ncomms15263, 2017.
- Duda, J.-P., Van Kranendonk, M. J., Thiel, V., Ionescu, D., Strauss, H., Schäfer, N., and Reitner, J.: A Rare Glimpse of Paleoproterozoic Life: Geobiology of an Exceptionally Preserved Microbial Mat Facies from the 3.4 Ga Strelley Pool Formation, Western Australia, *PLoS ONE*, 11, e0147629, 10.1371/journal.pone.0147629, 2016.
- Duda, J.-P., Thiel, V., Bauersachs, T., Mißbach, H., Reinhardt, M., Schäfer, N., Van Kranendonk, M. J., and Reitner, J.: Ideas and perspectives: hydrothermally driven redistribution and sequestration of early Archaean biomass – the “hydrothermal pump hypothesis”, *Biogeosciences*, 15, 1535–1548, 10.5194/bg-15-1535-2018, 2018.
- Durand, B.: Sedimentary organic matter and kerogen. Definition and quantitative importance of kerogen, in: *Kerogen: Insoluble Organic Matter from Sedimentary Rocks*, edited by: Durand, B., Editions Technip., Paris, 13–34, 1980.
- Eglinton, G., and Hamilton, R. J.: Leaf Epicuticular Waxes, *Science*, 156, 1322–1335, 10.1126/science.156.3780.1322 1967.
- Eugster, H. P.: Hydrous Sodium Silicates from Lake Magadi, Kenya: Precursors of Bedded Chert, *Science*, 157, 1177–1180, 10.1126/science.157.3793.1177, 1967.
- Eugster, H. P.: Inorganic bedded cherts from the Magadi area, Kenya, *Contrib. Mineral. Petrol.*, 22, 1–31, 10.1007/BF00388011, 1969.
- Eugster, H. P.: Chemistry and origin of the brines of Lake Magadi, Kenya, *Mineral. Soc. Amer. Spec. Pap.*, 3, 213–235, 1970.
- Eugster, H. P.: Lake Magadi, Kenya: a model for rift valley hydrochemistry and sedimentation?, *Geol. Soc. Spec. Publ.*, 25, 177–189, 10.1144/GSL.SP.1986.025.01.15, 1986.
- Eugster, H. P., and Jones, B. F.: Gels Composed of Sodium-Aluminium Silicate, Lake Magadi, Kenya, *Science*, 161, 160–163, 10.1126/science.161.3837.160, 1968.
- Fairhead, J. D., Mitchell, J. G., and Williams, L. A. J.: New K/Ar Determinations on Rift Volcanics of S. Kenya and their Bearing on Age of Rift Faulting, *Nature Physical Science*, 238, 66–69, 10.1038/physci238066a0, 1972.

- Farrimond, P., Griffiths, T., and Evdokiadis, E.: Hopanoic acids in Mesozoic sedimentary rocks: their origin and relationship with hopanes, *Org. Geochem.*, 33, 965–977, 10.1016/S0146-6380(02)00059-1, 2002.
- French, K. L., Hallmann, C., Hope, J. M., Schoon, P. L., Zumberge, J. A., Hoshino, Y., Peters, C. A., George, S. C., Love, G. D., Brocks, J. J., Buick, R., and Summons, R. E.: Reappraisal of hydrocarbon biomarkers in Archean rocks, *PNAS*, 112, 5915–5920, 10.1073/pnas.1419563112, 2015.
- George, S. C., and Jardine, D. R.: Ketones in a Proterozoic dolerite sill, *Org. Geochem.*, 21, 829–839, 10.1016/0146-6380(94)90042-6, 1994.
- Glikson, M., Duck, L. J., Golding, S. D., Hofmann, A., Bolhar, R., Webb, R., Baiano, J. C. F., and Sly, L. I.: Microbial remains in some earliest Earth rocks: Comparison with a potential modern analogue, *Precambrian Res.*, 164, 187–200, 10.1016/j.precamres.2008.05.002, 2008.
- Goetz, C., and Hillaire-Marcel, C.: U-series disequilibria in early diagenetic minerals from Lake Magadi sediments, Kenya: Dating potential, *Geochim. Cosmochim. Acta*, 56, 1331–1341, 10.1016/0016-7037(92)90065-Q, 1992.
- Golubic, S., Friedmann, E. I., and Schneider, J.: The lithobiontic ecological niche, with special reference to microorganisms, *J. Sediment. Petrol.*, 51, 475–478, 10.1306/212F7CB6-2B24-11D7-8648000102C1865D, 1981.
- Goñi, M. A., and Eglinton, T. I.: Stable carbon isotopic analyses of lignin-derived CuO oxidation products by isotope ratio monitoring-gas chromatography-mass spectrometry (irm-GC-MS), *Org. Geochem.*, 24, 601–615, 10.1016/0146-6380(96)00052-6, 1996.
- Grant, W. D., Pinch, G., Harris, J. E., De Rosa, M., and Gambacorta, A.: Polar Lipids in Methanogen Taxonomy *J. Gen. Microbiol.*, 131, 3277–3286, 10.1099/00221287-131-12-3277, 1985.
- Greenwood, P. F., and Summons, R. E.: GC–MS detection and significance of crocetane and pentamethylcosane in sediments and crude oils, *Org. Geochem.*, 34, 1211–1222, 10.1016/S0146-6380(03)00062-7, 2003.
- Hallmann, C., Friedenberger, H., Hause-Reitner, D., and Hoppert, M.: Depth profiles of microbial colonization in sandstones, *Geomicrobiol. J.*, 32, 365–379, 10.1080/01490451.2014.929762, 2015.
- Hamilton-Brehm, S. D., Gibson, R. A., Green, S. J., Hopmans, E. C., Schouten, S., van der Meer, M. T. J., Shields, J. P., Sinninghe Damsté, J. S., and Elkins, J. G.: *Thermodesulfobacterium geofontis* sp. nov., a hyperthermophilic, sulfate-reducing bacterium isolated from Obsidian Pool, Yellowstone National Park, *Extremophiles*, 17, 251–263, 10.1007/s00792-013-0512-1, 2013.
- Harvey, H. R., and McManus, G. B.: Marine ciliates as a widespread source of tetrahymanol and hopan-3 $\beta$ -ol in sediments, *Geochim. Cosmochim. Acta*, 55, 3387–3390, 10.1016/0016-7037(91)90496-R, 1991.
- Hautevelle, Y., Michels, R., Malartre, F., and Trouiller, A.: Vascular plant biomarkers as proxies for palaeoflora and palaeoclimatic changes at the Dogger/Malm transition of the Paris Basin (France), *Org. Geochem.*, 37, 610–625, 10.1016/j.orggeochem.2005.12.010, 2006.
- ten Haven, H. L., de Leeuw, J. W., Rullkötter, J., and Sinninghe Damsté, J. S.: Restricted utility of the pristane/phytane ratio as a palaeoenvironmental indicator, *Nature*, 330, 641–643, 10.1038/330641a0, 1987.

- ten Haven, H. L., Rohmer, M., Rullkötter, J., and Bisseret, P.: Tetrahymanol, the most likely precursor of gammacerane, occurs ubiquitously in marine sediments, *Geochim. Cosmochim. Acta*, 53, 3073–3079, 10.1016/0016-7037(89)90186-5, 1989.
- Hawkes, J. A., Rossel, P. E., Stubbins, A., Butterfield, D., Connelly, D. P., Achterberg, E. P., Koschinsky, A., Chavagnac, V., Hansen, C. T., Bach, W., and Dittmar, T.: Efficient removal of recalcitrant deep-ocean dissolved organic matter during hydrothermal circulation, *Nat. Geosci.*, 8, 856–860, 10.1038/ngeo2543, 2015.
- Hawkes, J. A., Hansen, C. T., Goldhammer, T., Bach, W., and Dittmar, T.: Molecular alteration of marine dissolved organic matter under experimental hydrothermal conditions, *Geochim. Cosmochim. Acta*, 175, 68–85, 10.1016/j.gca.2015.11.025, 2016.
- Hay, R. L.: Chert and its sodium-silicate precursors in sodium-carbonate lakes of East Africa, *Contrib. Mineral. Petrol.*, 17, 255–274, 10.1007/BF00380740, 1968.
- Hickman-Lewis, K., Cavalazzi, B., Foucher, F., and Westall, F.: Most ancient evidence for life in the Barberton greenstone belt: Microbial mats and biofabrics of the ~3.47 Ga Middle Marker horizon, *Precambrian Res.*, 312, 45–67, 10.1016/j.precamres.2018.04.007, 2018.
- Huber, R., Wilharm, T., Huber, D., Tricone, A., Burggraf, S., König, H., Reinhard, R., Rockinger, I., Fricke, H., and Stetter, K. O.: *Aquifex pyrophilus* gen. nov. sp. nov., Represents a Novel Group of Marine Hyperthermophilic Hydrogen-Oxidizing Bacteria, *Syst. Appl. Microbiol.*, 15, 340–351, 10.1016/S0723-2020(11)80206-7, 1992.
- Ingram, L. L., Ellis, J., Crisp, P. T., and Cook, A. C.: Comparative study of oil shales and shale oils from the Mahogany Zone, Green River Formation (U.S.A.) and Kerosene Creek Seam, Rundle Formation (Australia), *Chem. Geol.*, 38, 185–212, 10.1016/0009-2541(83)90054-2, 1983.
- Jahnke, L., Eder, W., Huber, R., Hope, J. M., Hinrichs, K.-U., Hayes, J. M., Des Marais, D. J., Cady, S. L., and Summons, R. E.: Signature Lipids and Stable Carbon Isotope Analyses of Octopus Spring Hyperthermophilic Communities Compared with Those of Aquificales Representatives, *Appl. Environ. Microbiol.*, 67, 5179–5189, 10.1128/AEM.67.11.5179-5189.2001 2001.
- Jones, B., and Renaut, R. W.: Formation of silica oncoids around geysers and hot springs at El Tatio, northern Chile, *Sedimentology*, 44, 287–304, 10.1111/j.1365-3091.1997.tb01525.x, 1997.
- Jones, B., and Renaut, R. W.: Impact of Seasonal Changes on the Formation and Accumulation of Soft Siliceous Sediments on the Discharge Apron of Geysir, *Iceland Journal of Sedimentary Research*, 80, 17–35, 10.2110/jsr.2010.008, 2010.
- Jones, B., Renaut, R. W., Torfason, H., and Owen, R. B.: The geological history of Geysir, Iceland: a tephrochronological approach to the dating of sinter, *J. Geol. Soc. (London, U.K.)*, 164, 1241–1252, 10.1144/0016-76492006-178, 2007.
- Jones, B. F., Eugster, H. P., and Rettig, S. L.: Hydrochemistry of the Lake Magadi basin, Kenya, *Geochim. Cosmochim. Acta*, 41, 53–72, 10.1016/0016-7037(77)90186-7, 1977.
- Kambura, A. K., Mwirichia, R. K., Kasili, R. W., Karanja, E. N., Makonde, H. M., and Boga, H. I.: Bacteria and Archaea diversity within the hot springs of Lake Magadi and Little Magadi in Kenya, *BMC Microbiol.*, 16, 10.1186/s12866-016-0748-x, 2016.

- Kemp, P., Lander, D. J., and Orpin, C. G.: The Lipids of the Rumen Fungus *Piromonas communis*, *J. Gen. Microbiol.*, 139, 27–37, 10.1099/00221287-130-1-27, 1983.
- Killops, S., and Killops, V.: *Introduction to Organic Geochemistry*, 2nd ed., Blackwell Publishing, Oxford, 2005.
- 5 Kleemann, G., Poralla, K., Englert, G., Kjøsén, H., Liaaen-Jensen, S., Neunlist, S., and Rohmer, M.: Tetrahymanol from the phototrophic bacterium *Rhodospirillum rubrum*: first report of a gammacerane triterpene from a prokaryote, *J. Gen. Microbiol.*, 136, 2551–2553, 10.1099/00221287-136-12-2551, 1990.
- Koga, Y., Nishihara, M., Morii, H., and Akagawa-Matsushita, M.: Ether polar lipids of methanogenic bacteria: structures, comparative aspects, and biosyntheses, *Microbiol. Mol. Biol. Rev.*, 57, 164–182, 1993.
- 10 Kolattukudi, P. E.: Biopolyester Membranes of Plants: Cutin and Suberin, *Science*, 208, 990–1000, 10.1126/science.208.4447.990, 1980.
- Konn, C., Charlou, J. L., Donval, J. P., Holm, N. G., Dehairs, F., and Bouillon, S.: Hydrocarbons and oxidized organic compounds in hydrothermal fluids from Rainbow and Lost City ultramafic-hosted vents, *Chem. Geol.*, 258, 299–314, 10.1016/j.chemgeo.2008.10.034, 2009.
- Krooss, B. M., Brothers, L., and Engel, M. H.: Geochromatography in petroleum migration: a review, in: *Petroleum Migration*, edited by: England, W. A., and Fleet, A. J., *Geol. Soc. Spec. Publ.*, London, 149–163, 1991.
- 15 Langworthy, T. A., Holzer, G., Zeikus, J. G., and Tornabene, T. G.: Iso- and Anteiso-Branched Glycerol Diethers of the Thermophilic Anaerobe *Thermodesulfobacterium commune*, *Syst. Appl. Microbiol.*, 4, 1–17, 10.1016/S0723-2020(83)80029-0, 1983.
- Leif, R. N., and Simoneit, B. R. T.: Ketones in hydrothermal petroleums and sediment extracts from Guaymas Basin, Gulf of California, *Org. Geochem.*, 23, 889–904, 10.1016/0146-6380(95)00085-2, 1995.
- 20 Love, G. D., Snape, C. E., Carr, A. D., and Houghton, R. C.: Release of covalently-bound alkane biomarkers in high yields from kerogen via catalytic hydrolysis, *Org. Geochem.*, 23, 981–986, 10.1016/0146-6380(95)00075-5, 1995.
- Love, G. D., McAulay, A. D., and Snape, C. E.: Effect of Process Variables in Catalytic Hydrolysis on the Release of Covalently Bound Aliphatic Hydrocarbons from Sedimentary Organic Matter, *Energy Fuels*, 11, 522–531, 10.1021/ef960194x, 1997.
- 25 Luque, F. J., Ortega, L., Barrenechea, J. F., Millward, D., Beyssac, O., and Huizenga, J.-M.: Deposition of highly crystalline graphite from moderate-temperature fluids, *Geology*, 37, 275–278, 10.1130/G25284A.1, 2009.
- Mallory, F. B., Gordon, J. T., and Conner, R. L.: The isolation of a pentacyclic triterpenoid alcohol from a protozoan, *J. Am. Chem. Soc.*, 85, 1362–1363, 1963.
- 30 Marshall, C. P., Love, G. D., Snape, C. E., Hill, A. C., Allwood, A. C., Walter, M. R., Van Kranendonk, M. J., Bowden, S. A., Sylva, S. P., and Summons, R. E.: Structural characterization of kerogen in 3.4 Ga Archaean cherts from the Pilbara Craton, Western Australia, *Precambrian Res.*, 155, 1–23, 10.1016/j.precamres.2006.12.014, 2007.

- McCollom, T. M., and Seewald, J. S.: Experimental study of the hydrothermal reactivity of organic acids and acid anions: II. Acetic acid, acetate, and valeric acid, *Geochim. Cosmochim. Acta*, 67, 3645–3664, 10.1016/S0016-7037(03)00135-2, 2003.
- McCollom, T. M., Seewald, J. S., and German, C. R.: Investigation of extractable organic compounds in deep-sea hydrothermal vent fluids along the Mid-Atlantic Ridge, *Geochim. Cosmochim. Acta*, 156, 122–144, 10.1016/j.gca.2015.02.022, 2015.
- 5 Meredith, W., Russell, C. A., Cooper, M., Snape, C. E., Love, G. D., Fabbri, D., and Vane, C. H.: Trapping hydropyrolysates on silica and their subsequent thermal desorption to facilitate rapid fingerprinting by GC–MS, *Org. Geochem.*, 35, 73–89, 10.1016/j.orggeochem.2003.07.002, 2004.
- Meredith, W., Snape, C. E., and Love, G. D.: Development and Use of Catalytic Hydropyrolysis (HyPy) as an Analytical Tool for Organic Geochemical Applications, in: *Principles and Practice of Analytical Techniques in Geosciences*, edited by: Grice, K., Royal Society of Chemistry, 171–208, 2014.
- 10 Mißbach, H., Schmidt, B. C., Duda, J.-P., Lünsdorf, N. K., Goetz, W., and Thiel, V.: Assessing the diversity of lipids formed via Fischer-Tropsch-type reactions, *Org. Geochem.*, 119, 110–121, 10.1016/j.orggeochem.2018.02.012, 2018.
- Morag, N., Williford, K. H., Kitajima, K., Philippot, P., Van Kranendonk, M. J., Lepot, K., Thomazo, C., and Valley, J. W.: Microstructure-specific carbon isotopic signatures of organic matter from ~3.5 Ga cherts of the Pilbara Craton support a biologic origin, *Precambrian Res.*, 275, 429–449, 10.1016/j.precamres.2016.01.014, 2016.
- 15 Nicolau, C., Reich, M., and Lynne, B.: Physico-chemical and environmental controls on siliceous sinter formation at the high-altitude El Tatio geothermal field, Chile, *J. Volcanol. Geotherm. Res.*, 282, 60–76, 10.1016/j.jvolgeores.2014.06.012, 2014.
- Olcott Marshall, A., Emry, J. R., and Marshall, C. P.: Multiple Generations of Carbon in the Apex Chert and Implications for Preservation of Microfossils, *Astrobiology*, 12, 160–166, 10.1089/ast.2011.0729, 2012.
- 20 Otto, A., and Simoneit, B. R. T.: Biomarkers of Holocene buried conifer logs from Bella Coola and north Vancouver, British Columbia, Canada, *Org. Geochem.*, 33, 1241–1251, 10.1016/S0146-6380(02)00139-0, 2002.
- Owen, R. B., Renaut, R. W., Muiruri, V. M., Rabideaux, N. M., Lowenstein, T. K., McNulty, E. P., Leet, K., Deocampo, D., Luo, S., Deino, A. L., Cohen, A., Sier, M. J., Campisano, C., Shen, C.-C., Billingsley, A., Mbuthia, A., and Stockhecke, M.: Quaternary history of the Lake Magadi Basin, southern Kenya Rift: Tectonic and climatic controls, *Palaeogeogr. Palaeoclimatol. Palaeoecol.*, 518, 97–118, 10.1016/j.palaeo.2019.01.017, 2019.
- 25 Pancost, R. D., Coleman, J. M., Love, G. D., Chatzi, A., Bouloubassi, I., and Snape, C. E.: Kerogen-bound glycerol dialkyl tetraether lipids released by hydrolysis of marine sediments: A bias against incorporation of sedimentary organisms?, *Org. Geochem.*, 39, 1359–1371, 10.1016/j.orggeochem.2008.05.002, 2008.
- 30 Pancost, R. D., McClymont, E. L., Bingham, E. M., Roberts, Z., Charman, D. J., Hornibrook, E. R. C., Blundell, A., Chambers, F. M., Lim, K. L. H., and Evershed, R. P.: Archaeol as a methanogen biomarker in ombrotrophic bogs, *Org. Geochem.*, 42, 1279–1287, 10.1016/j.orggeochem.2011.07.003, 2011.
- Parkes, R. J., and Taylor, J.: The relationship between fatty acid distributions and bacterial respiratory types in contemporary marine sediments, *Eustuarine Coastal Shelf Sci.*, 16, 175–189, 10.1016/0272-7714(83)90139-7, 1983.



- Peters, K. E., Walters, C. C., and Moldowan, J. M.: The Biomarker Guide: I. Biomarkers and Isotopes in the Environment and Human History, 2nd ed., Cambridge University Press., Cambridge, 471 pp., 2005a.
- Peters, K. E., Walters, C. C., and Moldowan, J. M.: The Biomarker Guide: II. Biomarkers and Isotopes in Petroleum Exploration and Earth History, 2nd ed., Cambridge University Press, Cambridge, 1155 pp., ~~2005~~2005b.
- 5 Pirajno, F., and van Kranendonk, M. J.: Review of hydrothermal processes and systems on Earth and implications for Martian analogues, *Aust. J. Earth Sci.*, 52, 329–351, 10.1080/08120090500134571, 2005.
- Qu, Y., Engdahl, A., Zhu, S., Vajda, V., McLoughlin, N.: Ultrastructural Heterogeneity of Carbonaceous Material in Ancient Cherts: Investigating Biosignature Origin and Preservation, *Astrobiology*, 15, 10.1089/ast.2015.1298, 2015.
- Radke, M., and Welte, D. H.: The Methylphenanthrene Index (MPI): a maturity parameter based on aromatic hydrocarbons, 10 in: *Advances in Organic Geochemistry 1981*, edited by: Bjorøy et al., M., Wiley, 504–512, 1983.
- Rebelo, S. L. H., Guedes, A., Szeferczyk, M. E., Pereira, A. M., Araújo, J. P., and Freire, C.: Progress in the Raman spectra analysis of covalently functionalized multiwalled carbon nanotubes: unraveling disorder in graphitic materials, *Phys. Chem. Chem. Phys.*, 18, 12784–12796, 10.1039/C5CP06519D, 2016.
- Renaut, R. W., Jones, B., Tiercelin, J.-J., and Tarits, C.: Sublacustrine precipitation of hydrothermal silica in rift lakes: evidence 15 from Lake Baringo, central Kenya Rift Valley, *Sediment. Geol.*, 148, 235–257, 10.1016/S0037-0738(01)00220-2, 2002.
- Risatti, J. B., Rowland, S. J., Yon, D. A., and Maxwell, J. R.: Stereochemical studies of acyclic isoprenoids—XII. Lipids of methanogenic bacteria and possible contributions to sediments, *Org. Geochem.*, 6, 93–104, 10.1016/0146-6380(84)90030-5, 1984.
- Roberts, N., Taieb, M., Barker, P., Damnati, B., Icole, M., and Williamson, D.: Timing of the Younger Dryas event in East 20 Africa from lake-level changes, *Nature*, 366, 146–148, 10.1038/366146a0, 1993.
- Rossel, P. E., Stubbins, A., Rebling, T., Koschinsky, A., Hawkes, J. A., and Dittmar, T.: Thermally altered marine dissolved organic matter in hydrothermal fluids, *Org. Geochem.*, 110, 73–86, 10.1016/j.orggeochem.2017.05.003, 2017.
- Rushdi, A. I., and Simoneit, B. R. T.: Lipid Formation by Aqueous Fischer-Tropsch-Type Synthesis over a Temperature Range of 100 to 400 °C, *Origins Life Evol. Biosphere*, 31, 103–118, 10.1023/A:1006702503954, 2001.
- 25 Röhricht, C.: *Lithologie und Genese der Chertserien des Magadi Beckens, Lake Magadi, Kenia*, Papierflieger, Clausthal-Zellerfeld, 108 pp., 1999.
- Scalan, E. S., and Smith, J. E.: An improved measure of the odd-even predominance in the normal alkanes of sediment extracts and petroleum, *Geochim. Cosmochim. Acta*, 34, 611–620, 10.1016/0016-7037(70)90019-0, 1970.
- Schidlowski, M.: A 3,800-million-year isotopic record of life from carbon in sedimentary rocks, *Nature*, 333, 313–318, 30 10.1038/333313a0, 1988.
- Schidlowski, M.: Carbon isotopes as biogeochemical recorders of life over 3.8 Ga of Earth history: evolution of a concept, *Precambrian Res.*, 106, 117–134, 10.1016/S0301-9268(00)00128-5, 2001.
- Schidlowski, M., Matzigkeit, U., and Krumbein, W. E.: Superheavy Organic Carbon from Hypersaline Microbial Mats, *Naturwissenschaften*, 71, 303–308, 1984.

- Schidlowski, M., Gorzawski, H., and Dor, I.: Carbon isotope variations in a solar pond microbial mat: Role of environmental gradients as steering variables, *Geochim. Cosmochim. Acta*, 58, 2289–2298, 10.1016/0016-7037(94)90011-6, 1994.
- Schito, A., Romano, C., Corrado, S., Grigo, D., and Poe, B.: Diagenetic thermal evolution of organic matter by Raman spectroscopy, *Org. Geochem.*, 106, 57–67, 0.1016/j.orggeochem.2016.12.006, 2017.
- 5 Schmidt, M. W. I., and Noack, A. G.: Black carbon in soils and sediments: Analysis, distribution, implications, and current challenges, *Global Biogeochem. Cycles*, 14, 777–793, 10.1029/1999GB001208, 2000.
- Schouten, S., Hartgers, W. A., Lòpez, J. F., Grimalt, J. O., and Sinninghe Damsté, J. S.: A molecular isotopic study of <sup>13</sup>C-enriched organic matter in evaporitic deposits: recognition of CO<sub>2</sub>-limited ecosystems, *Org. Geochem.*, 32, 277–286, 10.1016/S0146-6380(00)00177-7, 2001.
- 10 Sforna, M. C., van Zuilen, M. A., and Philippot, P.: Structural characterization by Raman hyperspectral mapping of organic carbon in the 3.46 billion-year-old Apex chert, Western Australia, *Geochim. Cosmochim. Acta*, 124, 18–33, 10.1016/j.gca.2013.09.031, 2014.
- Simoneit, B. R. T.: Hydrothermal effects on organic matter—high vs low temperature components, *Org. Geochem.*, 6, 857–864, 10.1016/0146-6380(84)90108-6, 1984.
- 15 Simoneit, B. R. T., Grimalt, J. O., Hayes, J. M., and Hartman, H.: Low temperature hydrothermal maturation of organic matter in sediments from the Atlantis II Deep, Red Sea, *Geochim. Cosmochim. Acta*, 51, 879–894, 10.1016/0016-7037(87)90101-3, 1987.
- Simoneit, B. R. T., Deamer, D. W., and Kompanichenko, V.: Characterization of hydrothermally generated oil from the Uzon caldera, Kamchatka, *Appl. Geochem.*, 24, 303–309, 10.1016/j.apgeochem.2008.10.007, 2009.
- 20 Sinninghe Damsté, J. S., and de Leeuw, J. W.: Analysis, structure and geochemical significance of organically-bound Sulphur in the geosphere: State of the art and future research, *Org. Geochem.*, 16, 1077–1101, 10.1016/0146-6380(90)90145-P, 1990.
- Still, C. J., Berry, J. A., Collatz, G. J., and DeFries, R. S.: Global distribution of C<sub>3</sub> and C<sub>4</sub> vegetation: Carbon cycle implications, *Global Biogeochem. Cycles*, 17, 6-1–6-14, 10.1029/2001GB001807, 2003.
- 25 Sugitani, K., Yamamoto, K., Wada, H., Binu-Lal, S. S., and Yoneshige, M.: Geochemistry of Archean carbonaceous cherts deposited at immature island-arc setting in the Pilbara Block, Western Australia, *Sediment. Geol.*, 151, 45–66, 10.1016/S0037-0738(01)00230-5, 2002.
- Taipale, S. J., Strandberg, U., Peltomaa, E., Galloway, A. W. E., Ojala, A., and Brett, M. T.: Fatty acid composition as biomarkers of freshwater microalgae: analysis of 37 strains of microalgae in 22 genera and in seven classes, *Aquat. Microb. Ecol.*, 71, 165–178, 10.3354/ame01671, 2013.
- 30 Taipale, S. J., Hiltunen, M., Vuorio, K., and Peltomaa, E.: Suitability of Phytosterols Alongside Fatty Acids as Chemotaxonomic Biomarkers for Phytoplankton, *Front. Plant Sci.*, 7, 10.3389/fpls.2016.00212, 2016.
- Teixidor, P., Grimalt, J. O., Pueyo, J. J., and Rodriguez-Valera, F.: Isopranylglycerol diethers in non-alkaline evaporitic environments, *Geochim. Cosmochim. Acta*, 57, 4479–4489, 10.1016/0016-7037(93)90497-K, 1993.

- Thiel, V., Jenisch, A., Landmann, G., Reimer, A., and Michaelis, W.: Unusual distributions of long-chain alkenones and tetrahymanol from the highly alkaline Lake Van, Turkey, *Geochim. Cosmochim. Acta*, 61, 2053–2064, 10.1016/S0016-7037(97)00038-0, 1997.
- Tice, M. M., and Lowe, D. R.: The origin of carbonaceous matter in pre-3.0 Ga greenstone terrains: A review and new evidence from the 3.42 Ga Buck Reef Chert, *Earth Sci. Rev.*, 76, 259–300, 10.1016/j.earscirev.2006.03.003, 2006.
- 5 Tindall, B. J.: Qualitative and Quantitative Distribution of Diether Lipids in Haloalkaliphilic Archaeobacteria, *Syst. Appl. Microbiol.*, 6, 243–246, 10.1016/S0723-2020(85)80025-4, 1985.
- Tindall, B. J., Ross, H. N. M., and Grant, W. D.: *Natronobacterium* gen. nov. and *Natronococcus* gen. nov., Two New Genera of Haloalkaliphilic Archaeobacteria, *Syst. Appl. Microbiol.*, 5, 41–57, 10.1016/S0723-2020(84)80050-8, 1984.
- 10 Tissot, B. P., and Welte, D. H.: *Petroleum formation and occurrence*. 2nd ed., Springer, Berlin, 1984.
- Ueno, Y., Yoshioka, H., Maruyama, S., and Isozaki, Y.: Carbon isotopes and petrography of kerogens in ~3.5-Ga hydrothermal silica dikes in the North Pole area, Western Australia, *Geochim. Cosmochim. Acta*, 68, 573–589, 10.1016/S0016-7037(03)00462-9, 2004.
- Villanueva, L., Sinninghe Damsté, J. S., and Schouten, S.: A re-evaluation of the archaeal membrane lipid biosynthetic pathway, *Nat. Rev. Microbiol.*, 12, 438–448, 10.1038/nrmicro3260, 2014.
- 15 Vinçon-Laugier, A., Grossi, V., Pacton, M., Escarguel, G., and Cravo-Laureau, C.: The alkyl glycerol ether lipid composition of heterotrophic sulfate reducing bacteria strongly depends on growth substrate, *Org. Geochem.*, 98, 141–154, 10.1016/j.orggeochem.2016.05.015, 2016.
- 20 Wakeham, S. G., Sinninghe Damsté, J. S., Kohlen, M. E. L., and de Leeuw, J. W.: *Organic sulfur compounds formed during early diagenesis in Black Sea sediments*, *Geochim. Cosmochim. Acta*, 59, 521–533, 10.1016/0016-7037(94)00361-O, 1995.
- Weston, R. J., and Woolhouse, A. D.: Organic geochemistry of the sedimentary basins of New Zealand part IV. A biomarker study of the petroleum seepage and some well core bitumens from the geothermal region of Ngawha Springs, *Appl. Geochem.*, 2, 305–319, 10.1016/0883-2927(87)90046-1, 1987.
- 25 Wheildon, J., Morgan, P., Williamson, K. H., Evans, T. R., and Swanberg, C. A.: Heat flow in the Kenya rift zone, *Tectonophysics*, 236, 131–149, 10.1016/0040-1951(94)90173-2, 1994.
- Williamson, D., Taieb, M., Damnati, B., Icole, M., and Thouveny, N.: Equatorial extension of the younger Dryas event: rock magnetic evidence from Lake Magadi (Kenya), *Global Planet. Change*, 7, 235–242, 10.1016/0921-8181(93)90053-Q, 1993.
- 30 Yang, H., Zheng, F., Xiao, W., and Xie, S.: Distinct distribution revealing multiple bacterial sources for 1-O-monoalkyl glycerol ethers in terrestrial and lake environments, *Sci. China Earth Sci.*, 58, 1005–1017, 10.1007/s11430-014-5016-z, 2015.

Yunker, M. B., Macdonald, R. W., Vingarzan, R., Mitchell, R. H., Goyette, D., and Sylvestre, S.: PAHs in the Fraser River basin: a critical appraisal of PAH ratios as indicators of PAH source and composition, *Org. Geochem.*, 33, 489–515, 10.1016/S0146-6380(02)00002-5, 2002.

5 Zander, J. M., Caspi, E., Pandey, G. N., and Mitra, C. R.: The presence of tetrahymanol in *Oleandra wallichii*, *Phytochemistry*, 8, 2265–2267, 10.1016/S0031-9422(00)88195-9, 1969.

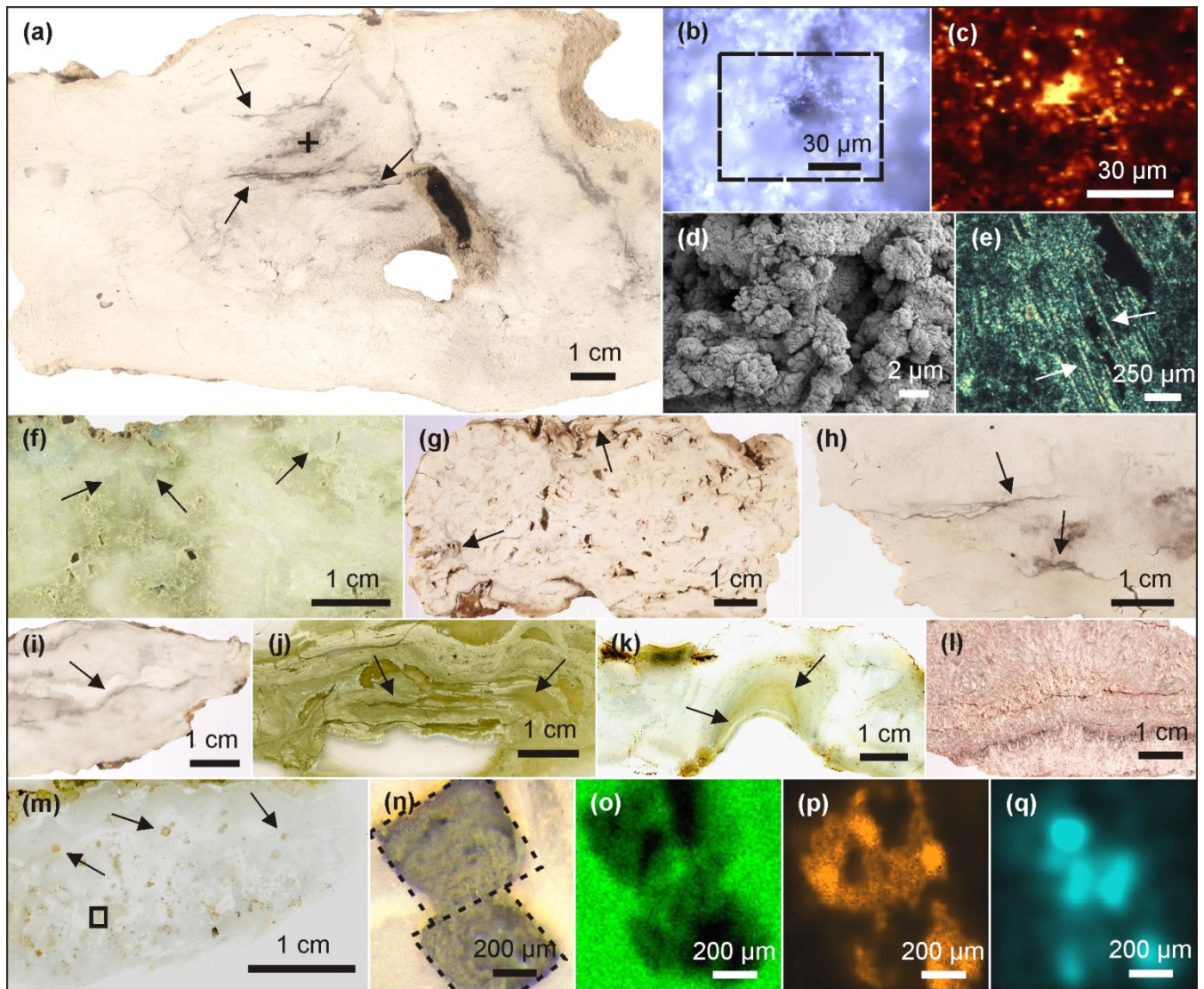


**Figure 1.** Petrographic characteristics of Lake Magadi cherts. (a) Polished slice of LM-1692, revealing organic matter in the silica matrix (arrows). The cross marks the spot for Raman mapping (detailed in b–c). (b) Area of Raman mapping at  $-2.5 \mu\text{m}$  (dashed box, image scan  $94 \times 72$  pixels). (c) Raman mapping result, yellow color indicates high abundances of organic matter. (d) SEM image from LM-1692, showing a porous matrix of microcrystalline quartz. (e) Silicified bacterial filaments from LM-1699 under polarized light (see arrows). (f) Brecciated texture (arrows) in LM-1699. (g) Cloudy microbial features (arrows) in LM-1694. (h) Layered organic matter (arrow) in LM-1693. (i–k) Laminated microbial mat patterns (arrows) preserved in LM-1695 (i), LM-1697 (j) and LM-1698 (k). (l) Silica sinter from Great Geysir, Iceland (IC-1700). (m) Carbonate rhombs (arrows) enclosed in the chert matrix of LM-1696. The box marks the area for  $\mu$ -XRF scanning (n–q). (n) Close-up of boxed area showing carbonate rhombs under reflected light. (o–q)  $\mu$ -XRF analyses of the same area showing

silica (o), calcium (p), and sulfur (q) distributions (a brighter color indicates a higher concentration). Sulfur enrichments accompanied by calcium point to the presence of gypsum associated with the carbonate rhombs.

5

10

15

20



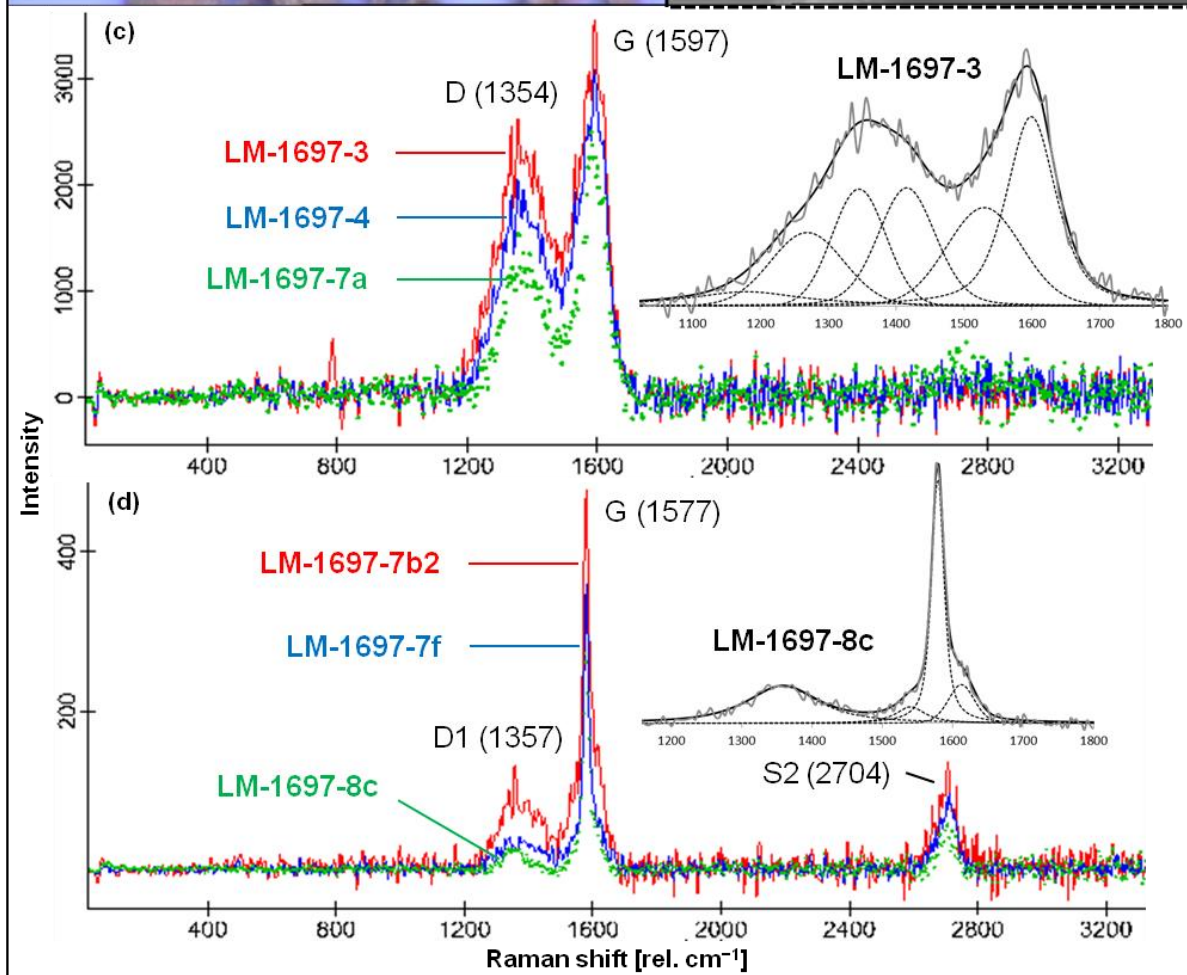
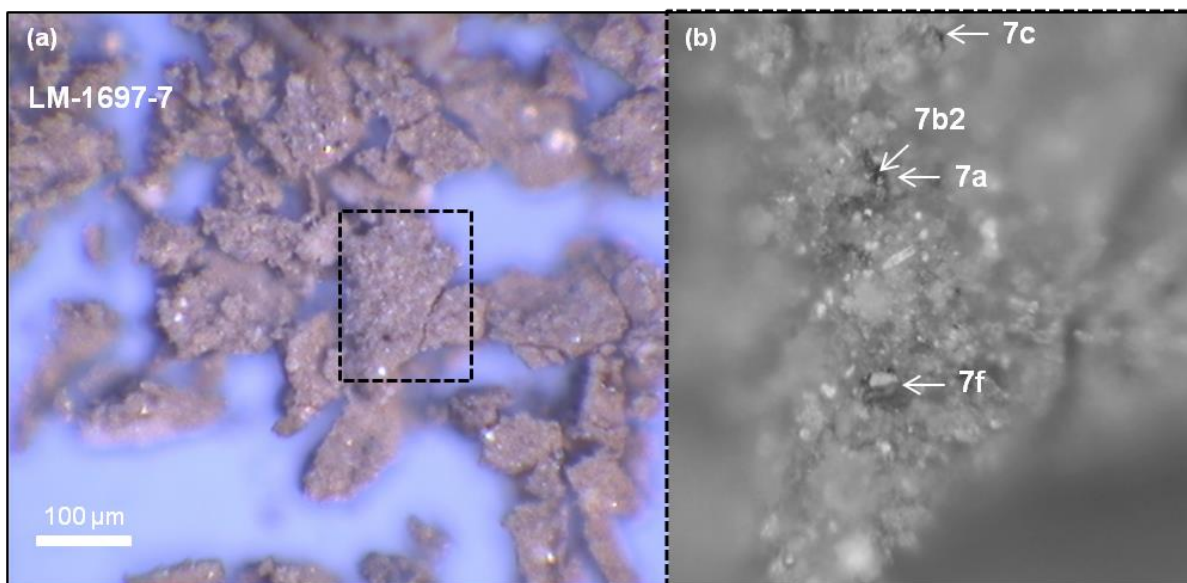


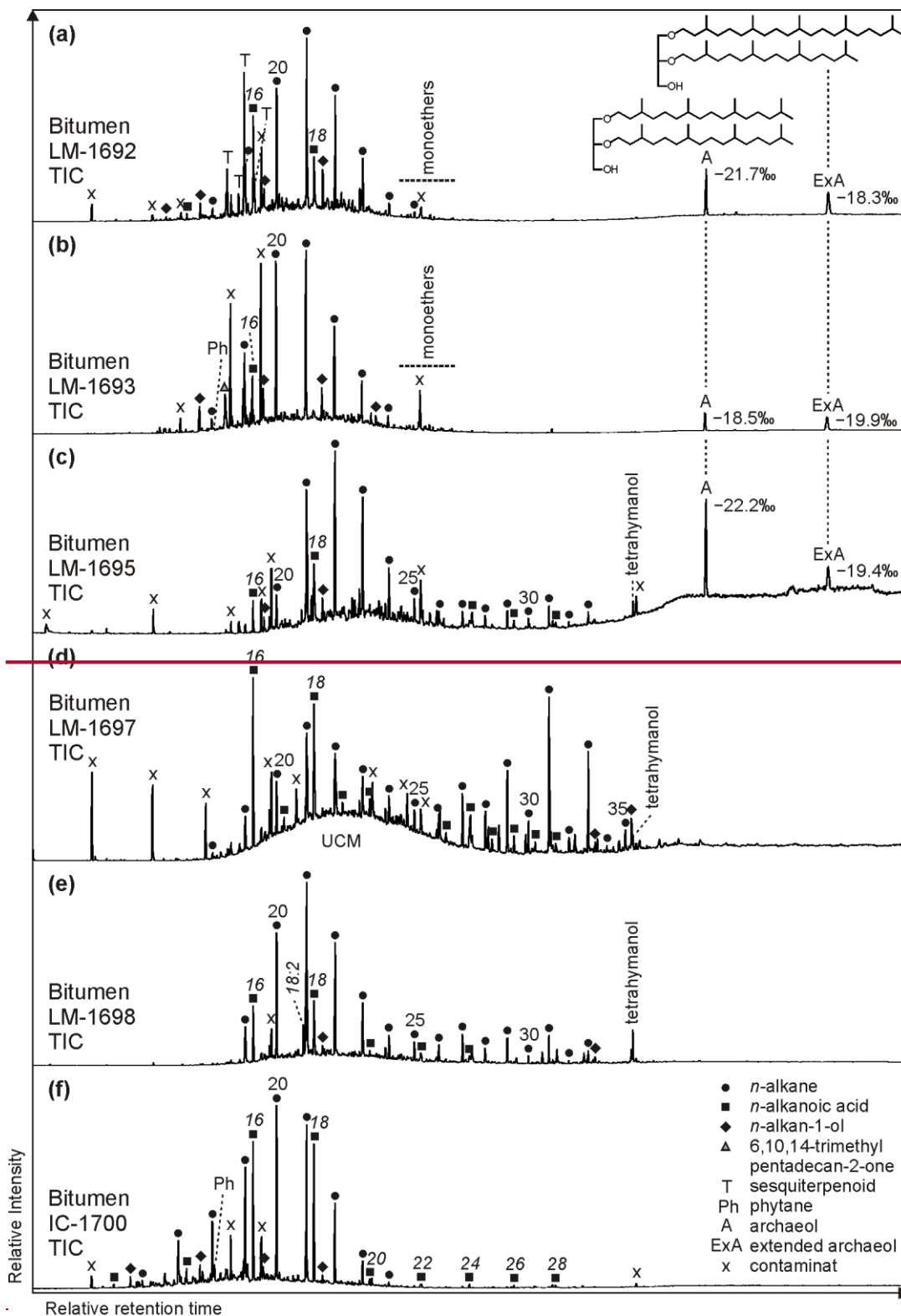
**Figure 2.** Raman spectroscopy of kerogen isolated from Green Bed chert sample LM-1697. (a) Kerogen flakes under reflected light. (b) Detail from (a; dashed box) showing selected spots analyzed via Raman (arrows). (c, d) Raman spectra obtained from several spots on the kerogen flakes, including those denoted in (b); insets magnify the spectral range of ca. 1100–1800  $\text{rel. cm}^{-1}$  and show fits representative for kerogen populations (band order in c: S, D1, D, Dr, G1, G; Rebelo et al., 2016; band order in d: D1, D3, G, D2; Beyssac et al., 2002). Note the close spatial association of kerogen populations of low (immature; c) and high thermal maturity (graphitic; d) within the same sample.

10

15

20





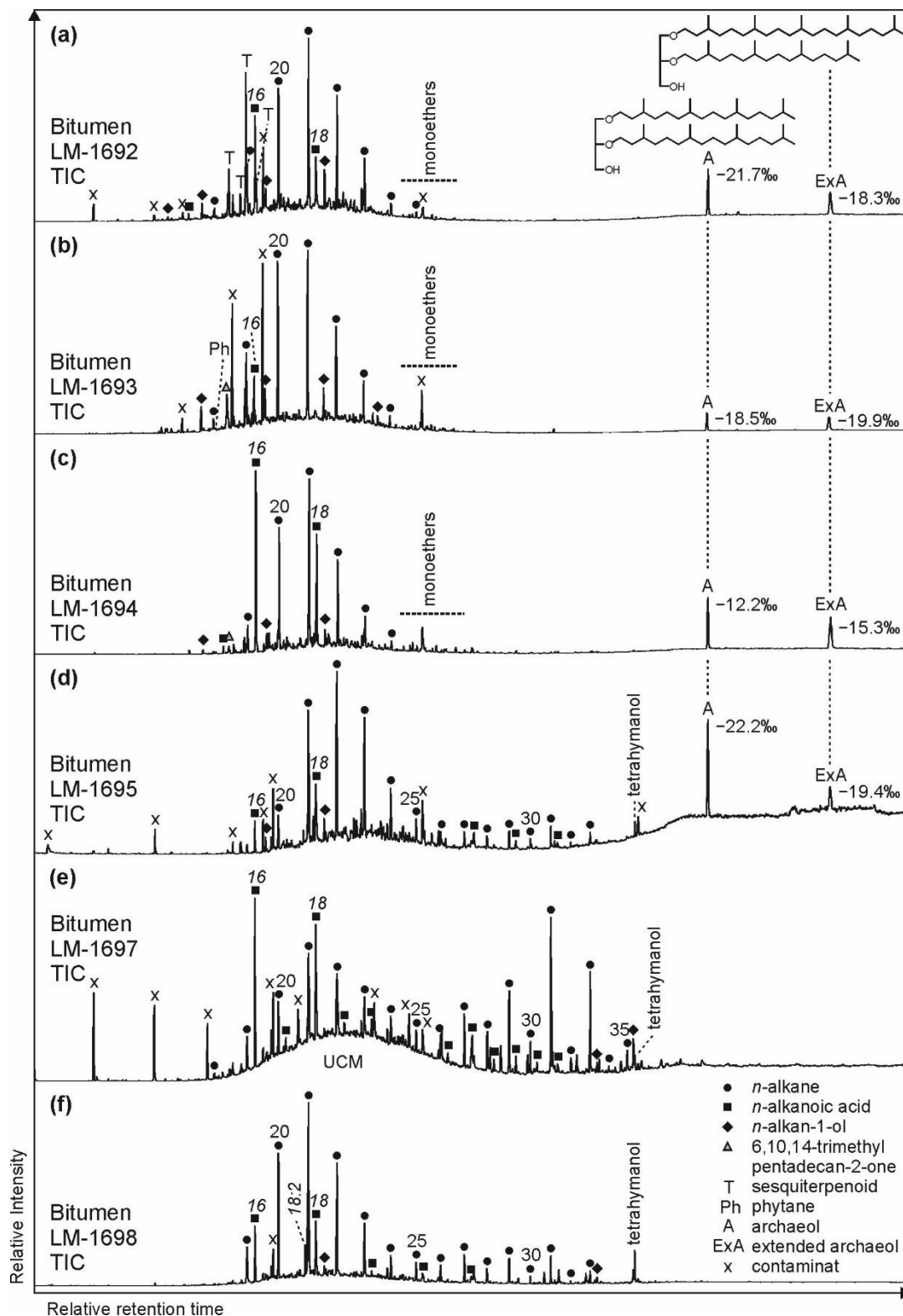
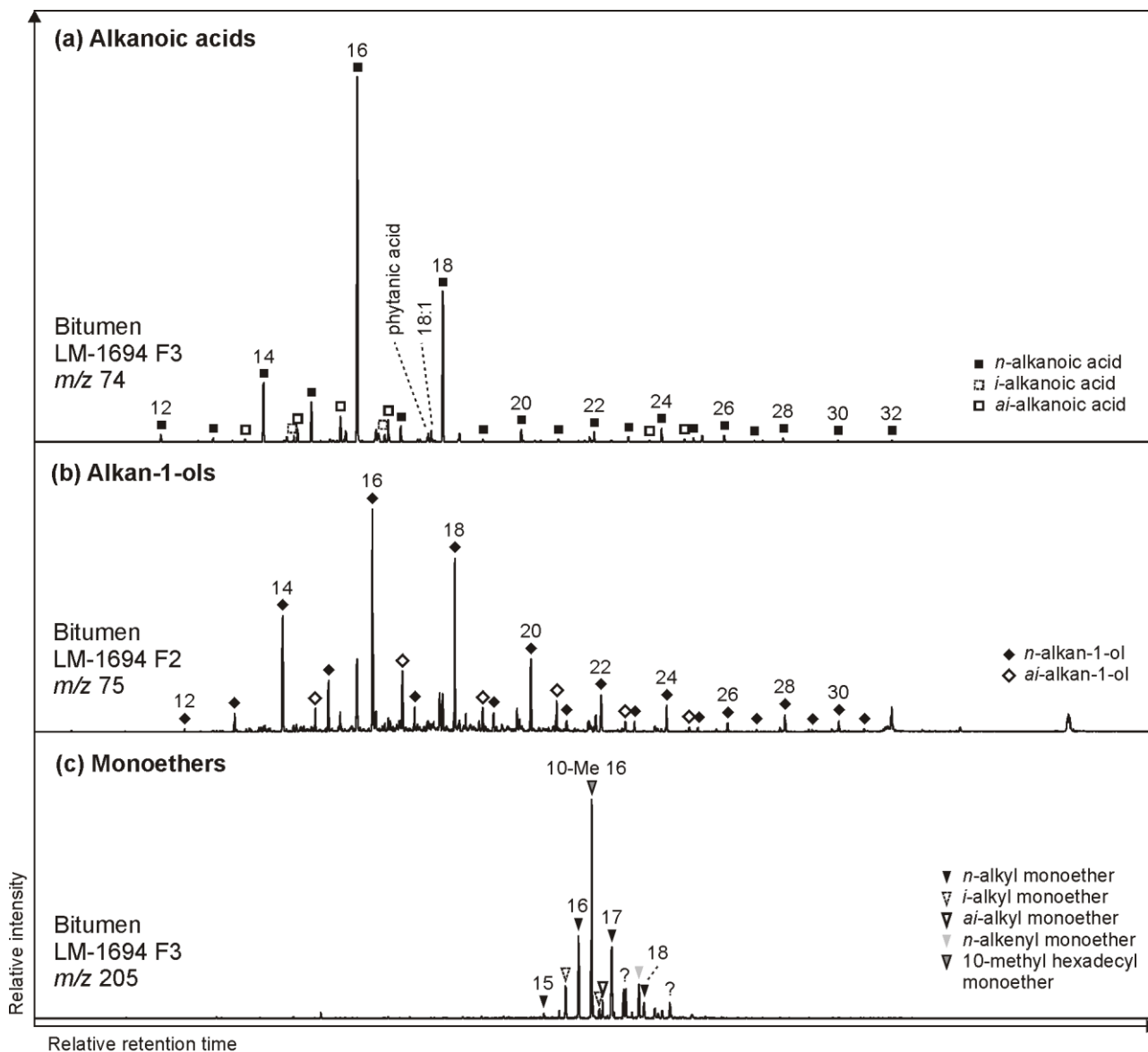


**Figure 3.** Total ion chromatograms (TICs; 10–65 min) of the derivatized bitumens (alcohols were measured as trimethylsilyl ethers, carboxylic acids as methyl esters) from the High Magadi Bed cherts (a–e), d, and the Green Bed cherts (d, e), ~~and the Great Geysir silica sinter (f)~~. Note pronounced *n*-alkanes showing a bell-shaped distribution in the medium-chain range (maxima at *n*-C<sub>20</sub>, *n*-C<sub>21</sub> or *n*-C<sub>22</sub>) in all chromatograms except LM-1697 (maximum at *n*-C<sub>31</sub>). Other prominent compounds are hexa- and octadecanoic acid (all samples), tetrahymanol (LM-1695, LM-1697, LM-1698), glycerol monoethers (LM-1692–~~1693~~1694), and the glycerol diethers archaeol ( $\delta^{13}\text{C}_{\text{V-PDB}}$  between ~~-18.5~~-12.2 and -22.2 ‰) and extended archaeol ( $\delta^{13}\text{C}_{\text{V-PDB}}$  between ~~-18~~-15.3 and -19.9 ‰; LM-1692–1693 and LM-1695). Siloxanes and phthalates were identified as contaminants.

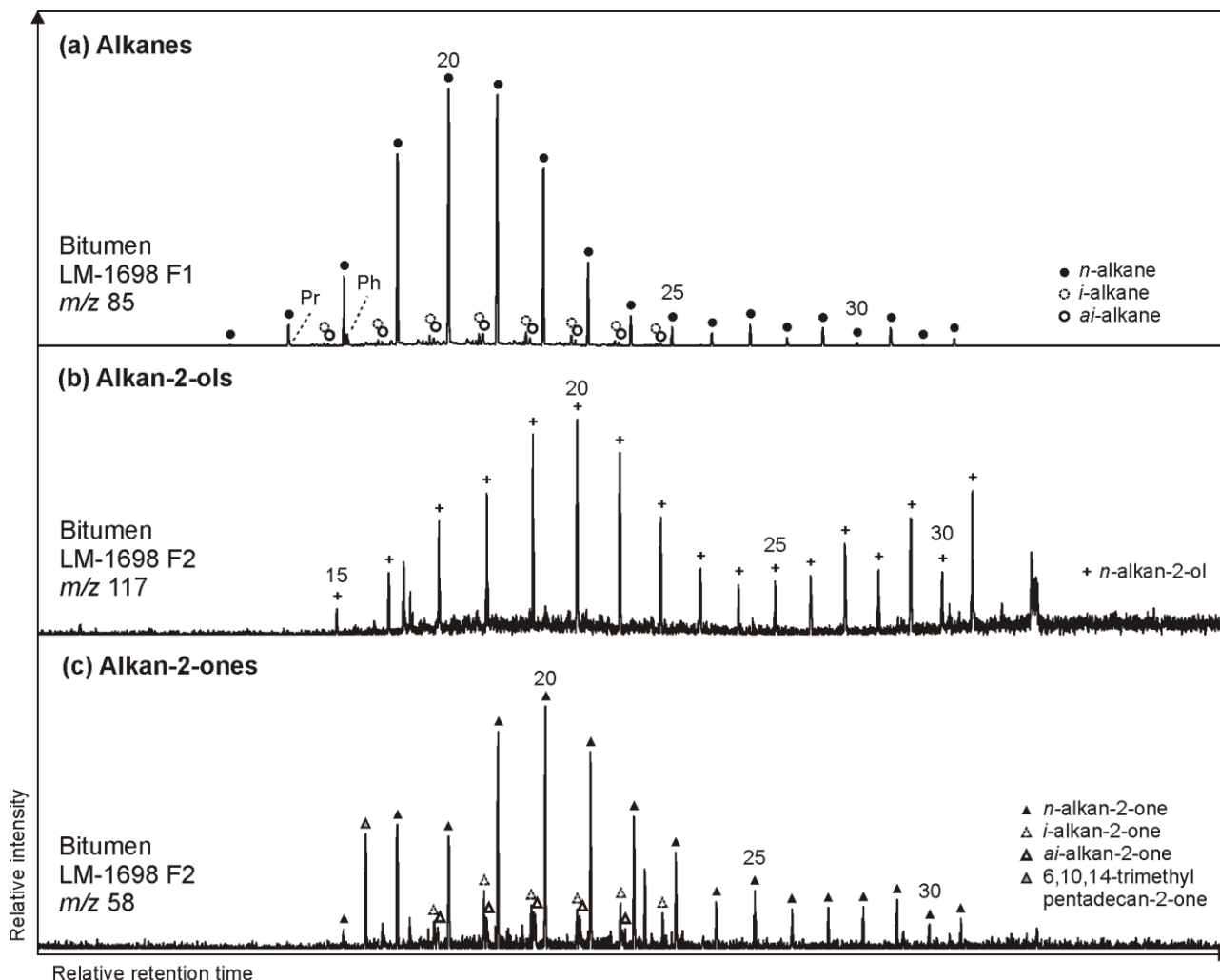
10

15

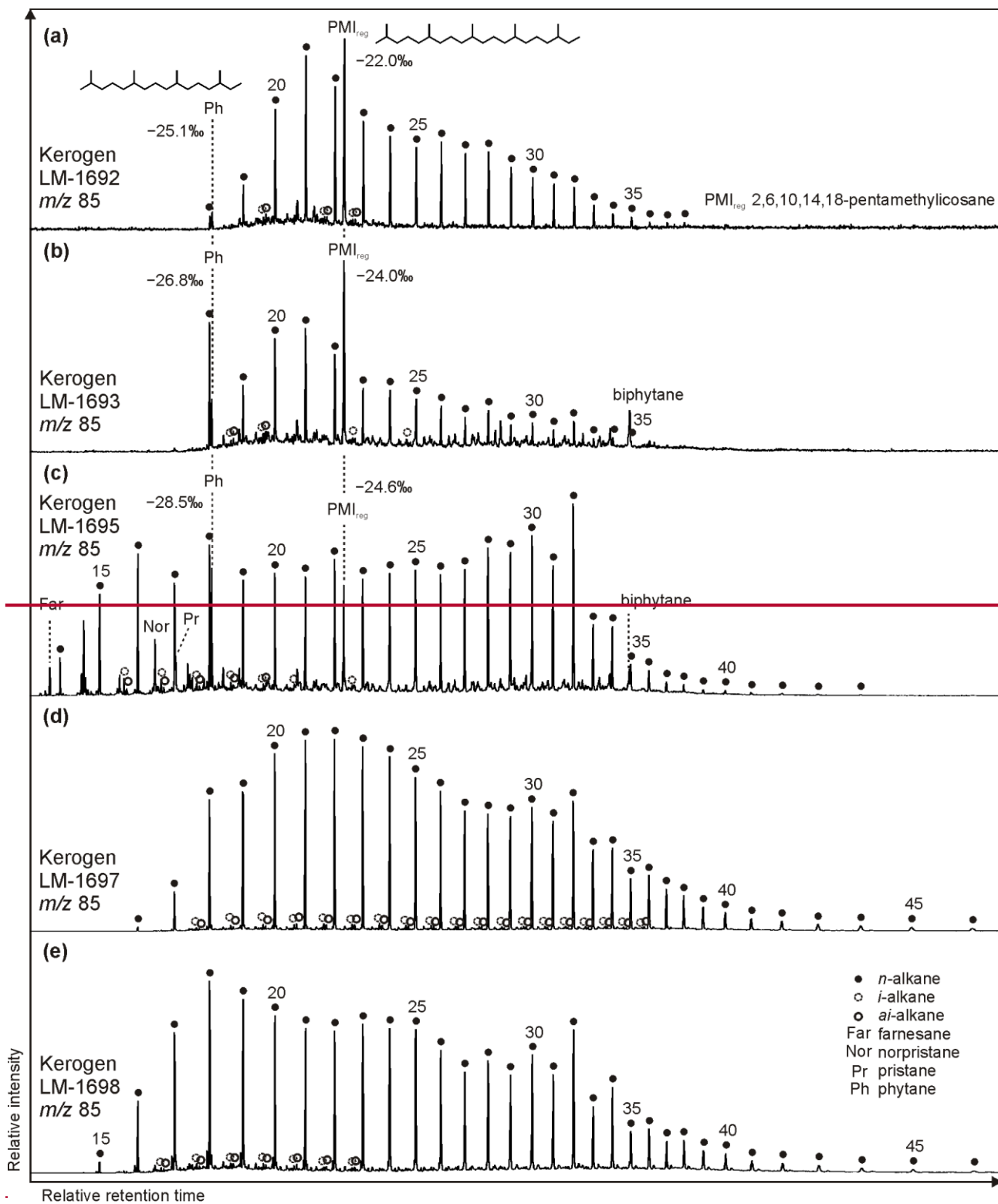
20



**Figure 4.** Partial GC-MS ion chromatograms (10–60 min) of the derivatized alcohol/ketone (F2; alcohols were measured as trimethylsilyl ethers) and polar (F3; carboxylic acids were measured as methyl esters) fractions from bitumen of the High Magadi Bed chert LM-1694. Alkanoic acids ( $m/z$  74; a) and alkan-1-ols ( $m/z$  75; b) show a clear even-over-odd-predominance and dominances of linear C<sub>16</sub> and C<sub>18</sub> homologues. (c) Distribution of glycerol monoethers ( $m/z$  205).



**Figure 5.** Partial GC-MS ion chromatograms (10–55 min) of the hydrocarbon (F1) and derivatized alcohol/ketone fraction (F2; alcohols were measured as trimethylsilyl ethers) from bitumen of the Green Bed chert LM-1698. Medium-chain (~C<sub>20</sub>) alkanes (*m/z* 85; a), alkan-2-ols (*m/z* 117; b) and alkan-2-ones (*m/z* 85; c) show similar distributions with no chain-length-predominance, while long-chain compounds reveal a clear odd-over-even-predominance particularly for alkanes and alkan-2-ols. Hydrothermal cracking of kerogen may produce alkanes that are then converted into alkan-2-ols and subsequently alkan-2-ones (Leif and Simoneit, 1995).



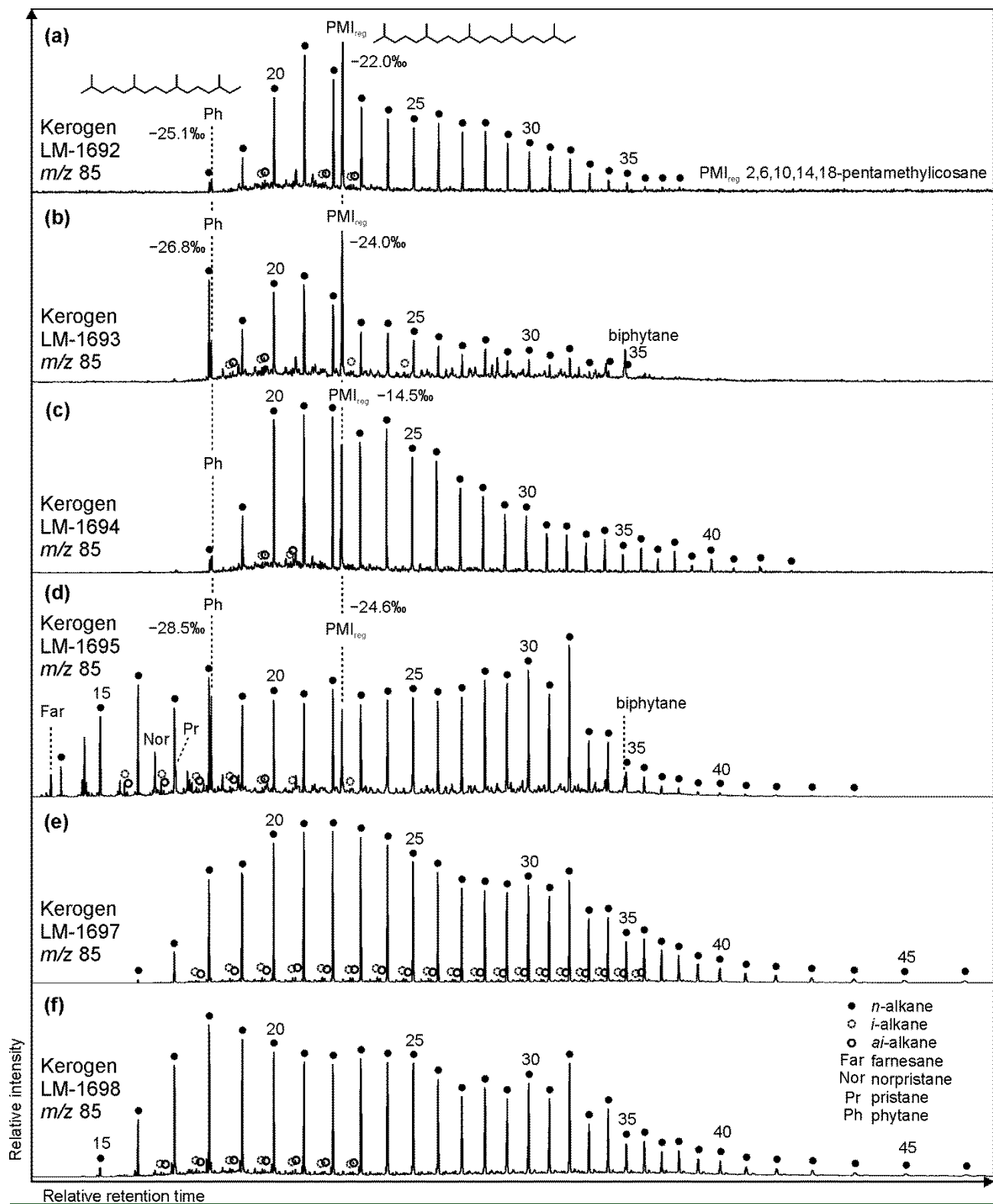


**Figure 6.** Partial GC-MS ion chromatograms ( $m/z$  85; 10–70 min) from kerogen HyPy pyrolysates (high temperature step, up to 520 °C) of High Magadi Bed cherts (a–ed), and Green Bed cherts (d, e, f).  $\delta^{13}\text{C}_{\text{V-PDB}}$  values are given for selected compounds. Note different  $n$ -alkane distributions in the kerogens, with LM-1698 showing the broadest range ( $n$ -C<sub>15</sub> to  $n$ -C<sub>46</sub>). Also note that the regular acyclic isoprenoids phytane and 2,6,10,14,18-pentamethyl icosane are only present in High Magadi Bed chert kerogens (a, b, ed). Furthermore, farnesane, norpristane and pristane appear in LM-1695, while biphytane is visible in LM-1693 and LM-1695.

10

15

20

25

30



**Table 1.** Geochemical bulk data (C, N, S)

	<b>C<sub>org</sub></b>		<b>C<sub>inorg</sub></b>		<b>calc. CaCO<sub>3</sub></b>		<b>N</b>		<b>S</b>	
	wt.%	±	wt.%	±	wt.%	±	wt.%	±	wt.%	±
LM-1692	0.13	0.001					0.004	0.001	0.002	0.001
LM-1693	0.34	0.003	0.01	0.001	0.11	0.001	0.009	0.001	0.002	0.001
LM-1694	0.21	0.002	0.54	0.005	4.47	0.04	0.024	0.012	0.048	0.024
LM-1695	0.04	0.002	0.01	0.001	0.05	0.003	0.002	0.001	0.005	0.001
LM-1696	0.03	0.002	0.04	0.002	0.29	0.003	0.001	0.001	0.002	0.001
LM-1697	0.02	0.001	0.13	0.001	1.06	0.01	0.004	0.001	0.001	0.001
LM-1698	0.02	0.001	0.08	0.004	0.68	0.007	0.002	0.001	0.009	0.001
LM-1699	0.03	0.002	0.01	0.001	0.11	0.001	0.001	0.001	0.003	0.001
IC-1700	0.01	0.001					0.004	0.001	0.003	0.001

5

10

15

20

**Table 2.** Environmental and maturity parameters from biomarker analysis (GC-MS) and Raman spectroscopy. The C<sub>31</sub> hopane S/(S+R) ratios (3<sup>rd</sup> column) are all in the range of 0.5 to 0.6 and therefore near saturation, implying that most organic compounds may have reached early-oil-window (vitrinite reflectance  $\geq 0.6$ ; Killops and Killops, 2005). These results are fully consistent with reflectances inferred from MPI-1 (5<sup>th</sup> and 6<sup>th</sup> column). Raman data (right-most two columns) have been acquired on few specific sample points and therefore reflect the heterogeneity of the sample rather than its bulk properties.

	Pr/Ph <sup>a</sup>	Ph/ <i>n</i> -C <sub>18</sub> <sup>b</sup>	<sup>C<sub>31</sub></sup> S/(S+R) <sup>c</sup>	Phe/MP <sup>d</sup>	MPI-1 <sup>e</sup>	%R <sub>c</sub> <sup>f</sup>	Flu/(Flu+Py) <sup>g</sup>	%R <sub>0</sub> <sup>h</sup>	T <sub>max</sub> [°C] <sup>i</sup>
<i>Bitumen</i>									
LM-1692	0.10	0.49	0.50	0.42	1.02	0.94	0.69		
LM-1693	0.18	0.36	0.58	0.62	0.63	0.66	0.66		
LM-1694	0.06	0.29	0.55	0.37	0.84	0.81	0.60		
LM-1695	0.37	0.39	0.49	0.61	0.69	0.70	0.48		
LM-1696	0.21	0.31	0.59	0.71	0.56	0.61	0.74		
LM-1697	0.25	0.37	0.61	0.95	0.48	0.56	0.79		
LM-1698	0.09	0.26	0.57	0.19	0.99	0.91	0.77		
LM-1699		0.29					0.61		
IC-1700	0.36	0.35		0.93	0.59	0.63	0.96		
<i>Kerogen</i>									
LM-1692		1.89		0.22	1.25	1.10	0.32	0.72	110
LM-1693		0.49		0.10	1.69	1.41	0.44	0.69	110
LM-1694		<u>1.53</u>						0.54	90
LM-1695	0.24	0.99		0.53	1.03	0.94	0.33	0.51	80
LM-1696								0.63	100
LM-1697				0.56	1.00	0.92	0.23	0.32	40
									440 <sup>j</sup>
LM-1698				0.72	0.89	0.85	0.32	0.35	50

<sup>a</sup>Pristane(Pr)/phytane(Ph) ratio

<sup>b</sup>Phytane(Ph)/*n*-octadecane(*n*-C<sub>18</sub>) ratio

<sup>c</sup>17 $\alpha$ , 21 $\beta$ (H)-C<sub>31</sub> hopane 22S/(S+R) ratio

<sup>d</sup>Phenanthrene(Phe)/methylphenanthrene(MP) ratio

10 <sup>e</sup>Methylphenanthrene index = 1.5·(2-MP+3-MP)/(Phe+1-MP+9-MP); Radke and Welte, 1983

<sup>f</sup>Computed vitrinite reflectance = 0.7·MPI-1+0.22 (Boreham et al., 1988), if Phe/MP <1(Brocks et al., 2003a)

<sup>g</sup>Fluoranthene(Flu)/(Flu+pyrene(Py)) ratio

<sup>h</sup>Vitrinite reflectance, calculated from Raman band ratio RA2 (Schito et al., 2017)

<sup>i</sup>Mean maximum temperature, calculated from  $R_0$  (Barker and Pavlewicz, 1994)

<sup>j</sup>Mean maximum temperature, calculated from Raman band ratio R2 (Beysac et al., 2002)

5

10

15

20

25

**Table 3.** Odd-to-even-predominances (OEPs; Scalan and Smith, 1970) in bitumens and kerogens

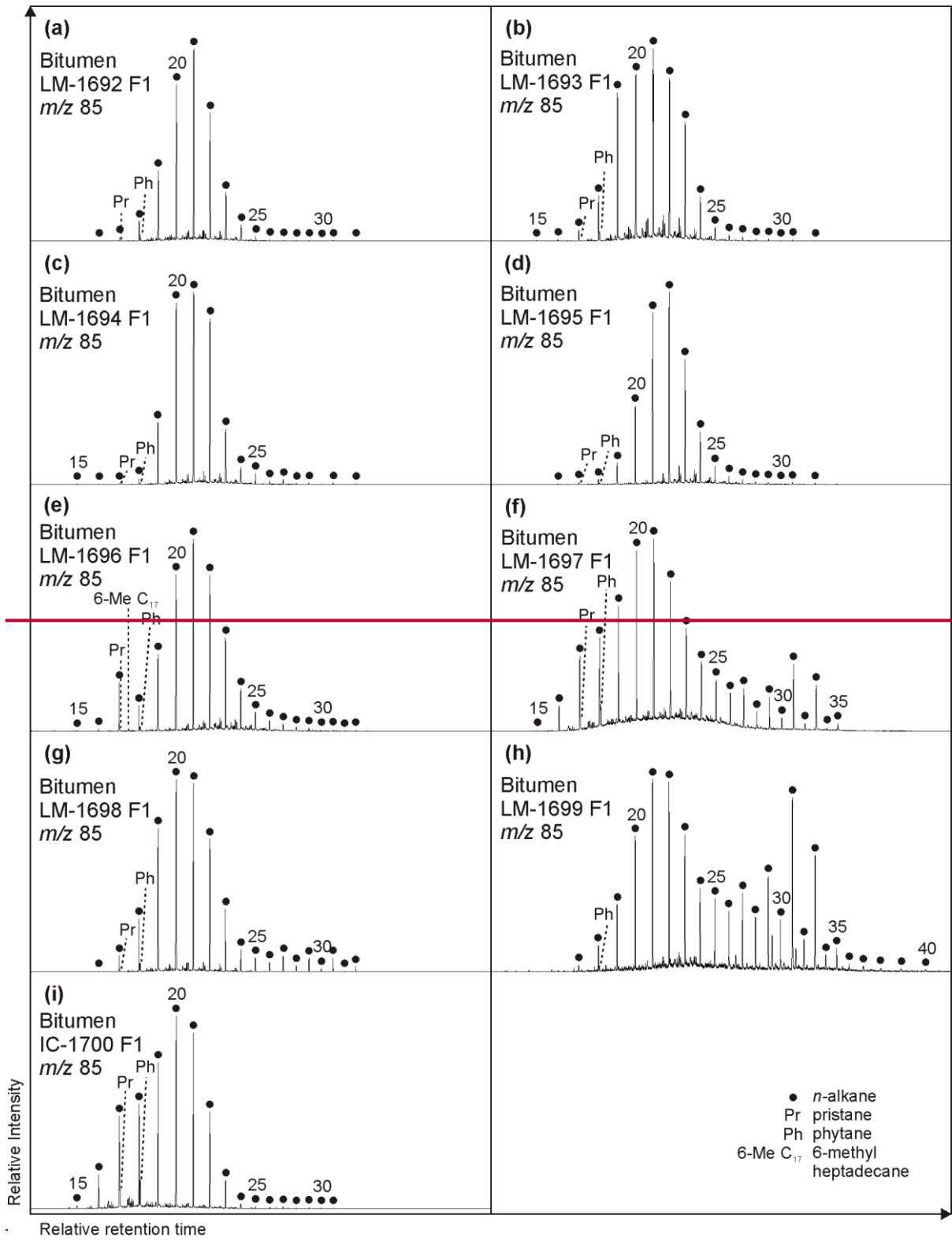
	<i>Alkanoic acids</i>		<i>Alkan-1-ols</i>		<i>Alkan-2-ols</i>		<i>Alkan-2-ones</i>		<i>n-Alkanes</i>	
	OEP 15	OEP 29	OEP 17	OEP 29	OEP 21	OEP 29	OEP 21	OEP 29	OEP 21	OEP 31
<i>Bitumen</i>										
LM-1692	0.2	0.3	0.1	<0.1	1.1		2.1		1.2	2.8
LM-1693	0.4	0.4	0.2	0.1	1.0	2.3	1.5		1.1	3.3
LM-1694	0.1	0.3	0.1	0.1	1.0	5.9	1.8		1.1	5.2
LM-1695	0.1	0.3	0.1	0.1	1.0		1.3		1.1	3.5
LM-1696	0.2	0.4	0.1	<0.1	1.0	2.2	1.3		1.1	2.3
LM-1697	0.2	0.5	0.2	0.3	0.9	1.9	1.1	1.2	1.0	6.5
LM-1698	0.1	0.5	0.2	0.2	1.0	1.9	1.1	1.5	1.0	7.0
LM-1699	0.2	0.4	0.1	0.1	0.8	4.5			1.0	4.0
IC-1700	0.1	0.2	0.2	<0.1	1.1		1.0		1.1	1.8
<i>Kerogen</i>										
LM-1692									1.0	0.9
LM-1693									1.0	0.7
<u>LM-1694</u>									<u>0.8</u>	<u>0.9</u>
LM-1695									1.0	0.7
LM-1697									1.0	0.8
LM-1698									1.0	0.7

$$OEP_n = (C_{n-2} + 6 \cdot C_n + C_{n+2}) / (4 \cdot C_{n-1} + 4 \cdot C_{n+1})^{((-1)^{(n+1)})}$$

**Table 4.** Mean  $\delta^{13}\text{C}_{\text{V-PDB}}$  values in ‰ of key compound classes and selected biomarkers in bitumens and kerogens

	LM-1692	LM-1693	LM-1694	LM-1695	LM-1696	LM-1697	LM-1698	LM-1699	IC-1700
<i>Bitumen</i>									
Long-chain <i>n</i> -alkanoic acids (C <sub>24–28</sub> )	-25.2	-27.0	-26.3	-28.9	-22.4	-25.1	-27.4	-29.6	-32.5
Long-chain <i>n</i> -alkan-1-ols (C <sub>24–32</sub> )	-25.0	-32.3	-20.2	-29.1	-25.1	-23.7	-23.2	-24.0	-26.1
Long-chain <i>n</i> -alkanes (C <sub>25–33</sub> )				-30.9	-30.1	-31.5	-26.2	-26.5	
Short-chain <i>n</i> -alkanoic acids (C <sub>12–18</sub> )	-27.6	-26.5	-26.8	-28.9	-24.0	-25.8	-25.6	-27.0	-25.2
Short-chain <i>n</i> -alkan-1-ols (C <sub>12–18</sub> )	-33.5	-32.2	-35.9	-30.5	-32.6	-33.1	-29.4	-31.8	-27.7
Medium-chain <i>n</i> -alkanes (C <sub>17–24</sub> )	-32.1	-31.7	-31.7	-32.8	-32.6	-33.3	-33.3	-29.7	-35.7
Phytane	-33.3	-30.9	-30.0	-36.1	-34.7	-33.8	-35.3		-38.6
Archaeol	-21.7	-18.5	-12.2	-22.2	-14.8			-16.6	
Extended archaeol	-18.3	-19.9	-15.3	-19.4	-19.6				
Monoethers	-20.2	-20.2	-10.9	-18.6					
<i>Kerogen</i>									
Long-chain <i>n</i> -alkanes (C <sub>25–40</sub> )	-27.6	-30.2	<u>-22.7</u>	-24.9		-21.9	-27.1		
Medium-chain <i>n</i> -alkanes (C <sub>17–24</sub> )	-30.5	-31.4	<u>-27.3</u>	-28.3		-23.5	-34.2		
Phytane	-25.1	-26.8		-28.5					
PMI <sub>reg</sub> <sup>a</sup>	-22.0	-24.0	<u>-14.5</u>	-24.6					

<sup>a</sup>2,6,10,14,18-pentamethylcosane (regular acyclic C<sub>25</sub> isoprenoid)



## Supplementary information for:

### Organic signatures in Pleistocene cherts from Lake Magadi (Kenya)—implications for early Earth hydrothermal deposits

Manuel Reinhardt, Walter Goetz, Jan-Peter Duda, Christine Heim, Joachim Reitner, Volker Thiel

5 Correspondence to: Manuel Reinhardt (mreinha@gwdg.de)

#### Interior-versus-exterior experiments (LM-1692 and LM-1695)

10 Crushed and powdered surface cut-offs (exterior) and the inner blocks (interior) of LM-1692 and LM-1695 were extracted and derivatized using a similar protocol as described in Section 2.2. In brief, 10 g sample powder (2 × interior and 2 × exterior per sample) was ultrasonically extracted with 20 mL DCM/MeOH (2/1, v/v), DCM/MeOH (3/1, v/v) and DCM (10 min, respectively). All TOEs were desulfurized with reduced Cu and hydrolyzed using TMCS/MeOH (1/9, v/v; heated at 80 °C for 1 h 30 min). Subsequently, the extracts were derivatized with BSTFA/pyridine (3/2, v/v; heated at 40 °C for 1h). All samples were analyzed via GC–MS using the parameters described in Section 2.4.

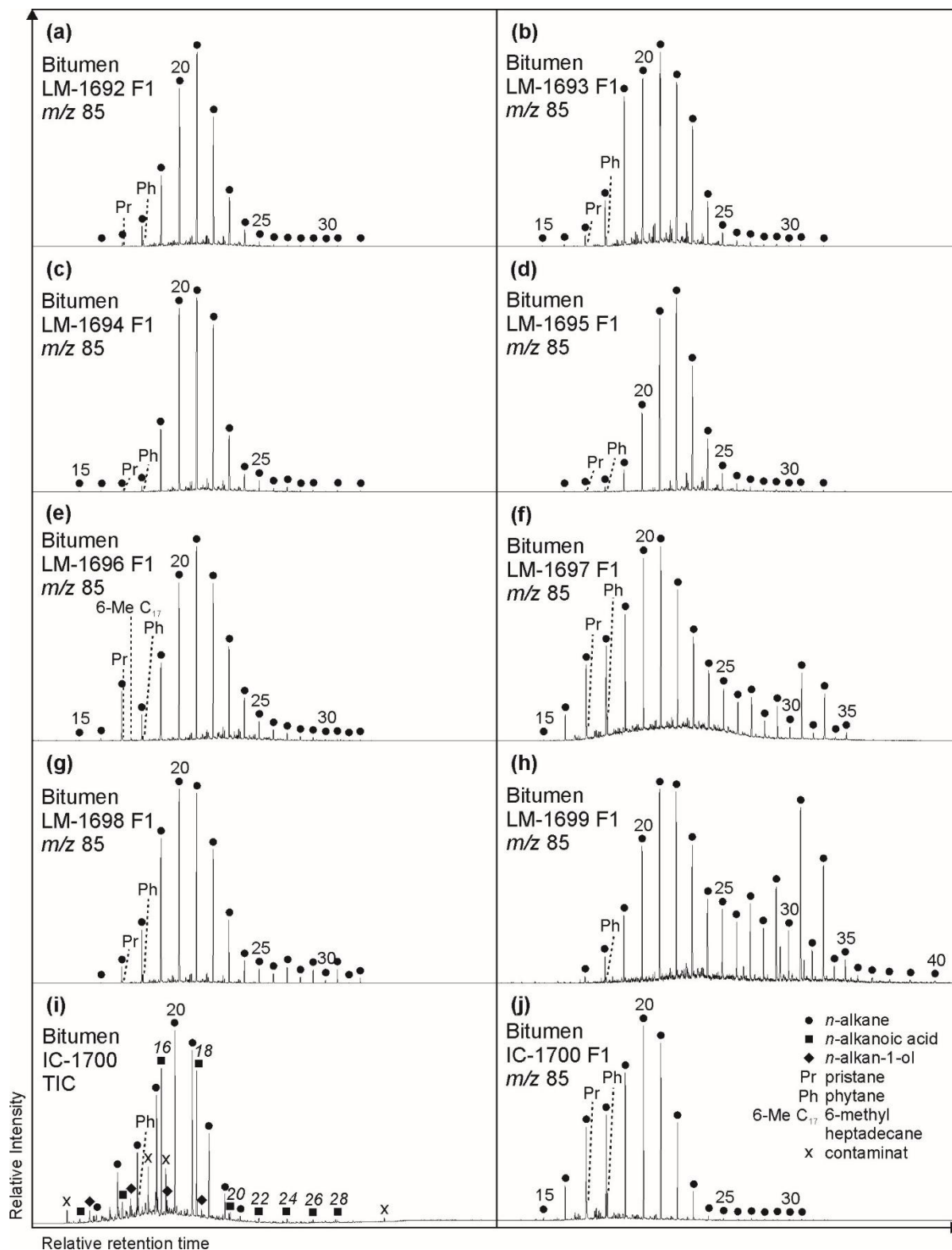




**Figure S1.** Partial GC-MS ion chromatograms ( $m/z$  85; 10–60 min) of the hydrocarbon fractions (F1) from bitumens of the Magadi cherts (LM-1692–1699; a–h). A total GC-MS ion chromatogram (TIC; 10–60 min) and a partial GC-MS ion chromatogram ( $m/z$  85; 10–60 min) of the Great Geysir reference sinter (IC-1700; ~~i~~) is shown in (~~i~~) and (j), respectively. A narrow bell-shaped  $n$ -alkane distribution in the mid-chain range (around  $n$ -C<sub>21</sub>) is visible in all samples analyzed.

5 Additionally, odd-numbered long-chain  $n$ -alkanes are abundant in bitumens from most of the Green Bed cherts (LM-1697–1699; f–h). Notably, 6-methyl heptadecane appears in LM-1696 (e).

10

15

20

25

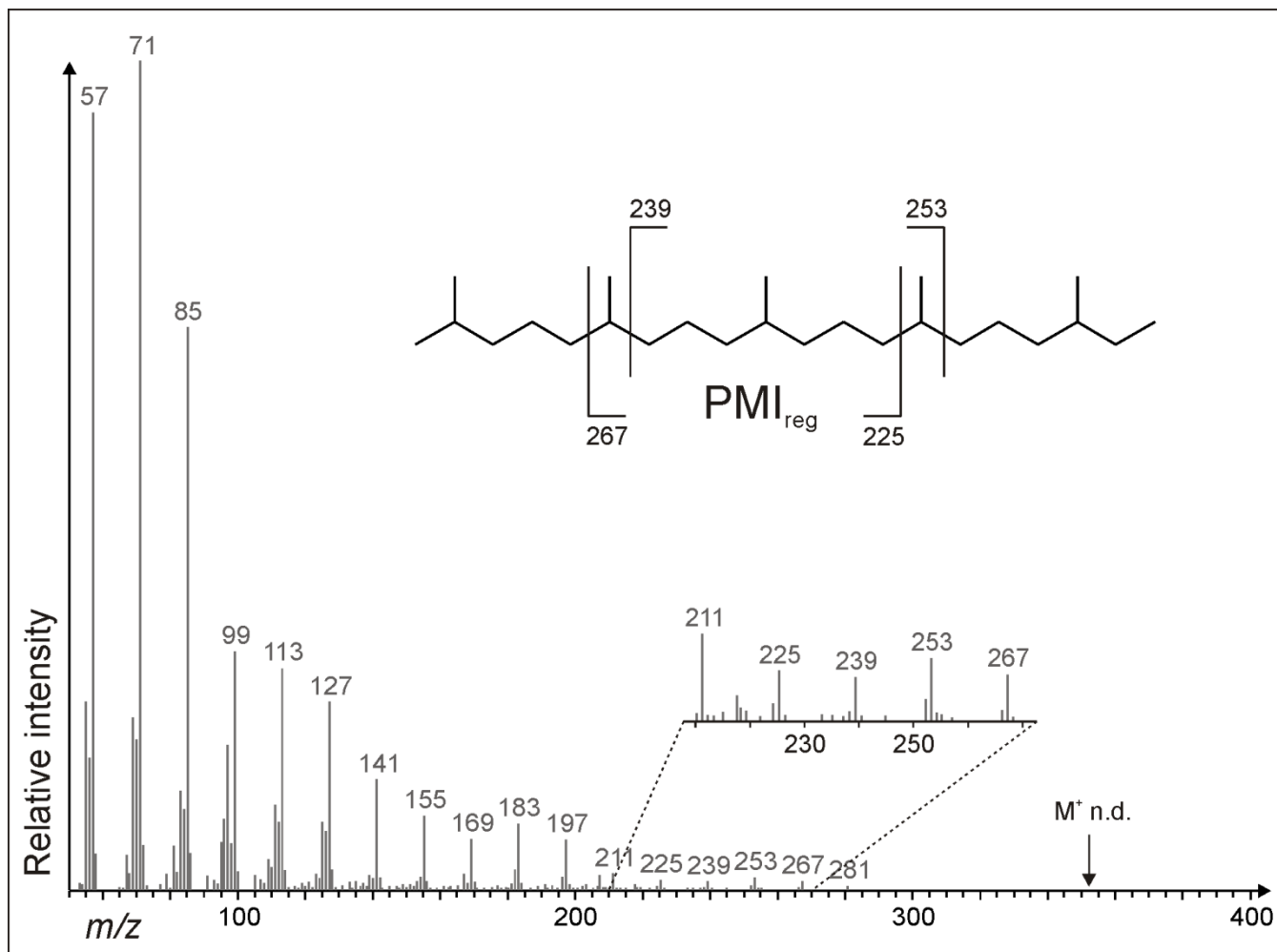


**Figure S2.** Mass spectrum of the regular C<sub>25</sub> isoprenoid 2,6,10,14,18-pentamethylcosane (PMI<sub>reg</sub>) from kerogen of LM-1693 (similar in kerogen pyrolysates from LM-1692 and LM-1695). Typical for this C<sub>25</sub> isoprenoid isomer is the high higher abundance of the fragments at 225 and 253 amu, as compared to 239 and 267 amu (Risatti et al., 1984; Greenwood and Summons, 2003). The molecular ion (M<sup>+</sup>) at 352 amu was not detected (n.d.).

**Table S1.** Mean  $\delta^{13}\text{C}_{\text{V-PDB}}$  values in ‰ of fatty acids from bitumens

	LM-1692		LM-1693		LM-1694		LM-1695		LM-1696		LM-1697		LM-1698		LM-1699		IC-1700	
	Mean	±	Mean	±	Mean	±	Mean	±	Mean	±	Mean	±	Mean	±	Mean	±	Mean	±
C <sub>12:0</sub>	-25.7	0.1	-25.0	0.1													-26.5	0.1
C <sub>13:0</sub>			-26.1	0.5													-21.2	0.2
C <sub>14:0</sub>	-26.1	<0.1	-27.5	0.1	-27.4	<0.1	-32.2	0.1			-28.5	0.8					-26.4	0.2
<i>i</i> -C <sub>15:0</sub>			-25.3	<0.1	-27.3	0.1											-18.2	<0.1
<i>ai</i> -C <sub>15:0</sub>	-30.9	<0.1	-28.8	0.1	-29.5	0.1											-21.2	0.7
C <sub>15:0</sub>	-27.8	0.1	-28.0	0.2	-26.1	0.1	-31.4	0.2			-21.5	0.4	-29.2	<0.1	-23.9	0.1	-24.8	0.2
C <sub>16:1</sub>													-26.9	0.5				
C <sub>16:1</sub>													-23.7	0.5				
C <sub>16:0</sub>	-28.3	<0.1	-25.3	<0.1	-26.4	<0.1	-23.9	0.1	-27.0	0.5	-27.5	0.1	-23.9	<0.1	-25.3	0.1	-26.1	<0.1
<i>ai</i> -C <sub>17:0</sub>	-34.0	<0.1	-30.0	0.3	-25.7	0.1												
C <sub>17:0</sub>	-29.4	0.2	-27.3	0.2	-24.8	0.7	-27.3	<0.1	-18.8	0.1	-22.8	0.1	-24.1	0.9	-30.5	0.5	-24.2	0.2
C <sub>18:2</sub>			-27.8	1.0	-18.3	0.7			-35.2	0.2			-27.5	0.2				
C <sub>18:1</sub>	-29.1	0.1	-26.5	0.1	-25.8	<0.1			-26.9	<0.1	-28.1	0.5	-23.2	0.2	-30.2	0.1		
C <sub>18:1</sub>	-21.7	0.2	-22.5	0.1									-21.2	0.2				
C <sub>18:0</sub>	-28.3	0.2	-26.3	0.1	-29.1	0.1	-29.6	0.1	-26.2	0.4	-28.7	0.1	-25.1	0.2	-28.4	0.7	-27.2	0.1
C <sub>19:0</sub>											-22.1	0.1	-32.0	0.1			-27.9	<0.1
C <sub>20:0</sub>	-28.8	0.6	-28.2	<0.1	-27.2	<0.1			-20.2	0.1	-20.8	0.1	-27.3	0.7	-27.5	0.2	-21.1	0.1
C <sub>21:0</sub>											-21.3	<0.1	-30.9	0.3				
C <sub>22:0</sub>								-30.5	0.3	-24.3	0.1	-28.0	0.7	-26.7	<0.1	-33.7	0.3	
C <sub>23:0</sub>											-25.7	<0.1	-30.8	0.1			-30.6	<0.1
C <sub>24:0</sub>	-24.5	0.1	-28.0	0.1	-22.2	0.1	-28.9	0.1	-28.5	0.3	-26.3	0.1	-27.5	0.1	-28.8	<0.1	-29.5	0.1
<i>i</i> -C <sub>25:0</sub>			-24.8	0.2														
<i>ai</i> -C <sub>25:0</sub>			-27.1	0.2														
C <sub>25:0</sub>			-22.5	0.2							-26.8	0.1	-24.7	0.7			-33.8	0.1
C <sub>26:0</sub>	-25.8	0.2	-30.6	<0.1	-30.4	0.4			-16.3	0.2	-24.6	0.2	-30.0	0.3	-30.5	0.3	-35.4	0.1
C <sub>27:0</sub>											-22.5	0.2					-31.9	0.2
C <sub>28:0</sub>											-25.4	<0.1					-32.0	<0.1

**Table S2.** Mean  $\delta^{13}\text{C}_{\text{V-PDB}}$  values in ‰ of alcohols, ketones, mono- and diethers from bitumens

	LM-1692		LM-1693		LM-1694		LM-1695		LM-1696		LM-1697		LM-1698		LM-1699		IC-1700				
	Mean	±	Mean	±	Mean	±	Mean	±	Mean	±	Mean	±	Mean	±	Mean	±	Mean	±			
<i>Alkan-1-ols</i>																					
C <sub>12</sub>																		-29.9	0.4		
C <sub>13</sub>																			-25.2	0.1	
C <sub>14</sub>	-28.5	0.2	-39.5	0.1	-37.3	0.1	-19.6	0.5	-27.1	0.7			-19.4	0.2					-30.2	0.1	
C <sub>15</sub>																				-27.3	<0.1
C <sub>16</sub>	-34.8	0.2	-25.1	<0.1	-35.5	0.4	-36.0	0.3	-35.9	0.2	-33.1	0.2	-33.6	0.4	-30.9	0.3				-24.4	0.1
C <sub>18</sub>	-37.2	0.3	-31.9	0.2	-35.0	0.3	-35.9	0.4	-34.8	0.1	-33.2	<0.1	-35.1	0.4	-32.8	0.4				-29.4	0.3
C <sub>20</sub>	-30.9	0.1	-29.9	0.6	-32.7	0.1	-30.3	0.2	-29.8	0.1	-24.8	0.2	-29.5	0.1	-30.9	0.1					
C <sub>21</sub>							-33.3	0.2													
C <sub>22</sub>	-29.6	0.4	-32.4	0.3	-28.7	0.1	-30.3	0.2	-25.2	0.4	-34.6	0.2	-26.7	0.3	-31.5	0.3				-25.9	0.2
C <sub>23</sub>													-31.1	0.1	-20.2	0.4					
C <sub>24</sub>	-20.2	0.3	-36.5	0.1	-28.3	0.3	-32.3	0.6	-30.1	0.7	-22.6	0.8	-25.0	0.2	-30.0	0.3				-24.0	0.1
C <sub>25</sub>													-17.5	0.2	-25.3	0.2					
C <sub>26</sub>	-32.1	0.5	-33.8	0.7	-17.4	0.2	-28.5	0.9	-26.5	0.3	-29.2	0.1	-21.7	0.3	-21.8	0.2				-27.7	0.5
C <sub>27</sub>													-26.4	0.3							
C <sub>28</sub>	-21.3	1.0	-26.7	0.5	-20.6	0.4	-26.6	1.0	-18.7	0.3	-22.8	0.1	-25.4	<0.1	-23.5	0.1				-23.0	0.2
C <sub>30</sub>					-14.6	0.3					-20.3	0.7			-19.6	0.1				-29.5	0.5
C <sub>32</sub>	-26.4	0.7																			
<i>Glycerol mono- and diethers</i>																					
<i>i</i> -C <sub>16:0</sub>	-21.8	0.1	-20.3	<0.1	-12.2	<0.1															
C <sub>16:0</sub>	-20.4	0.1	-20.2	0.7	-11.4	0.4															
10Me-C <sub>16:0</sub>	-21.5	0.1	-23.0	0.1	-19.7	<0.1															
<i>i</i> -C <sub>17:0</sub>	-25.2	0.2	-21.3	0.5																	
<i>ai</i> -C <sub>17:0</sub>	-17.4	0.1	-25.0	0.7																	
C <sub>17:0</sub>	-19.0	0.1	-26.9	0.1	-10.7	0.2															
Me-C <sub>17:0</sub>	-22.1	0.1	-17.9	0.4	-10.9	0.1															
Me-C <sub>17:0</sub>	-22.5	0.3	-9.8	<0.1	-9.4	<0.1	-18.6	0.1													
C <sub>18:1</sub>	-20.9	0.2	-15.7	0.1																	
C <sub>18:1</sub>	-19.1	0.8	-22.9	0.7	-7.0	0.2															
C <sub>18:0</sub>	-12.5	0.2	-19.0	0.8	-5.7	0.4															
A	-21.7	0.4	-18.5	0.5	-12.2	0.4	-22.2	0.1	-14.8	0.5					-16.6	0.4					
ExA	-18.3	0.6	-19.9	0.2	-15.3	0.4	-19.4	0.5	-19.6	0.5											
<i>Other compounds</i>																					
Tetrahyd.							-33.3	0.3	-27.7	0.1	-25.4	0.2	-24.1	0.5	-29.3	0.2					

**Table S3.** Mean  $\delta^{13}\text{C}_{\text{V-PDB}}$  values in ‰ of alkanes and isoprenoids from bitumens

	LM-1692		LM-1693		LM-1694		LM-1695		LM-1696		LM-1697		LM-1698		LM-1699		IC-1700			
	Mean	±	Mean	±	Mean	±	Mean	±	Mean	±	Mean	±	Mean	±	Mean	±	Mean	±		
<i>n</i> -C <sub>16</sub>																	-37.1	0.1		
<i>n</i> -C <sub>17</sub>			-30.5	0.6					-30.1	0.6	-38.0	1.2							-32.9	<0.1
6Me-C <sub>17</sub>									-30.3	0.2										
<i>n</i> -C <sub>18</sub>	-32.5	<0.1	-32.1	<0.1	-31.8	0.5	-35.6	0.5	-33.8	<0.1	-34.4	0.1	-34.3	0.1					-33.4	<0.1
<i>n</i> -C <sub>19</sub>	-32.0	0.2	-31.6	0.1	-32.0	0.1	-33.3	0.3	-32.9	0.5	-33.3	0.4	-32.9	<0.1	-14.7	0.5			-35.2	0.1
<i>i</i> -C <sub>20</sub>	-31.1	0.1	-30.0	<0.1	-34.1	0.3							-29.8	0.2						
<i>ai</i> -C <sub>20</sub>	-32.1	0.8	-33.2	0.1	-29.0	0.8							-27.5	0.1						
<i>n</i> -C <sub>20</sub>	-31.4	<0.1	-30.7	0.2	-30.9	0.3	-32.3	0.4	-33.2	<0.1	-32.6	0.4	-32.7	0.2	-38.9	0.3			-33.6	<0.1
<i>i</i> -C <sub>21</sub>	-32.3	<0.1	-31.2	<0.1	-32.7	<0.1	-30.9	0.1	-34.4	0.7	-35.3	0.5	-33.2	0.3						
<i>ai</i> -C <sub>21</sub>	-29.8	<0.1	-31.5	<0.1	-30.5	0.3	-31.9	0.4	-28.6	0.1	-36.5	0.3	-32.2	0.1						
<i>n</i> -C <sub>21</sub>	-31.6	<0.1	-31.0	0.2	-31.2	0.4	-31.9	0.1	-32.9	<0.1	-31.6	<0.1	-33.6	<0.1	-35.0	0.7			-34.0	<0.1
<i>i</i> -C <sub>22</sub>	-29.9	0.8	-33.2	0.1	-29.6	0.1	-34.0	0.3	-34.1	0.1	-34.9	0.1	-33.6	0.1						
<i>ai</i> -C <sub>22</sub>	-29.1	0.2	-37.4	0.8	-28.9	0.1	-34.4	0.2	-33.3	<0.1	-32.6	0.1	-33.3	0.3						
<i>n</i> -C <sub>22</sub>	-32.1	0.2	-31.7	<0.1	-32.0	0.3	-32.3	0.1	-32.8	<0.1	-31.6	0.2	-34.4	0.2	-36.7	0.3			-37.5	<0.1
<i>i</i> -C <sub>23</sub>	-33.8	0.1	-30.3	0.1	-29.1	0.1	-32.1	<0.1	-31.4	<0.1	-36.5	0.1	-31.3	0.2						
<i>ai</i> -C <sub>23</sub>	-33.7	0.2	-27.3	0.1	-28.8	0.1	-33.1	0.1	-32.1	0.1	-39.1	0.4	-30.2	0.4						
<i>n</i> -C <sub>23</sub>	-32.1	<0.1	-32.2	0.2	-32.2	<0.1	-32.4	0.1	-32.6	0.3	-34.5	<0.1	-33.4	0.1	-25.4	0.1			-39.6	0.1
<i>i</i> -C <sub>24</sub>	-31.8	<0.1	-33.9	0.1	-32.5	<0.1	-29.8	0.4	-35.2	<0.1			-36.3	0.3						
<i>ai</i> -C <sub>24</sub>	-26.2	0.5	-32.6	0.2	-31.5	0.1	-29.0	0.1	-34.3	0.3			-29.5	0.7						
<i>n</i> -C <sub>24</sub>	-32.7	0.2	-33.7	<0.1	-31.6	<0.1	-31.8	0.2	-32.5	0.5	-30.6	0.2	-32.2	0.1	-27.6	0.2			-39.2	<0.1
<i>i</i> -C <sub>25</sub>	-30.8	<0.1	-31.2	0.4	-25.3	<0.1	-34.6	0.1	-28.4	0.4										
<i>ai</i> -C <sub>25</sub>	-26.8	0.4	-35.9	0.4	-22.6	0.2	-30.4	0.7	-28.0	0.2										
<i>n</i> -C <sub>25</sub>							-32.0	<0.1	-30.2	0.1	-34.7	0.1	-34.9	0.2	-25.6	0.1				
<i>n</i> -C <sub>26</sub>							-29.8	0.1	-29.9	0.2	-34.0	0.2	-25.8	<0.1	-34.8	0.3				
<i>n</i> -C <sub>27</sub>											-36.3	0.2	-23.7	0.1	-30.8	0.1				
<i>n</i> -C <sub>28</sub>											-33.8	0.2	-24.2	0.3	-27.9	0.1				
<i>n</i> -C <sub>29</sub>											-28.8	0.4	-23.9	0.5	-21.5	0.2				
<i>n</i> -C <sub>30</sub>															-26.9	0.1				
<i>n</i> -C <sub>31</sub>											-20.9	0.6	-24.4	0.1	-21.1	0.4				
<i>n</i> -C <sub>32</sub>															-24.5	0.2				
<i>n</i> -C <sub>33</sub>															-25.8	<0.1				
<i>Isoprenoids</i>																				
Pr			-31.7	0.1					-30.2	0.1	-32.2	0.2	-35.8	0.1					-34.5	0.2
Ph	-33.3	<0.1	-30.9	0.4	-30.0	0.6	-36.1	1.2	-34.7	0.1	-33.8	0.1	-35.3	<0.1					-38.6	0.1

**Table S4.** Mean  $\delta^{13}\text{C}_{\text{V-PDB}}$  values in ‰ of alkanes and isoprenoids from kerogens

	LM- 1692	LM- 1693	LM- <u>1694</u>	LM- 1695	LM- 1697	LM- 1698	-			
	Mean	±	Mean	±	Mean	±	<u>Mean</u>	±		
<i>n</i> -C <sub>15</sub>				-30.5	0.6					
<i>n</i> -C <sub>16</sub>				-30.4	0.1		-30.9	0.1		
<i>n</i> -C <sub>17</sub>				-30.3	<0.1	-26.0	0.3	-31.3 <0.1		
<i>n</i> -C <sub>18</sub>	-36.3	0.7	-35.0	0.9	-31.5	0.2	-25.4	0.4	-34.9 <0.1	
<i>n</i> -C <sub>19</sub>	-32.0	0.3	-29.2	0.7	-27.2	0.1	-24.0	<0.1	-34.6 0.1	
<i>n</i> -C <sub>20</sub>	-27.8	0.6	-33.7	0.8	<u>-34.6</u>	<u>0.6</u>	-26.9	0.1	-22.1 <0.1	-35.8 0.2
<i>n</i> -C <sub>21</sub>	-28.1	0.4	-31.5	0.3	<u>-29.6</u>	<u>0.5</u>	-27.6	0.7	-22.0 0.2	-34.3 0.8
<i>n</i> -C <sub>22</sub>	-31.1	<0.1	-30.9	0.2	<u>-26.6</u>	<u>0.1</u>	-28.8	0.1	-23.0 0.9	-32.9 0.1
<i>n</i> -C <sub>23</sub>	-31.8	0.1	-29.3	0.4	<u>-21.0</u>	<u>0.1</u>	-27.3	<0.1	-22.4 0.1	-34.5 0.8
<i>n</i> -C <sub>24</sub>	-26.5	0.6	-30.5	0.3	<u>-24.7</u>	<u>0.4</u>	-26.9	0.2	-22.9 0.5	-35.3 0.2
<i>n</i> -C <sub>25</sub>	-28.7	0.5	-30.9	1.0	<u>-22.7</u>	<u>0.2</u>	-27.3	<0.1	-24.4 0.3	-34.9 <0.1
<i>n</i> -C <sub>26</sub>	-26.6	0.5	-27.4	0.1	<u>-23.3</u>	<u>0.2</u>	-25.4	<0.1	-24.1 0.1	-29.7 0.1
<i>n</i> -C <sub>27</sub>	-29.8	0.3	-30.6	0.1	<u>-18.9</u>	<u>0.1</u>	-24.8	<0.1	-22.9 0.4	-28.0 0.1
<i>n</i> -C <sub>28</sub>	-30.4	0.4	-28.8	0.7	<u>-24.3</u>	<u>0.4</u>	-23.6	0.3	-22.6 0.3	-28.0 0.1
<i>n</i> -C <sub>29</sub>	-25.9	<0.1	-29.1	0.8	<u>-16.8</u>	<u>1.0</u>	-25.8	0.2	-22.8 0.2	-26.3 0.3
<i>n</i> -C <sub>30</sub>	-29.6	0.6	-32.3	0.4	<u>-22.0</u>	<u>0.8</u>	-24.3	0.3	-22.1 <0.1	-26.0 0.1
<i>n</i> -C <sub>31</sub>	-24.7	0.2	-31.0	0.4	<u>-23.0</u>	<u>0.4</u>	-23.5	<0.1	-22.4 0.1	-27.1 0.6
<i>n</i> -C <sub>32</sub>	-26.7	0.4	-31.3	1.0	<u>-21.9</u>	<u>0.6</u>	-22.6	0.4	-21.5 <0.1	-24.1 0.6
<i>n</i> -C <sub>33</sub>	-24.8	0.7			<u>-26.0</u>	<u>0.3</u>	-23.6	0.2	-21.4 0.4	-26.2 0.2
<i>n</i> -C <sub>34</sub>	-27.6	0.1			<u>-24.6</u>	<u>1.0</u>	-23.2	0.1	-21.2 0.1	-25.4 <0.1
<i>n</i> -C <sub>35</sub>	-28.9	0.3			<u>-26.0</u>	<u>0.4</u>	-24.4	0.7	-20.4 0.5	-28.2 0.5
<i>n</i> -C <sub>36</sub>					<u>-26.1</u>	<u>0.2</u>	-27.4	0.7	-21.0 0.1	-23.7 0.4
<i>n</i> -C <sub>37</sub>							-27.7	0.9	-20.8 0.4	-26.9 0.2
<i>n</i> -C <sub>38</sub>							-25.6	<0.1	-19.3 0.6	-25.3 <0.1
<i>n</i> -C <sub>39</sub>									-21.8 0.1	
<i>n</i> -C <sub>40</sub>									-21.6 0.5	
<i>Isoprenoids</i>										
Far					-33.0	0.2				
Nor					-35.3	0.1				
Pr					-32.3	0.3				
Ph	-25.1	0.3	-26.8	0.2	-28.5	<0.1				
PMI <sub>reg</sub>	-22.0	0.3	-24.0	0.4	<u>-14.5</u>	<u>&lt;0.1</u>	-24.6	0.1		

**Table S5.** Coefficients of determination ( $R^2$ ) for Raman fittings

<u>-</u>	<u>LM-1692</u>	<u>LM-1693</u>	<u>LM-1694</u>	<u>LM-1695</u>	<u>LM-1696</u>	<u>LM-1697</u>	<u>LM-1698</u>
<u>Flake 1</u>	<u>0.995</u>	<u>0.996</u>	<u>0.995</u>	<u>0.975</u>	<u>0.985</u>	<u>0.984</u>	<u>0.989</u>
<u>Flake 2</u>	<u>0.996</u>	<u>0.997</u>	<u>0.995</u>	<u>0.989</u>	<u>0.992</u>	<u>0.987</u>	<u>0.975</u>
<u>Flake 3</u>	<u>0.994</u>	<u>0.998</u>	<u>0.992</u>	<u>0.982</u>	<u>0.989</u>	<u>0.987</u>	<u>0.984</u>
<u>Flake 4</u>	<u>0.988</u>	<u>0.992</u>	<u>0.994</u>	<u>0.986</u>	<u>0.994</u>	<u>0.987</u>	<u>0.991</u>
<u>Flake 5</u>	<u>0.996</u>	<u>0.997</u>	<u>0.989</u>	<u>0.992</u>	<u>0.997</u>	<u>0.984</u>	<u>0.986</u>
<u>Flake 6</u>	<u>0.996</u>	<u>0.997</u>	<u>0.994</u>	<u>0.974</u>	<u>0.989</u>	<u>0.986</u>	<u>0.985</u>
<u>Flake 7</u>	<u>0.996</u>	<u>0.997</u>	<u>0.995</u>	<u>0.954</u>	<u>0.992</u>	<u>0.979</u>	<u>0.986</u>
<u>Flake 8</u>	<u>0.995</u>	<u>0.998</u>	<u>0.979</u>	<u>0.992</u>	<u>0.982</u>	<u>0.970</u>	<u>0.981</u>
<u>Flake 9</u>	<u>0.997</u>	<u>0.998</u>	<u>0.988</u>	<u>0.987</u>	<u>0.992</u>	<u>0.985</u>	<u>0.986</u>
<u>Flake 10</u>	<u>0.998</u>	<u>0.995</u>	<u>0.991</u>	<u>0.991</u>	<u>0.989</u>	<u>0.987</u>	<u>0.992</u>
<u>Mean</u>	<u>0.995</u>	<u>0.996</u>	<u>0.991</u>	<u>0.982</u>	<u>0.990</u>	<u>0.984</u>	<u>0.986</u>

5

10

15

20

25

**Table S6.** Mean concentrations of selected *n*-alkanes, archaeol (A) and extended archaeol (ExA) in the interior and exterior of LM-1692 and LM-1695 (mg/g TOC).

	<u><i>n</i>-C<sub>18</sub></u>	<u><i>n</i>-C<sub>19</sub></u>	<u><i>n</i>-C<sub>20</sub></u>	<u><i>n</i>-C<sub>21</sub></u>	<u><i>n</i>-C<sub>22</sub></u>	<u><i>n</i>-C<sub>23</sub></u>	<u><i>n</i>-C<sub>24</sub></u>	<u><i>n</i>-C<sub>25</sub></u>	<u>A</u>	<u>ExA</u>
1692 exterior	<u>0.02</u>	<u>0.11</u>	<u>0.13</u>	<u>0.18</u>	<u>0.13</u>	<u>0.16</u>	<u>0.03</u>	<u>0.02</u>	<u>0.21</u>	<u>0.12</u>
1692 interior	<u>0.02</u>	<u>0.09</u>	<u>0.12</u>	<u>0.22</u>	<u>0.20</u>	<u>0.16</u>	<u>0.04</u>	<u>0.03</u>	<u>0.17</u>	<u>0.12</u>
1695 exterior	<u>0.08</u>	<u>0.35</u>	<u>0.42</u>	<u>1.20</u>	<u>0.96</u>	<u>0.74</u>	<u>0.42</u>	<u>0.25</u>	<u>0.24</u>	<u>0.09</u>
1695 interior	<u>0.07</u>	<u>0.32</u>	<u>0.49</u>	<u>1.83</u>	<u>1.33</u>	<u>0.76</u>	<u>0.32</u>	<u>0.13</u>	<u>0.42</u>	<u>0.16</u>